VOLUME FRACTION DEPENDENCE OF LINEAR VISCOELASTICITY OF STARCH SUSPENSION

by

Jinsha Li

A Dissertation

Submitted to the Faculty of Purdue University

In Partial Fulfillment of the Requirements for the degree of

Doctor of Philosophy

School of Agricultural & Biological Engineering

West Lafayette, Indiana

May 2019

THE PURDUE UNIVERSITY GRADUATE SCHOOL
STATEMENT OF COMMITTEE APPROVAL

Dr. Ganesan Narsimhan, Chair
School of Agricultural and Biological Engineering
Dr. Osvaldo Campanella
School of Agricultural and Biological Engineering
Dr. Martin Okos
School of Agricultural and Biological Engineering
Dr. Owen Jones
Department of Food Science
Dr. Vivek Narsimhan
Davidson School of Chemical Engineering

Approved by:
Dr. Nathan Mosier
Head of the Graduate Program

For Andrew, who always urges me to view stress more positively, who trusts me in handling life's challenges, and who ensures that I don't have to face them alone.

ACKNOWLEDGMENTS

First of all, I am deeply thankful to my advisor, Dr. Ganesan Narsimhan, for the opportunity to work in his lab and under great support. I have gained tremendous amount of scientific knowledge and life advice from working with him. I sincerely appreciate his contagiously positive attitude that pushes me to do my best work and feel confident in my competence.

The project is truly a collaborative work with the knowledge input from faculty members on my advisory committee, Dr. Osvaldo Campanella, Dr. Martin Okos, Dr. Owen Jones and Dr. Vivek Narsimhan. Dr. Campanella has kindly allowed me to use the rheology equipment in his lab and provided many hours of consultation on technical questions I had. He also offered me lots of career advice and helped me identify opportunities in the industry. Dr. Okos' office door was always open whenever I have to discuss with him some questions regarding to my research. His pumpkin patch has been one of the most memorable thing at Purdue ABE that I am looking forward to every year. I thank Dr. Jones for the trainings and permission to use the tensiometer, goniometer system and AFM in his lab. Nevertheless, I am also grateful to Dr. Vivek Narsimhan for teaching me the Stokesian Dynamic Simulation and his input in my project overall.

Throughout my years as an ABE graduate student working in the Food Science building, I have gotten so much help from people from both department technically and personally. From Department of Food Science, I would like to thank Dr. James BeMiller for his advice on the topics to focus for my thesis. Each conversation with him is so thought intriguing. I also would like to thank Dr. Suzanne Nielsen who was always there to support me when I was in crisis of any kind. From Department of ABE, I thank Dr. Mosier for giving me tremendous support during both my MS and PhD period, Dr, Engelberth for advocating the doctoral fellowship and being the advisor for my MS where I learned how to do research and publish paper in a systematic way, as well as Nikki Zimmerman for being the most helpful Graduate Program admin any student can ask for.

They say that "you are who your friends are". In that sense, I feel very lucky that I have been surrounded with those who have selflessly shared their knowledge with me, who see the goodness within me even when I do not see it myself, and who are my role models, mentors, and source of recharging. On top of my mind, I would like to thank (with no particular order) Fang Fang, Malithi

Wickramathilaka, Necla Mine Eren, Mahdieh Aghazadeh, Studie Red Corn, Maryam Ghadiry, Xiaowei Zhang, Xingyun Peng, Ning Xiang, Yuan Lyu, Ximing Zhang, Leyu Zhang, Lei Nie, Maya Fritriyanti, Gnana Prasuna Reddy, David Orrego, Jen Rich, Nimisha Bajaj, Joyatee Sarker, and Purdue Women in Engineering Program, in which I formed some life-long friendships.

This project was funded by Agriculture and Food Research Initiative Competitive Grant from the USDA National Institute of Food and Agriculture. A special gratitude goes out to Fredrick N. Andrews Fellowship and Whistler Center for Carbohydrate Research for sponsoring my PhD study. The Center also provided great resource for me to gain deeper understanding on science behind carbohydrate.

Nobody has been more important to me in the pursuit of this path than the members of my family, my parents who have been living a frugal life to support my education in the U.S. since 2008 and my fiancée Andrew who have put so much mileage in his car for the trip between Michigan and Indiana over the past three years. I am forever indebted to your patient, care and understanding with me. I love you guys so much and will try my best to be a better daughter and life partner to you.

TABLE OF CONTENTS

LIST OF TABLES

LIST OF FIGURES

ABSTRACT

Author: Li, Jinsha. PhD
Institution: Purdue University
Degree Received: May 2019
Title: Volume Fraction Dependence of Linear Viscoelasticity of Starch Suspensions
Committee Chair: Ganesan Narsimhan

When starch granules are gelatinized, many complex structural changes occur as a result of large quantity of water being absorbed. The enlargement of granule sizes and the leaching out water-soluble macromolecules contribute to the viscoelasticity. Starch pasting behavior greatly influences the texture of a variety of food products such as canned soup, sauces, baby foods, batter mixes etc. It is important to characterize the relationship between the structure, composition and architecture of the starch granules with its pasting behavior in order to arrive at a rational methodology to design modified starch of desirable digestion rate and texture. Five types of starch used in this study were waxy maize starch (WMS), normal maize starch (NMS), waxy rice starch (WRS), normal rice starch (NRS) and STMP cross linked normal maize starch. Evolution of volume fraction ϕ and pasting of 8% w/w starch suspension when heated at 60, 65, 70, 75, 80, 85 and 90 °C were characterized by particle size distribution and G', G" in the frequency range of 0.01 to 10 Hz respectively. As expected, granule swelling was more pronounced at higher temperatures. At a fixed temperature, most of the swelling occurred within the first 5 min of heating. The pastes exhibited elastic behavior with G' being much greater than G". G' increased with time for waxy maize and rice starch at all times. G' and G'' were found to correlated only to the temperature of pasting and not change much with the rate of heating. For WMS, WRS and STMP crosslinked NMS, G' approached a limiting value for long heating times (30 min and above) especially at heating temperatures of 85°C and above. This behavior is believed to be due to the predominant effect of swelling at small times. For normal maize and rice starch, however, G' reached a maximum and decreased at longer times for temperatures above 80 °C due to softening of granules as evidenced by peak force measurements. For each starch sample, the experimental data of G' at different heating temperatures and times could be collapsed into a single curve. The limiting value of G' at high volume fraction was related to granule size and granule interfacial energy using a foam rheology model. The interfacial free energy of granules were obtained from

contact angle measurements and was employed to evaluate the limiting G'. The experimental data of G' for all starches when subjected to different heating temperatures and times were normalized with respect to the limiting value at high volume fractions. The master curve for normalized G' was employed to predict the evolution of G' with time for different starches which was found to agree well with experimental data of storage modulus. A mechanistic model for starch swelling that is based on Flory Huggins polymer swelling theory was employed to predict the evolution of volume fraction of swollen granules. The model accounts for the structure and composition of different types of starches through starch-solvent interaction as quantified by static light scattering, gelatinization temperature and enthalpy of gelatinization, porosity and its variation with swelling and crosslinking of starch molecules within the granule from equilibrium swelling. Consequently, one could predict the evolution of texture of these starch suspension from the knowledge of their swelling behavior. Expressing the limiting storage modulus of complete swelling (volume fraction approaching unity) of starch suspension in terms of foam rheology, we were able to normalize the storage modulus of different types of starches with respect to its limiting value which is found to fall into a master curve. This master curve when employed along with the swelling model resulted in the successful prediction of development of texture for different types of starches. The above methodology can quantify the effects of structure and composition of starch on its pasting behavior and would therefore provide a rational guideline for modification and processing of starch-based material to obtain desirable texture and rheological properties.

CHAPTER 1. INTRODUCTION

1.1 Overview of the Thesis

Starches are important ingredients used in various food and non-food products. They are very useful in a number of food applications, where they may act as a source of calories, as well as thickening, stabilizing and gelling agents. Starches are obtained from seeds, particularly corn, wheat, rice, and from tubers or roots, particularly potato, sweet potato, and cassava (Whistler & BeMiller, 1997). Starch granules, occurs naturally as discrete particles, range in size from sub-micron elongated granules of chloroplasts to the relatively large oval granules of potato, which could be over 100 μm. Granule shapes include nearly perfect spheres and discs, and polyhedral or irregular granules(Chen, Yu, Chen, & Li, 2006). Starch granules are composed of a mixture of two polymers: a linear polysaccharide, amylose with (1-4) glucosidic bonds and a highly branched polysaccharide, amylopectin with 5% of (1-6) glucosidic bonds which lead to a unique branched structure capable of crystallizing. Starch granules are relatively dense, are insoluble in water, and hydrate only slightly at room temperature; the dispersions formed have a relatively low viscosity. Starch granules swell when heated in an aqueous medium because of uptake of water due to a chemical potential gradient. This swelling is resisted by the elasticity of the granule network which ruptures at some point leading to leaching of starch (predominantly amylose) into the aqueous medium, thus resulting in its increased viscosity. The combined effects of increased volume fraction of granules (due to swelling) and the increased aqueous phase viscosity result in thickening of the starch dispersion, a phenomenon known as starch pasting. Starch pasting behavior greatly influences the texture of a variety of food products such as canned soups, gravies, sauces, baby foods, fruit pie fillings, puddings, batter mixes for deep fried foods etc. In non-food products, starch dispersion rheology and its pasting behavior is important in operations that range from paper coating to the fabrication of paints. Thus, it is necessary to quantify the effect of starch structure and composition on its pasting behavior in order to develop rational guidelines for modification of starch through cross linking in order to obtain desirable texture and rheological properties. This would require understanding the swelling of starch granules, the conditions under which they will rupture, the extent of release of its contents to the aqueous medium upon rupture and the effect of these on the rheology of suspension.

1.2 Objectives of the Thesis

1. Characterization of swelling behavior of waxy maize starch, normal maize starch, waxy rice starch and normal rice starch.
2. Characterization of pasting behaviors of cross-linked and native maize and rice starch
3. Explore the dependency of viscoelasticity of maize and rice starch on volume fraction

This dissertation contains six main sections: a review of literature, material and research methodologies, the results of the three main studies, conclusion and future recommendations and reference.

.

CHAPTER 2. OVERVIEW OF LITERATURE

Starches isolated from different sources are known to have different molecular structures resulting in a wide range of different functionalities. Differences in functionality can be attributed to the morphology and size of the starch granules but also to the assembly and structure of the starch molecules within the starch granules. The ratio between amylose and amylopectin within the starch granules is considered important since this variable has profound effect on starch paste rheology as shown for amylose-free potato starch (Visser, Suurs, Steeneken, & Jacobsen, 1997) and high-amylose starch(Banks, Greenwood, & Muir, 1974). Other molecular properties such as starch molecular weight distribution (Blennow, Bay-Smidt, & Bauer, 2001), and the degree of amylopectin branching are also known to influence the functional properties of starches (Fredriksson, Silverio, Andersson, A.-C, & Åman, 1998). The end uses of different types of starches are related to the ability of the granules to undergo swelling (Okechukwu & Rao, 1995). In high amylopectin cereal starches like waxy maize starch, the granules tend to hydrate with ease, swell rapidly, and rupture to a great extent, resulting in the loss of paste viscosity, with weak bodied, stringy and cohesive pastes(Tattiyakul & Rao, 2000). Waxy maize starches, composed of nearly 100% amylopectin, have built-in viscosity stability due to the branched nature of the polymer molecule. Waxy maize is useful in a wide array of applications in the food industry because of its stability.

Two main types of crystalline starch structures have been detected by wide-angle X-ray scattering(Galliard & Bowler, 1987; Nara & Tsu, 1983): the A-type structure of cereal grain starches such as maize, wheat, and rice; and the B-type structure of tuber, fruit and stem starches such as potato, sago and banana starches. An additional C-type structure composed of both A- and B-type polymorphs, has been detected in bean seed starch (French, 1984; Jacobs et al., 1998; Sarko & Wu, 1978). The type A X-ray pattern of cereal starches is indicative of parallel, double helixes separated by interstitial water(Whistler & BeMiller, 1997). It has been shown(Stevenson, Jane, & Inglett, 2006) that molar mass, radius of gyration and density of pin oak acorn starch were comparable to other A-type starches. The molecular weight, radius of gyration and hydrodynamic radius of amylopectin have been investigated by laser light scattering and size exclusion chromatography (Bello-Perez, Roger, Colonna, & Paredes-Lopez, 1998; Durrani & Donald, 2000;

Galinsky & Burchard, 1995; Hanselmann, Burchard, Ehrat, & Widmer, 1996; Millard, Wolf, Dintzis, & Willett, 1999; Yoo & Jane, 2002). The molecular weight of non-degraded amylopectin was reported to range from 1.70×10^8 g/mol to 5.60×10^8 g/mol, and the radius of gyration of non-degraded amylopectin was reported to vary from 170 to 342 nm. The differences in the results obtained by different authors could be attributed to the different sources of samples and partly due to the sample preparation method(Cheng et al., 2006). In spite of extensive experimental investigations on starch pasting profile, quantitative prediction remains unsatisfactory.

Studies have proved that granule size and its ability to incorporate water and swell can affect the function and physical properties of starch population. The granule size distribution is normal for maize starch, bimodal for wheat starch, or trimodal for barley starch (Stapley & BeMiller, 2003). The initial average diameter or the length of major axis can be different among sources of starch and even within the same species or different part of the same plant. For example, the large A-type (disc-like) and small B-type granules (spherical or polygonal) in wheat endosperm started with average diameter of 10-35μm and 1-10μm, respectively (S. G. Choi & W. L. Kerr, 2004). At 80°C, the average diameter of native wheat starch granule increased from 20.42 to 44.64μm in 1 min and further increased to 54.27 in 30 min (S. g. Choi & W. L. Kerr, 2004). Rice starch granules, on the other hand, vary from 2 to 7 μm in their size (Wani et al., 2012).

Extensive investigations have been carried out on swelling of polymer gels(Flory, 1953; Hirotsu, Hirokawa, & Tanaka, 1987; Hooper, Baker, Blanch, & Prausnitz, 1990; Joanny & Leibler, 1990; Katchalsky, Lifson, & Eisenberg, 1951; Katchalsky, Lifson, & Mazur, 1953; Katchalsky & Michaeli, 1955; Ricka & Tanaka, 1984, 1985; Tanaka, 1978; Tanaka et al., 1980). It has been demonstrated that changes in temperature(Tanaka, 1978), solvent composition(Hirotsu et al., 1987) and ionic strength(Hooper et al., 1990; Ricka & Tanaka, 1985) can induce changes in the state of the swollen network. The validity of Flory-Rehner theory(Flory, 1953) has been demonstrated for a wide variety of systems(Baker, Hong, Blanch, & Prausnitz, 1994a; Prange, Hooper, & Prausnitz, 1989; Urayama & Kohjiya, 1996). In some cases(Brotzman & Eichinger, 1982; Zhao & Eichinger, 1992), the additivity assumption of free energies of mixing and deformation has been shown to be unsatisfactory. Monte Carlo simulations were presented for the equilibrium swelling of polymeric gels(Fernando A. Escobedo, 1996; F. A. Escobedo & Pablo, 1997).

2.1 Polymer Swelling

Polymer gel swelling contributes to the texture of material and thus has many applications in everyday life. Extensive investigations have been carried out on swelling of polymer gels (Flory, 1953; Hirotsu et al., 1987; Hooper et al., 1990; Joanny & Leibler, 1990; Katchalsky et al., 1951; Katchalsky et al., 1953; Katchalsky & Michaeli, 1955; Ricka & Tanaka, 1984, 1985; Tanaka, 1978; Tanaka et al., 1980). It has been demonstrated that changes in temperature(Tanaka, 1978), solvent composition(Hirotsu et al., 1987) and ionic strength (Hooper et al., 1990; Ricka & Tanaka, 1985) can induce changes in the state of the swollen network. The validity of Flory-Rehner theory(Flory, 1953) has been demonstrated for a wide variety of systems (Baker, Hong, Blanch, & Prausnitz, 1994b; Prange et al., 1989; Urayama & Kohjiya, 1996). In some cases (Brotzman & Eichinger, 1982; Zhao & Eichinger, 1992), the additivity assumption of free energies of mixing and deformation has been shown to be unsatisfactory. Flory's theory has been extended by adding empty sites to the lattice(Z. Y. Lu & Hentschke, 2002). Monte Carlo simulations were presented for the equilibrium swelling of polymeric gels(Fernando A. Escobedo, 1996; F. A. Escobedo & Pablo, 1997).

2.2 Flory-Huggins Polymer Swelling Theory

The sufficiently regular chain structure of polymers usually are susceptible to the spontaneous ordering of their configurations. The polymer chains line in bundles with chain axes parallel to one another when they are in the crystalline condition irrespective of whether the individual molecules are fully extended or in a less extended spiral configuration.

A three-dimensional network polymer such as Sephadex beads absorb a large quantity of solvent, in which they are placed in contact. Incorporation of solvent causes swelling with the same conditions as the formation of ordinary polymer solution of analogous linear polymers where solvent spontaneously enters the polymer network (Flory, 1953). The swollen gel is an elastic solution. This process will continue until the system reaches the most thermodynamically stable state and it is spontaneous as long as there is an increase in entropy. One way to increase the entropy is by adding volume and surface area of polymer network so that the solvent may spread. Therefore, the mixing can be expressed as the entropy of dilution. As the network is swollen by uptake of solvent, the chains between network junctions are required to assume elongated

configurations and a force similar to the elastic retractive force in rubber consequently develops to oppose to the swelling process. This force increases as swelling continues while the diluting force decreases. Polymer stops swelling when these two forces are in balance and that is the state of equilibrium. This swelling behavior is very similar to osmosis, where water molecules move across the semi- permeable membrane from an area of greater concentration (of water molecules) to a less concentrated area until system reaches osmotic equilibrium. The elastic reaction of the network structure is equivalent to osmotic pressure acting on the swollen gel. When the chemical potential of the solvent in the gel is increased by osmotic pressure to the same level as it is in the excess solvent surrounding the swollen gel, equilibrium state is achieved. The network structure performs as solute, osmotic membrane and pressure-generating device.

The change in free energy ΔF (Eq. 2-1) involved in the mixing of pure solvent with the initially pure, isotropic and amorphous polymeric network consists of two parts: the free energy of mixing ΔF_M (Eq. 2-2), and the elastic free energy ΔF_{el} (Eq. 2-3).

$$\Delta F = \Delta F_M + \Delta F_{el} \quad (2\text{-}1)$$

$$\Delta F_M = kT(n_1 ln\emptyset_1 + \chi_1 n_1 \emptyset_2) \quad (2\text{-}2)$$

$$\Delta F_{el} = (kT\nu_e/2)(3\alpha_s^2 - 3 - ln\alpha_s^3) \quad (2\text{-}3)$$

where ϕ_1 and ϕ_2 are volume fractions of solvent and polymer respectively,

$$\mu_1 - \mu_1^0 = N\left(\frac{\partial \Delta F_M}{\partial n_1}\right)_{T,P} + N\left(\frac{\partial \Delta F_{el}}{\partial \alpha_s}\right)_{T,P} N\left(\frac{\partial \alpha_s}{\partial n_1}\right)_{T,P} \quad (2\text{-}4)$$

$$\mu_1 - \mu_1^0 = RT\left[\ln(1-\phi) + \phi + \chi(T)\phi^2 + v_1\left(\frac{\nu_e}{V}\right)(\phi^{1/3} - \frac{\phi}{2})\right] \quad (2\text{-}5)$$

The Gibbs free energy is used in this condition where pressure and temperature stay constant, while the volume of the system expand. where, ϕ is the volume fraction of starch within the granule, χ (T) is the Flory Huggins parameter at temperature T, R is the gas constant, T is the temperature, v_1 is the molar volume of the un-swollen starch granule, V is the volume of the relaxed network, i.e., the volume occupied by the polymer when the cross-linkages were introduced into the random system, ν_e is the effective number of moles of chains in the network. The first two terms on the right hand side arise from entropy of mixing, the third term involving

Flory Huggins parameter arises from the enthalpy of mixing and the last term arises from the elastic resistance to swelling.

2.3 Starch Pasting and Gelatinization

It has been proposed that the behaviors of pasted starch systems were determined primarily by the phase volume of swollen granules and their deformability(I. D. Evans & Lips, 1992; Frith & Lips, 1995). However, it can also be concluded that the rigidity of the swollen granules and the hot-water soluble components or the continuous phase can also influence the rheological properties of starch pastes(C. I. Lu & Chen, 1980).

When the elastic network of swollen granules rupture, the granule's starch contents (primarily amylose) leach into the aqueous medium thus resulting in its increased viscosity. The combined effects of increased volume fraction of granules (due to swelling) and the increased aqueous phase viscosity results in thickening of the starch dispersion, a phenomenon known as starch pasting. Below describes the major rheological observations during gelatinization and pasting. During this process, the starch transforms from a primarily ordered, crystalline state to an amorphous one.

Starch is unique among carbohydrates because it occurs naturally as discrete particles, called granules. They are synthesized in a plant organelle called 'amyloplast' and function as energy storage units for plant (W. T. Kim, Franceschi, & Okita, 1989; Nelson & Pan, 1995; Pozueta-Romero, Frehner, Viale, & Akazawa, 1991; Preiss, 1982, 1998). Starch is unique in a sense that most of them are composed of mixture of two polymers: a linear polysaccharide called amylose with α (1-4) glucosidic bonds and a high branched polysaccharide called amylopectin with 5% of α (1-6) glucosidic bonds (Ball & Deschamps, 2009; Kornbrust, Forman, & Matveeva, 2012). Those components and structure give rise to physical and chemical properties of starch that affects its application in food and non-food products. The textural properties of many foods are greatly impacted by the functional characteristics of starch used in their formula as stabilizer, gelling agents, water retention or bulking agent to increase thermal and shear resistance (J. Singh, Kaur, & McCarthy, 2007). In pharmaceuticals, starches make a variety of contributions, from binders (Zhou, Yang, & Qu, 2007) to products as disparate as tablets for control of drug delivery (Ravenelle, Marchessault, Légaré, & Buschmann, 2002), liquid medicines and creams(de Paepe, 2002). In textiles industry, starch is used to size and stiffen fabric (Teli, Rohera, Sheikh, & Singhal,

2009). It has been added to individual yarns to increase mechanical strength and resistance to friction wear and help resist moisture penetration (Meshram, Patil, Mhaske, & Thorat, 2009). In paper industry, starch is used as binding agent for treatment of paper surface. In construction material, starch can be used as consolidator/binder and pore former to make porous concrete (Glenn, Gray, Orts, & Wood, 1999) and ceramics for thermal insulation and filters. Gelatinization can be achieved through heating the granules with presence of water. In a water excessive environment, gelatinization of starch granules result in change in flow behavior of the slurry as swollen granules, ruptured granules and leaked-out molecules form a dispersion (Zobel, 1984). Starch granules are water-insoluble. Therefore, gelatinization is a crucial step that disrupts the granular structure through granule hydration, swelling, and solublization of starch molecules (Pither, 2003; Ratnayake & Jackson, 2006).

Because of the difference in chemical potential, water from the continuous aqueous medium will diffuse into the three-dimensional network inside the starch granule thereby resulting in its swelling. Swelling is spontaneous since it results in an increase in entropy as a result of dilution of starch network. Elongation of starch network due to swelling is opposed by an elastic retractive force. Swelling eventually stops at which the chemical potential of water becomes equal inside and outside the granule. Swelling power varies among plant source, degree of crosslinking, heating time and temperature and the presence of other components such as hydrocolloids. Many starch-based products are in fluid or semisolid form during production. Therefore, it is crucial to study the rheology of dispersions of starch in order to provide a concise description on how process condition and the composition of foods affect its texture. In the past three decades, numerous rheological models were employed to study such characteristics during starch gelatinization. For example, the power law model described the shear-thinning and shear thickening behavior of starch dispersion (I. D. Evans & Haisman, 1980), the Krieger-Dougherty model that was based on fundamental concept was used to study the effects of volume fraction on viscosity assuming the spheres are uniform diameter (M. A. Rao, P. E. Okechukwu, P. M. S. Da Silva, & J. C. Oliveira, 1997), and structural models such as that of Cross (Cross, 1965) was used to characterize the flow behavior of polymer dispersions.

Pasting behavior of starch based system contains information that is useful to improve and control texture, stability and process design of product. The flow behavior of paste is routinely monitored

during production in industry by empirical methods in which non-uniform shear conditions might exist(Wong & Lelievre, 1981). It is concluded that when being cooked at shorter time, the starch dispersion has dilatant behavior, but the gelatinized starch suspensions cooked at longer times behaves like non-Newtonian shear-thinning fluids (Bagley & Christianson, 1982). Those measurement techniques are useful in predicting the performance of paste in specific application. However, for viscoelastic paste and weak gel, their rheological properties are more rigorously characterized by measurement of dynamic viscosity and rigidity as a function of frequency (Dickinson, 1992; Ferry, 1980). In real foods that contain several ingredients, the control of texture can be achieved through viscoelasticity measurements of carbohydrates mixtures at low concentrations. The viscoelastic behavior of starch pastes or gels can be characterized through stress-relaxation experiments (Eliasson & Bohlin, 1982), creep experiment (Pérez, Alvarez, & Vázquez, 2008) and other dynamic measurements with oscillatory shear (Gunasekaran & Ak, 2000). Starches from different botanical sources demonstrated a variety of viscoelastic behavior during hearing (Eliasson, 1986).

2.4 Rheology of Moderately Concentrated Suspension of Spherical Particles

Macroscopic properties such as rheology of a suspension of particles can be predicted through their microstructural mechanics. Microstructural mechanics includes nonhydrodynamic forces (Brownian force, interparticle electrostatic and steric forces and external force) and hydrodynamic forces acting on the particles, as well as their microstructure (spatial and temporal distribution). The reason that colloids have non-Newtonian behavior is because of the interparticle hydrodynamic interactions (exist even for neutral particles and become important only for moderate to large concentrations), colloidal forces such as electrostatic effects (if the ranges of colloidal attraction and repulsion are significant) and the effects due to polymer layers adsorbed on the particles. In order to understand the flow behavior of dispersions, one needs to understand the interaction among particles, physicochemical factors or features of the phenomena.

Figure 2.1 shows a schematic of apparent viscosity vs. time as a starch dispersion experiences heating and cooling over a span of ~10-30 minutes. The viscosity is constant at lower temperatures (see step 1), increases suddenly near the gelatinization temperature (step 2), reaches a maximum

(step 3), and then subsequently decreases at higher temperatures (step 4) (Lii, Tsai, & Tseng, 1996; Lil, Shao, & Tseng, 1995; Tsai, Li, & Lii, 1997). The decrease at high temperature is due to the rupture of the polymer network. During this process, amylose leaches out of the granule, but this leaching does not overcome the viscosity decrease due to granule destruction. The rate of temperature heating/cooling plays a significant role in the measured profile in step 4. Upon cooling, the starch recrystallizes and increases in viscosity– a process known as retrogradation (steps 6-8). In this proposal, we focus on steps 1-3 – the rheology change during the swelling of the granule. During this process, the volume fraction occupied by the granules goes from dilute ($\phi << 1$) to beyond the closed-packed limit of monodisperse spheres ($\phi = 0.64$).

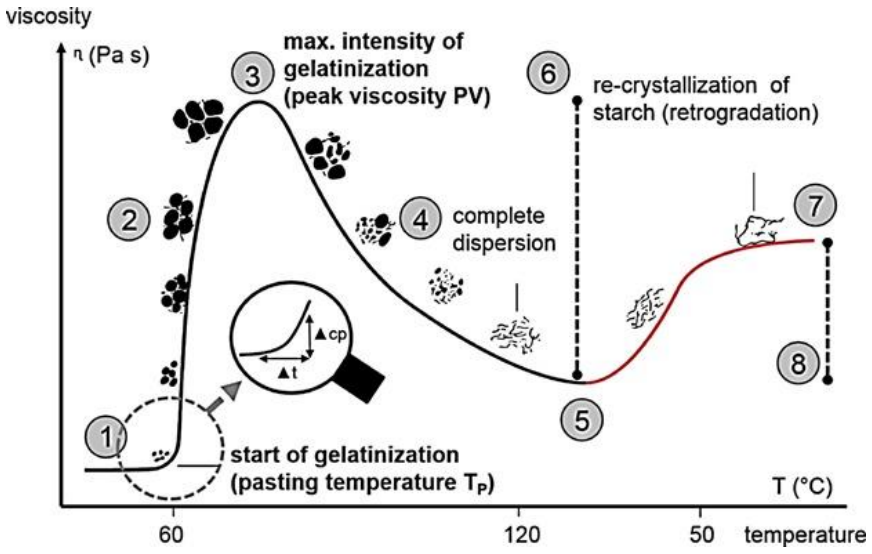

Figure 2.1: Schematic of viscosity vs. temperature during heating/cooling of starch dispersion. Reproduced from Schmirmer et al., 2015.

2.5 Effect of Granule Volume Fraction on Rheological Behavior of Polymer Suspension

The following factors play a dominant role in the rheology of starch dispersions during swelling: the phase volume of swollen granules, their deformability(Ellis, Ring, & Whittam, 1989; I. D. Evans & Lips, 1992; Frith & Lips, 1995), and the number fraction of large granules (Wong & Lelievre, 1981). In addition, the hot-water soluble components in the continuous phase can also influence the rheological properties of starch pastes (C. I. Lu & Chen, 1980). We note that granule size, granule shape, and composition of amylose/amylopectin have a profound effect on the factors

mentioned above (Vamadevan & Bertoft, 2015), as demonstrated for amylose-free potato starch (Visser et al., 1997; Hoover, 2001) and high-amylose starch (Banks et al., 1974; Srichuwong et al., 2005). Other molecular properties such as starch molecular weight distribution (Blennow et al., 2001), and the degree of amylopectin branching are also known to play a large role as well (Fredriksson et al., 1998; Singh et al., 2007). The end uses of different types of starches are related to the ability of the granules to undergo swelling (Okechukwu and Rao, 1995; Vroman and Tighzert, 2009). In high amylopectin cereal starches like waxy maize starch, the granules tend to hydrate with ease, swell rapidly, and rupture to a great extent, resulting in the loss of paste viscosity, with weak bodied, stringy and cohesive pastes (Tattiyakul and Rao, 2000). Waxy maize starches, composed of nearly 100% amylopectin, have built-in viscosity stability due to the branched nature of the polymer molecule. Waxy maize is useful in a wide array of applications in the food industry because of its stability.

2.6 Yield Stress and Shear Thinning Behavior

Yield stress is defined as the minimum shear stress that must be applied to the material to initiate flow(Dzuy & Boger, 1983). It is an important rheological property that many concentrated suspensions share. Yield stress is routinely measured and used in the food industry for basic process calculations, manufacturing, as well as a test for sensory and quality indices to determine the effect of composition and manufacturing procedures on structural and functional properties(Sun & Gunasekaran, 2009).

Many studies on the rheology of starch suspensions show that highly concentrated, gelatinized starch exhibits a yield stress. Below the temperature at which amylose solubilization increases rapidly (80°C) for cornstarch, the yield stress appears to be increase with increasing temperature and longer heating times. In general, experiments observe that the yield stress for wheat starch is larger than that of corn at the same volume fraction of swollen granules. Although the reasons for this observation are not fully understood at this point, it is believed that this behavior could be attributed to differences in inter-particle contact areas, granule particle size distribution or granule deformability(Christianson & Bagley, 1984).

Above the critical yield stress, many starch suspensions exhibit pronounced shear-thinning or shear-thickening behavior (Alloncle, Lefebvre, Llamas, & Doublier, 1989; I. D. Evans & Haisman,

1980). Currently, there appears to be no a priori theory to predict which behavior will occur for a given microstructure. Experiments suggest that polydispersity plays a major role in this process, with the extent of shear thinning increasing as polydispersity becomes wider. Polydispersity typically increases during the first 5-10 minutes of heating – in fact, in a few cases, this phenomenon can switch the starch's rheology from shear thickening to shear thinning. Researchers found that the suspension's temperature history plays a large role in determining the extent of shear thinning, probably because granules of different sizes swell at different rates. The molecular mechanisms behind these observations have yet to be elucidated, but simulations can play a big role in addressing how collections of polydisperse granules evolve/cluster under flow.

2.7 Effect of Granule Volume Fraction on Rheological Behavior of Polymer Suspension

It has been proposed that the behaviors of starch paste was determined primarily by the phase volume of swollen granules and their deformability(Ellis et al., 1989; I. D. Evans & Lips, 1992; Frith & Lips, 1995), as well as the number fraction of large granules and the volume fraction of swollen starch particles the paste contains (Wong & Lelievre, 1981). In addition, the rigidity of the swollen granules and the hot-water soluble components in the continuous phase can also influence the rheological properties of starch pastes (C. I. Lu & Chen, 1980). The influence of concentration of starch (Bagley & Christianson, 1982), source of starch (N. Singh, Singh, Kaur, Singh Sodhi, & Singh Gill, 2003) and method of paste preparation on rheological properties have been studied. The results suggest that under the conditions examined, the differences in the dynamic rigidity and viscosity of pastes may be attributed to the differences in the number fraction of large granules and the volume fraction of swollen starch particles they contain (Wong & Lelievre, 1981).

Pasting behavior varies among starch samples from the same species but with different amylose/amylopectin ratio. Literature usually assumes that the system, even though a bit like fluid, is a viscoelastic liquid (paste) and the cooled, more solid like system is a gel. The starch concentration is important as it affects the relative importance of the continuous and discontinuous phase of pastes and gels(H. R. Kim, Muhrbeck, & Eliasson, 1993). G' and G'' of normal corn and waxy maize starch dispersions increase to maximum values upon initial heating, then they decrease with further heating.

The flow and viscoelastic response of starch pastes have been extensively investigated (I. D. Evans & Lips, 1992; Frith & Lips, 1995; Genovese & Rao, 2003; Steeneken, 1989). When the particle volume fraction is close to and above close packing, it has been shown that the viscosity increases more rapidly with concentration for low swelling starches than for high-swelling ones. A direct correlation between granule size and viscosity-increase during gelatinization was reported by Tan et. al. (Tan, Torley, & Halley, 2008). When starch suspension was subjected to heating, the storage and loss moduli were constant at lower temperatures, increased suddenly at a certain temperature, reached a maximum and subsequently decreased at high temperatures (Lii et al., 1996; Lil et al., 1995; Tsai et al., 1997). Due to the irregular shape and unknown surface characteristics of granules, the study of viscoelasticity in starch suspension flow is scarce. However, from the study of suspension of solid particles, Kolli et. al. (2002) reported that the interparticle contacts play an important role especially at high granule volume fraction when the distance between individual particles become smaller.

The simplest theoretical colloid system is one in which the particle shape is spherical and the interactions are only volume exclusion, known as hard spheres systems. Behavior of hard sphere system has been extensively studied and well characterized (Fuchs & Ballauff, 2005). Due to the fixed size and volume of hard-sphere particles, the motion of particles is only confined by the its nearest neighbors(Pusey, 2008). As the volume fraction φ of particles increases, hard spheres undergo state changes due to the available space for particle motion becomes smaller. When φ is close to 0.64, known as maximum packing, the viscosity will diverge (Larson, 1999). For attractive particles, gel is an arrested state and is possible at lower particle concentration. The soft particles in gel can deform and attain larger volume fractions than hard sphere particles. Although they behave much like hard sphere particles at low concentration (Crassous, Ŕgisser, Ballauff, & Willenbacher, 2005), the high concentration leads to permanent contacts of particles when the soft particles start to deform, which strongly affect the rheological behavior of the suspension (van der Vaart, 2013).

2.8 Foam Rheology

Foam was described as a viscoelastic material because of its capability of maintaining the shape under small loading. The shear modulus can be calculated from the surface tension, initial deflection, the torqued applied, and the dimension (surface-to-volume ratio) of the sample. Stamenovic and Wilson (1984) measured the elastic response of foam to an applied torque for the first time and gave a range of values of the ratio of the shear modulus *G* to capillary pressure *Pc*. Based on their analysis, Budiansky and Kimmel (1987) came up with the dodecahedron model, where the aggregate of polyhedral cells in the foam was represented by a single regular dodecahedron (Figure 2.2). Narsimhan and Ruckenstein (1986) applied this model onto broad bubble size distribution in liquid environment and successfully predict the stability of foam bed at high superficial gas velocity, high viscosity and high inlet concentrations.

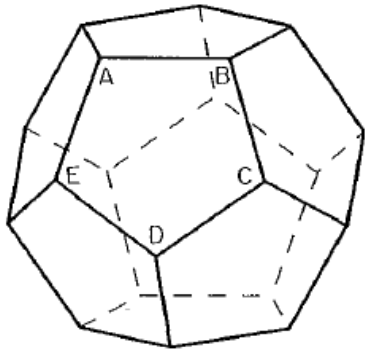

Figure 2.2: A single regular dodecahedron represent aggregate of polyhedral cells in the foam

When the volume fraction of swollen granules becomes greater than the maximum packing of solids, the granules deform and assume a dodecahedral structure, separated by thin films of aqueous phase. Three such films intersect at the dihedral angles of 120˚ in a channel called Plateau border. Four and only four these edges meet at a point at the angles of 109˚28’16” (the tetrahedral angles) to satisfy the laws of Plateau. The suspension therefore has a foam structure with thin films and interconnected Plateau borders. At low strains, the starch paste (suspension of swollen granule) is elastic with a modulus that is weakly dependent on the volume fraction. Above a yield stress, the paste flows and becomes plastic with a shear thinning behavior. In this project, we will be mainly concerned with the elastic behavior of the paste.

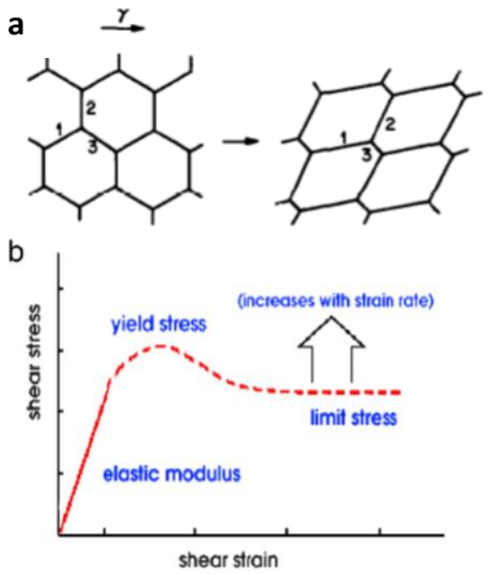

Figure 2.3: (a) dodecahedral structure of foam and (b) its deformation upon applied stress

The structure of a highly packed suspension of monodisperse, swollen granules can be pictured as a series of interconnected, elastic thin films in a dodecahedral structure, with the length of each microstructural element being $l_0 = 0.816R$, where R is the average particle radius. In the small deformation limit, the films are incompressible with principle stretches λ_1 and λ_2 in the directions normal and perpendicular to the dodecahedron surface. If we denote ε as the strain in the λ_1 direction, one can show that $\lambda_1 = (1 + 2\varepsilon)^{1/2}$, with $\lambda_2 = (\lambda_1)^{-1/2}$. The surface area of the deformed element is $S = 2l_0^2(2\lambda_1\lambda_2 + \lambda_2^2)$. If we assume the surface energy of the granule is $E = \gamma S$, where γ is the surface tension of the granule with the external fluid, the shear modulus is given by

$$G' = \frac{\gamma}{3V_0}\left(\frac{\partial^2 S}{\partial \varepsilon^2}\right)$$

Where $V_0 = 4\pi R^3/3$ is the granule volume. Substituting $l_0 = 0.816R$ from above, one obtains

$$G' = 0.053\frac{\gamma}{R}$$

This expression is valid for very high volume fraction (approaching unity) of starch pastes when the foam structure is dodecahedral. An initial estimate of G' for normal and cross-linked maize

starch is in the range of a few hundred Pascals for surface tension values in the range of 20 to 60 mN/m. This rough estimate of G' is consistent with measured, experimental data listed in previous sections. In this proposal, we will compare experimental measurements of shear modulus with predicted values for a wide range of starch varieties. To get quantitative comparison, we will obtain measurements of granule surface tensions as described in the Methods section.

At lower volume fractions, the granules are not fully deformed, and hence the above analysis needs to be modified. We anticipate the shear modulus will depend on the volume fraction in this regime, and we will develop analytical predictions accordingly.

CHAPTER 3. MATERIAL AND METHOD

3.1 Material and Methods

Waxy Maize Starch (Novation® 2300), Normal Maize Starch (Melojel), Waxy Rice Starch (Novation® 8300), Normal Rice Starch (Penpure 30), Waxy Potato Starch (Novation 1600) were provided by Ingredion. Sodium trimetaphosphate (STMP) for crosslinking is from Sigma Aldrich. DMSO used to dissolve starch is purchased from Fisher Scientific. Ethanol and acetone are both from Sigma Aldrich. Diiodomethane for measurement of interfacial tension of water and starch is from Fisher Scientific.

The Novation® clean label native starch brand that offers all the shear, pH and process tolerance, viscosity, shelf stability and texture of traditional modified starches. This waxy maize starch and waxy rice starch chosen for the study have been physically modified through heat-moisture treatment and are expected to have inhibited swelling. The exact making process of this line of starch is obviously a top trade secret. The key treatment done to these starch is called annealing, a hydrothermal process, consists of holding starch granules in an excess water at temperature above the glass transition temperature and below the gelatinization temperature (BeMiller & Huber, 2015; Sjoo, Nilsson, & Sjöö, 2018; S. Wang, Wang, Yu, & Wang, 2014). This process increases the onset and peak gelatinization temperature and lower the temperature range for phase transition. Though the extract reason for this change is not so clear, the widely accepted explanation for annealed waxy maize starch is that the thermal treatment increases the mobility of double-helical chain segments which improves the alignment of those chains. Because of the disruption of the less stable structures within both amorphous and crystalline regions, the more homogeneous and stable structure is formed (BeMiller & Huber, 2015).

3.2 Starch Pasting

Starch pasting was carried out in ARG2 Rheometer with a starch pasting cell. 2 g of Starch sample is mixed with 23 g of water (8% w/w). The temperature of pasting cell is increased from 25 ºC to 45 ºC at the rate of 15 ºC/min and the temperature is held at 45 ºC for 1 min. The temperature of the pasting cell was increased to the holding temperature at a rate of 15 ºC/min. The temperature

was then held constant for 2, 5, 10, 15, 30, 45 and 60 min, during which the starch solution sample was stirred at 16.75 rad/s by the paddle attached to the magnetic head. In order to collect valid measurement data point of G', the starch suspension has to form paste. The heating temperature therefore needs to equal or exceed the gelatinization temperature. As a result, the starting temperature for sample collection of WMS, NMS, WRS and NRS are 65℃, 70℃, 60℃ and 65℃ respectively.

3.3 Particle Size Distribution and calculation of volume fraction ϕ

2 g of starch paste from the sample was suspended in about 30 mL of DI water. The solution was mixed well in a vortex before size measurement to ensure good dispersion. Particle size measurement was carried out using a static light scattering with a Malvern Mastersizer 2000 with Hydro 2000MU (A) dispersing unit. Starch granules were modelled as spheres. The refractive index of starch and water are 1.53 and 1.33 respectively. The bulk density of starch was measured by the Tapped Density Tester (Agilent Technologies). $V_i\%$ is the volume percentage of granule with diameter d_i. Average volume of starch granules $\bar{V}(t)$ at different times i given by:

$$\bar{V}(t) = \sum_i \bar{\mathrm{v}}_i f(N_i) \tag{3-1}$$

Where $f(N_i)$ is the number fraction of granules in i^{th} interval which is related to volume fraction $f_{\mathrm{v}}(\mathrm{v}_i)$ and average granule volume $\bar{\mathrm{v}}_i$ in the interval via

$$f(N_i) = \frac{f_{\mathrm{v}}(\mathrm{v}_i)/\bar{\mathrm{v}}_i}{\sum_i f_{\mathrm{v}}(\mathrm{v}_i)/\bar{\mathrm{v}}_i} \tag{3-2}$$

Based on mass balance of starch inside the granule, the volume fraction $\phi(t)$ of swollen granule at time t is given by,

$$\phi(t) = \phi_0 \bar{V}(t) \tag{3-3}$$

Where the initial volume fraction ϕ_0 is related to the starch bulk density ρ_{bulk} by

$$\phi_0 = \frac{0.74w}{\bar{V}_0 \rho_{bulk}} \tag{3-4}$$

w being the weight fraction of starch suspension. In writing the above equation, it is assumed that the starch granules are close packed with a volume fraction of 0.74 during bulk density measurements.

3.4 Static Light Scattering

Sample was prepared by dissolving a gram of Waxy Maize Starch in 20 ml of 95% DMSO, with magnetic stirring for 3 days at room temperature. The sample was then precipitated with ethanol (60mL) and stored overnight at 4°C. The precipitate was filtered over a Whatman 2.5 μm ashless circle filter paper, washed successively with acetone (10ml), air- dried under a hood for a few hours to eliminate solvents, and finally dried in an oven at 60°C for 24hours. The dried sample was then dissolved in water at a concentration of 1.15 g/dm3.

The light scattering experiments were conducted at 25°C in a ALV CGS-3 compact Goniometer system with the angular ranges from 30-150° in 10 degree increment. It is in homodyne mode with full photon-counting detection using a ALV/LSE-5004 Light scattering Electronics and multiple Tau Digital correlator. The Berry Plot was generated in ALV/Static and Dynamic Fit and Plot Program The refractive index (dn/dc) was taken at 0.146 mL/g (White Jr, 1999). Optical alignment was checked over the angular range described using toluene. The sample was diluted by 10% each time with water to produce a concentration gradient from 1.15 g/dm3 to 0.55 g/dm3.

3.5 Porosity with X-Ray CT Scanning

X-Ray Micro CT (Microstructure) Skyscan 1272 X-ray Micro CT was used to perform scanning. Micro-computed tomography can be applied for visualization of the inner structure of starch granule. The image analysis is important in micro-CT to obtain quantitative parameters from scanned datasets. The analysis software CTAn developed by SkyScan is used to evaluate the porosity and porosity network. The quantitative measurement of porosity was based on binary images **Error! Reference source not found.** (b) and (c), which contain only black and white pixels, representing the solid and void space of selected particles. The while pixels are known as “object”, within which, CTAn can identify pores, represented as black pixels surrounded by the white ones. In CTAn, the binatization of images is done by thresholding. Segmented images are the result of this process.

Because of the small diameters of starch granules, they are packed densely in a plastic coffee stirrer straw to ensure that all the particles stay in place as the sample holder rotates slowly during the scanning **Error! Reference source not found.**(a). Image size is 162 W/H. Total of 137 images were taken where 137 are inside volume of interest. Pixel size is 1 μm. The threshold ranges from 47 to 200. Scanning lasts 6 hours. The main reconstruction is performed by NRECON software while INSTARecon software speeds up the process. Both software need to be open for fast reconstruction.

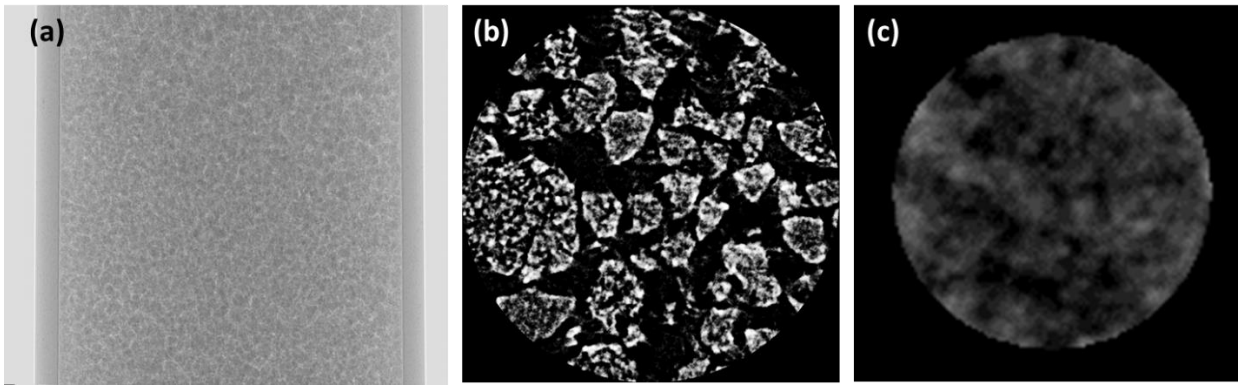

Figure 3.1: X-Ray CT Scanning (a) coronal view of the coffee stirrer straw packed with starch granules, (b) Region of Interest and (c) cross-section of starch granule where black and white picels represent the solid and void space, respectively

3.6 Bulk Density measurement

The bulk density, ρb, of granules was determined by the weight of granules filled into a 50 ml graduated cylinder. The graduated cylinder was tapped 2000 times using Agilent Technologies Tapped Density Tester. The bulk density is calculated by using the weight of the sample divided by the volume after tapping.

3.7 G’ and G’’ measurement

The amplitude range ensured the complex modulus G* is constant, i.e. where stress and strain waves are set at such low values that stress is proportional to strain. The viscoelasticity measured in such region is linear. The rheological parameters used to evaluate the dynamic mechanical behaviour of starch paste were the storage or elastic modulus (G’) and loss/viscous mudulus (G’’).

In the Small Amplitude Oscillatory Shear (SAOS) Experiment, oscillatory shear mechanical measurements were employed to determine the frequency-dependent G'and G'' moduli in the linear response regime. Starch pasted as described in the previous section was transferred immediately to the 40mm parallel plate on DHR3 rheometer with 1mm measuring gap. The paste was subjected to 0.01 strain at 40°C controlled environment. The frequency sweep was performed from 0.01 to 10 Hz.

3.8 Yield stress and apparent viscosity measurement

Yield stress is a material property defined as the stress at which a material begins to deform. In other word, once the applied stress is greater than the yield stress, the paste begins to flow. Apparent viscosity was measured through flow sweep where the shear rate was set to vary between 0.01 to 10 /s. The apparent viscosity was then plotted against the shear stress. Yield stress is the stress at which the apparent viscosity asymptotically approaches infinity.

3.9 Hardness of granules

Hardness of the granule was also measured on DHR3 Rheometerm equiped with a 40 mm Peltier plate cartridge immediately after pasting. The starting gap was 1mm, which ensured the force at the beginning of measurement is negligible. The sample was trimmed to fit right at the plate edge. The sample was first subjected to a shear at the rate of 5/s for 30s and was equalibrated for 60s. The upper plate was then lowered at 5um/s speed to reach the final gap of 10 µm (for rice starch) and 15 µm (for maize starch) , after which the sample was subjected to 0.01% shear strain and its stress relaxation was monitored for 3 min . All measurements were carried out at 40 ºC. The final gap between the plates was less than the average granule size of starch subjected to 65 C for 5 min. This ensured that only one layer of starch granule can fit under the gap. The force required to indent the gel to the final gap size is directly related to the deformation/hardness of a single layer of starch granules.

3.10 Preparation of cross-linked native maize starch with STMP

Cross-linked starches were prepared according to the method of Woo and Seib (Woo & Seib, 2002). Corn starch (50 g) was mixed with different amounts (0.1 and 0.2% (w/w), based on dry weight

of starch) of STMP and dissolved in 75 mL water, which were designated as Crosslink 1 and Crosslink 2, respectively. After the pH was adjusted to 11.5 with 0.1 N NaOH, the slurry was mixed at 30 C for 5 h using a magnetic stirrer. The suspensions were neutralized to pH 5.5±0.5 with 0.1 N HCl, washed with distilled water four times, and air dried at room temperature for 24 hours. The dried samples were then grounded in a mortar and sieved (200 mesh sifter). The starch subjected to the cross-linking condition without STMP was used as a control in each experiment.

3.11 Cryo- SEM

The microstructure of WMS was observed using Cryo-Scanning Electron Microscopy technique in the GATANAlto 2500 cryo system (FANNON & BEMILLER, 1992). After the pasting process, small amount of starch paste was taken and dispersed in 35 mL of water. The dispersed samples were centrifuged at 2000g (4358 RPM) for 20 min. Supernatant was removed and water was added into the tube to make it 35 mL. This process was repeated for three times. The starch paste sediment was then dispersed in 3 mL of water and vortex evenly. The control sample is un-heated WMS powder dissolved in 3 mL of water. A droplet of the sample was placed in the flat plate cryo holder and plunged into liquid nitrogen at 190˚ C. Sample was sublimated at 90 C for about 10 min. The sublimated sample was then sputter coated for 2 min with platinum to minimize charge build-up, and transferred to SEM cryo-stage at 150˚ C for imaging. The cryo sample was observed using an ETD (Everhart- Thornley) detector at a 5-Kv accelerating voltage.

CHAPTER 4. CHARACTERIZATION OF SWELLING BEHAVIOR OF MAIZE AND RICE STARCHES

4.1 Pasting properties for all starches

The RVA result (Figure 4.1) shows that both NRS and NMS have pasting curve similar to the typical measurement in Figure 2.1. However, because of the thermal treatment done on the Novation® starch, the peak viscosity temperatures are much higher. For WRS, the viscosity reaches the peak around 95°C, whereas the viscosity WMS keeps going up throughout the entire viscosity profile.

Table 4.1: Properties and functionality of selected starch

	Novation 2300	Melojel	Novation 8300	PenPure 30
Amylose%	1-2	27	1-2	20-25
Avg. Particle Size (μm)	12-14	10-11	6-7	4-5
Functionality	Function like modified starch; Resistant to high T, high shear or low pH	Strong gel formed after cooling a cooked dispersion.	Excellent freeze/ thaw stability Resistant to high T, high shear or low pH	High viscosity, water-holding capacity and binding ability firm consistency, crispness and smooth texture

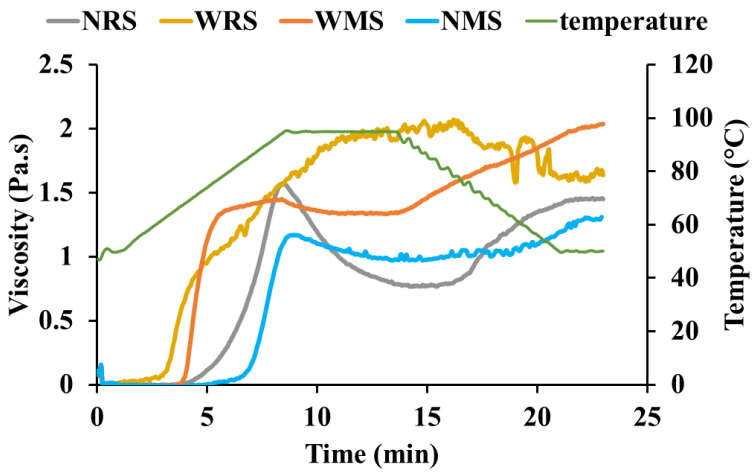

Figure 4.1: Plots of observed apparent viscosity versus time for normal rice starch, waxy rice starch, waxy maize starch and normal maize starch using data from RVA at 6% w/w.

4.2 Granule size distribution for waxy maize starch

Granule size distribution for waxy maize starch as a plot of number density vs granule size at different times of exposure at 65, 70, 75, 80, 85 and 90°C are given in Figure 4.2. It can be observed from the graphs that with increase in hold time the distribution shifts to the right, while the number density of lower particle size decreases. The increase of higher particle size indicates the swelling increases with holding time. The shift of size distribution curve at 2 minutes hold time is significant from 1-minute hold time particles, whereas the change is very minor in the following holding times.

It is also shown that for all hold times, the increase in temperature is always associated with a decrease in number density of lower particle size and an increase for higher particle size. This, again, indicates that swelling increases with temperature. The volume fraction vs time at different temperatures is shown in Figure 4.3. At all temperatures there is a sudden increase in volume fraction from 0 minutes to 5 minutes. Subsequent increase in granule size with time is found to be slower and the granule size approaches an equilibrium at longer times (after 45 min). As expected, swelling was more at higher temperature with a larger granule size at longer times.

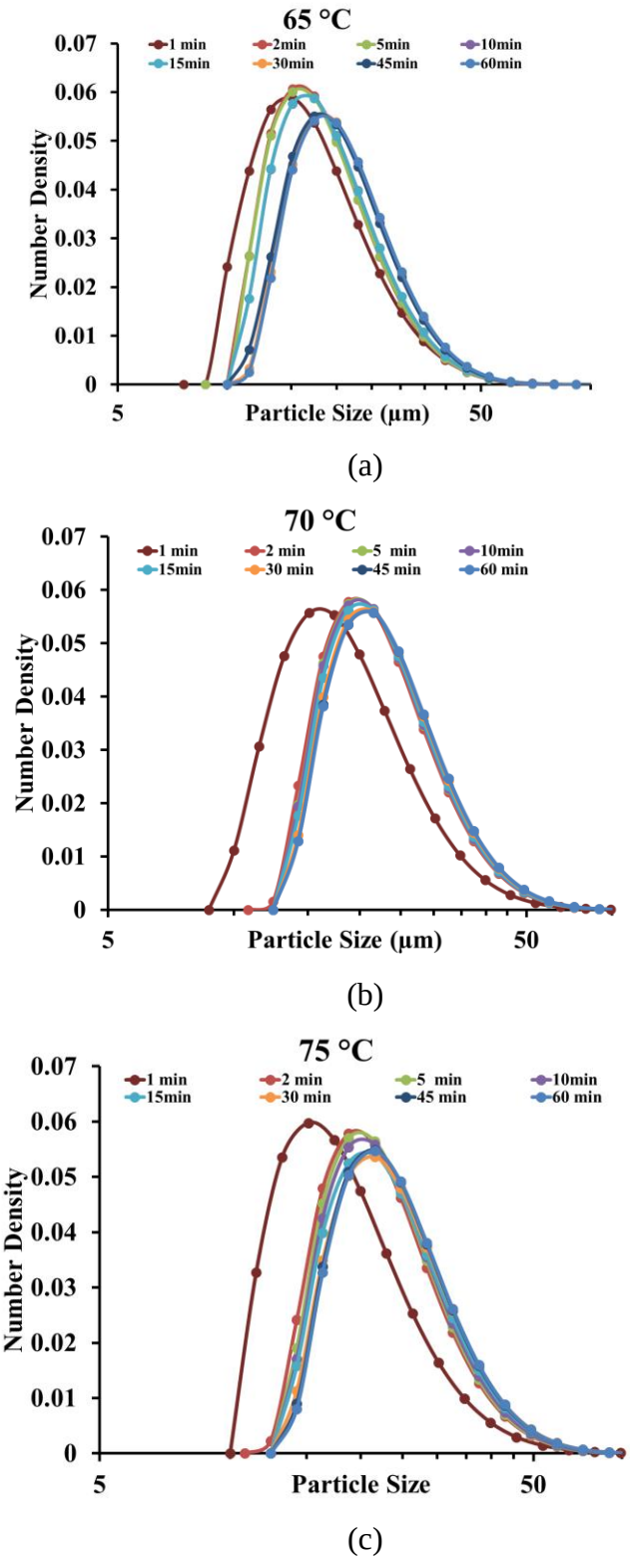

Figure 4.2: Size distribution of waxy maize starch heated at (a) 65°C, (b) 70°C, (c) 75°C, (d) 80°C**,** (e) 85°C and (f) 90°C for 1, 2, 5, 10, 15, 30, 45 and 60 min

Figure 4.2 continued

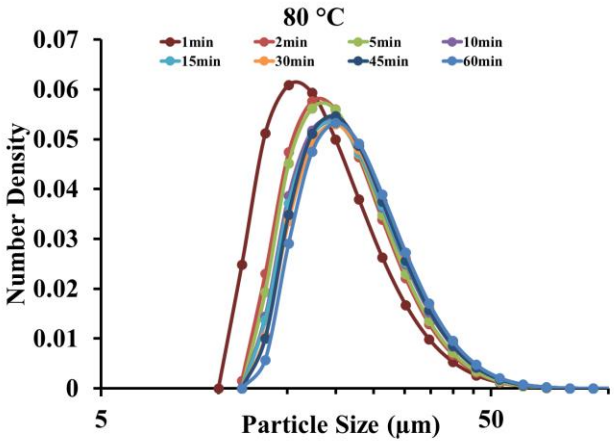

(d)

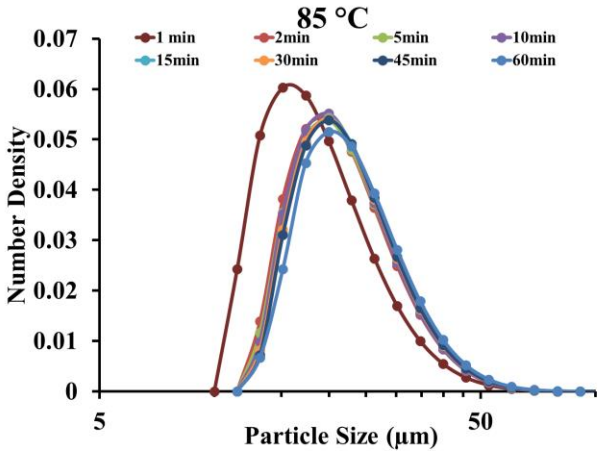

(e)

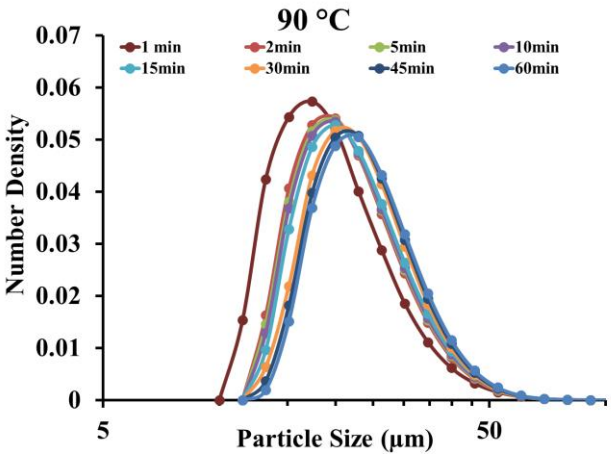

(f)

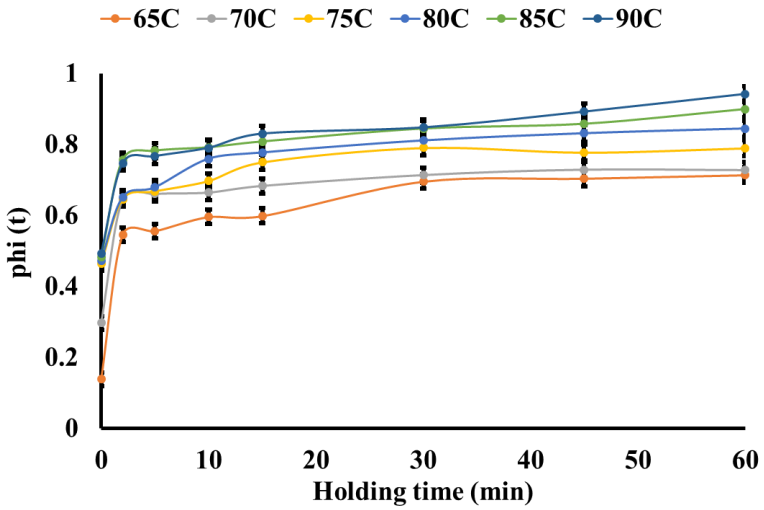

Figure 4.3: Volume fraction of 8 % w/w suspension of waxy maize starch versus holding time at different temperatures

4.3 Granule size distribution for normal maize starch

One can learn from Figure 4.1 that normal maize has a smaller peak viscosity compare to waxy maize starch and the gelatinization temperature is higher. Therefore, the starch paste sample was collected starting at 70°C. Similar to the waxy maize starch, the size distribution for normal maize starch shows the same trend at 70°C and 75°C Figure 4.4 (a) and (b). However, when temperature increased to 80°C, those granules being held for longer time (45 min and 60 min) ruptured and the size distribution shift to the smaller end. The volume fraction has slight decrease because there are still granules undergo swelling Figure 4.5. At 90°C, the size distribution is irregular at short hold time (5 min) and the volume fraction starts to decrease after 5min..

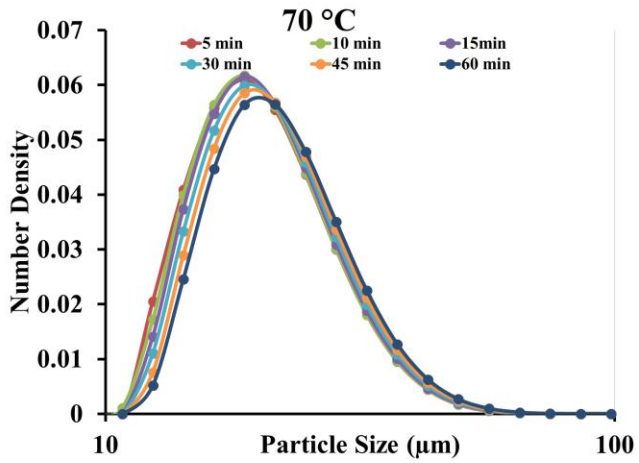

(a)

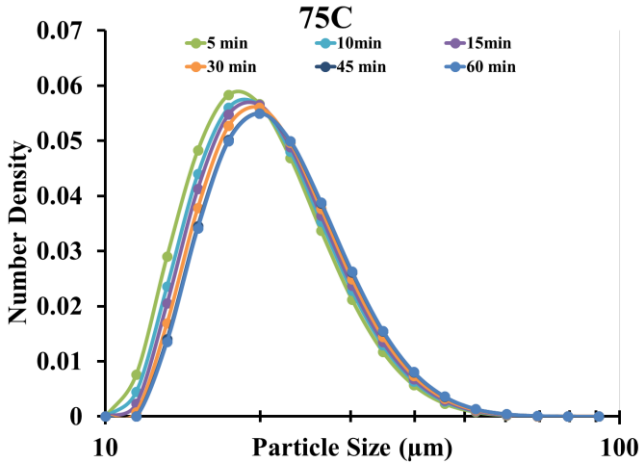

(b)

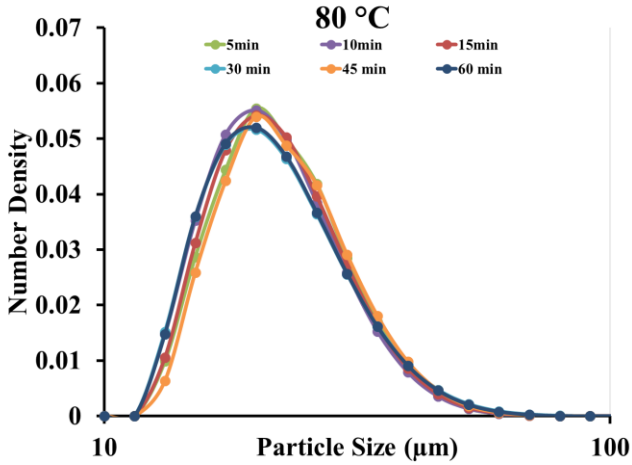

(c)

Figure 4.4: Size distribution of normal maize starch heated at (a) 70°C, (b) 75°C, (c) 80°C, (d) 85°C and (e) 90°C for 1, 2, 5, 10, 15, 30, 45 and 60 min

Figure 4.4 continued

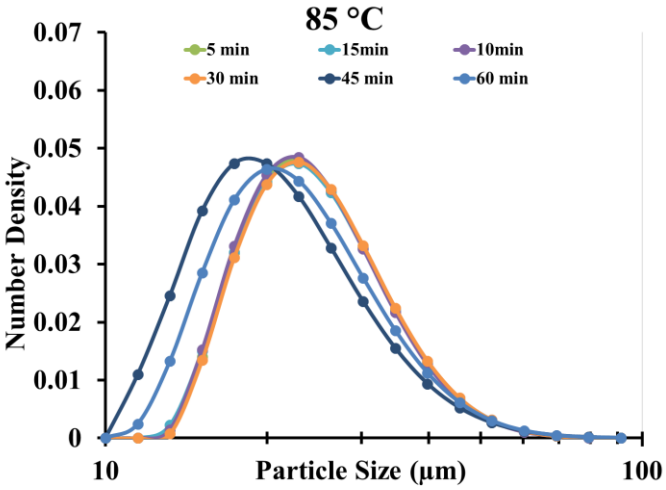

(d)

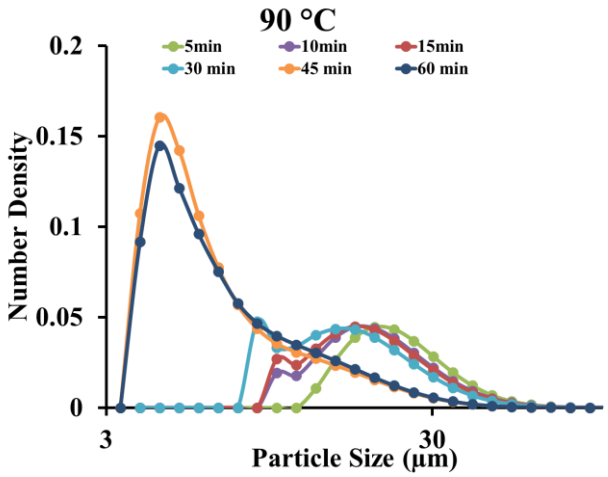

(e)

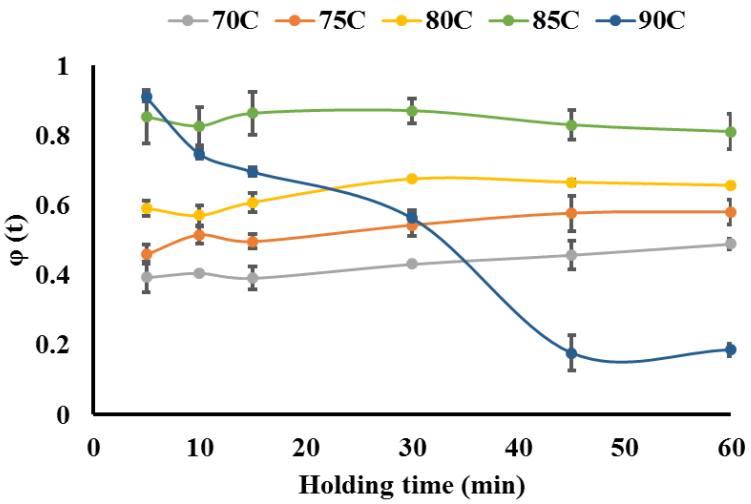

Figure 4.5: Volume fraction of 8 % w/w suspension of normal maize starch versus holding time at different temperatures.

4.4 Granule size distribution for waxy rice starch

When heated to different temperatures, the size distribution of waxy, regular and cross linked starch granules shift to larger sizes with time due to swelling as reported in our previous papers (Desam, Li, Chen, Campanella, & Narsimhan, 2018b). The volume fraction of starch granules was obtained from the number density as described in the methods section. Bulk density of WMS and NMS are 0.6909 and 0.5017 g/mL, respectively. The volume fraction of waxy rice starch increased over temperature at all hold times. A rapid increase in the starch volume fraction was observed in the first five minutes of heating at all temperatures. Subsequent increase in the starch volume fraction with time was found to be slower and it approached an equilibrium at longer times (after 45 min). Even at 90°C, the starch granules can remain intact. Therefore, the size distribution for 90°C is the largest among all. Waxy rice starch also has wider range of volume fraction and average granule sizes compared to waxy maize and normal maize starch. Swelling is more drastic in rice starch.

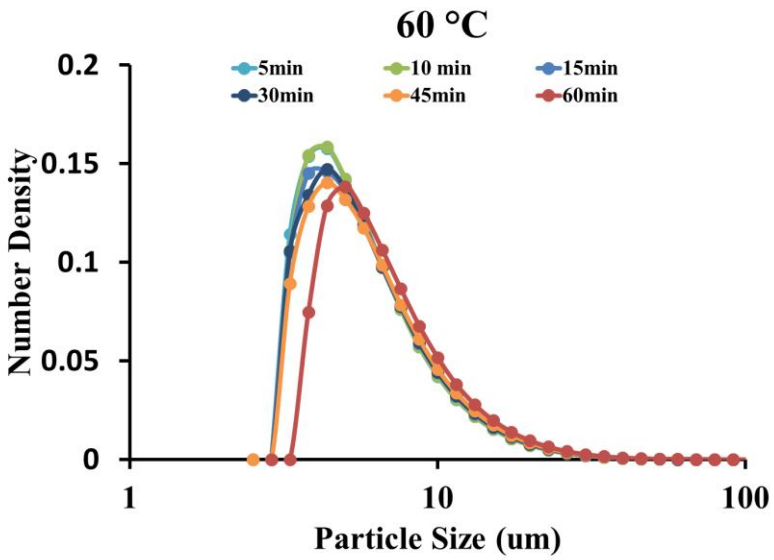

(a)

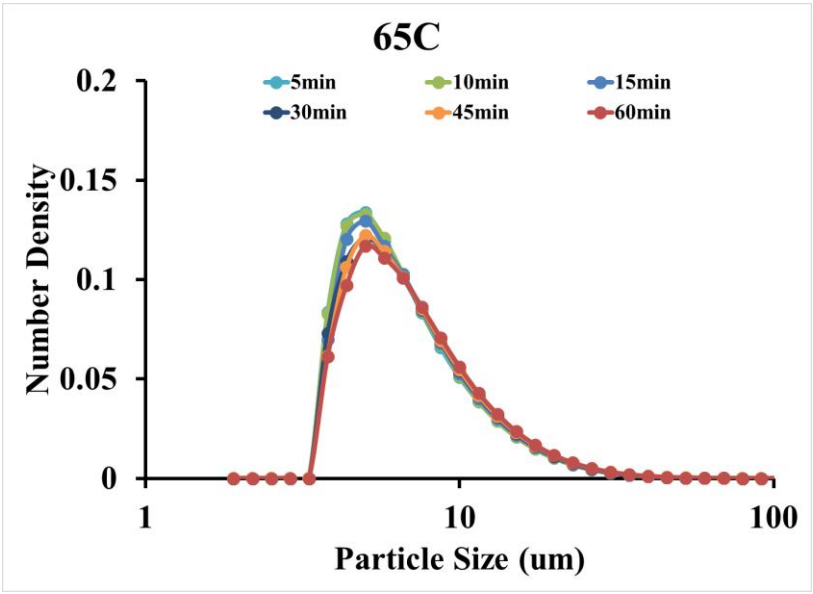

(b)

Figure 4.6: Size distribution of waxy rice starch heated at (a) 60°C, (b) 65°C, (c) 70°C, (d) 75°C, (e) 80°C, (f) 85°C and (g) 90°C for 5, 10, 15, 30, 45 and 60 min

Figure 4.6 continued

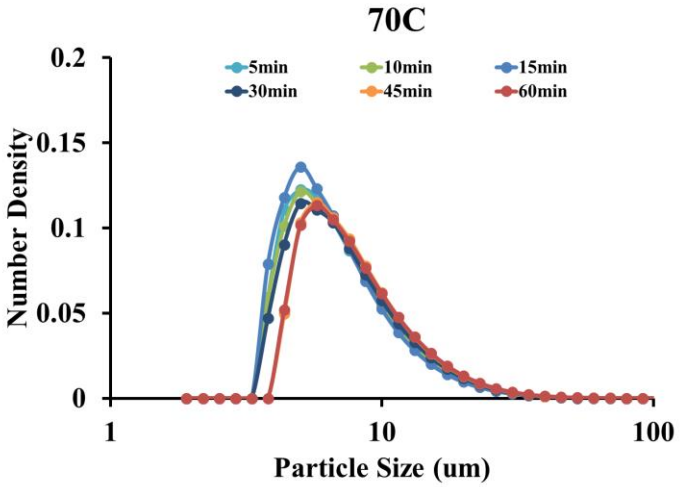

(c)

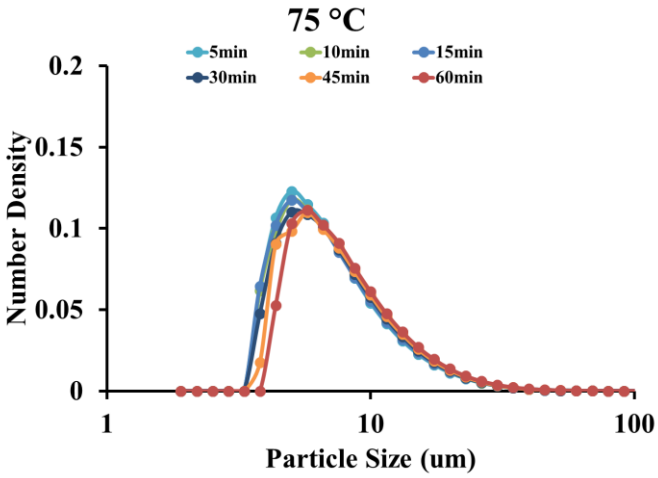

(d)

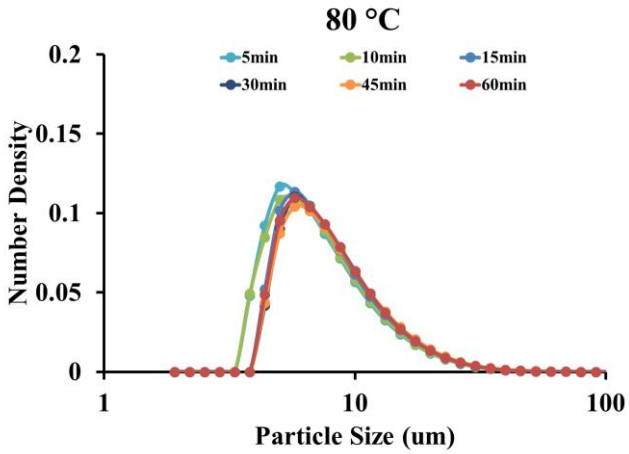

(e)

Figure 4.6 continued

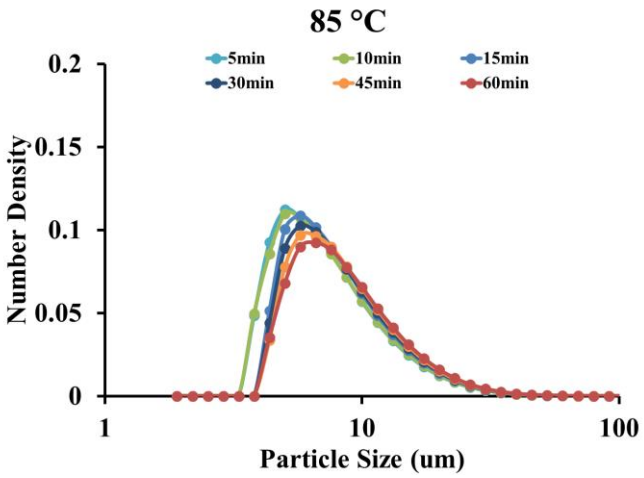

(f)

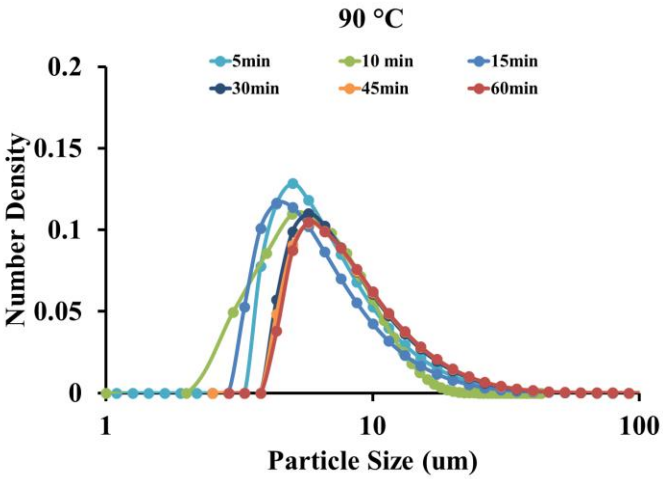

(g)

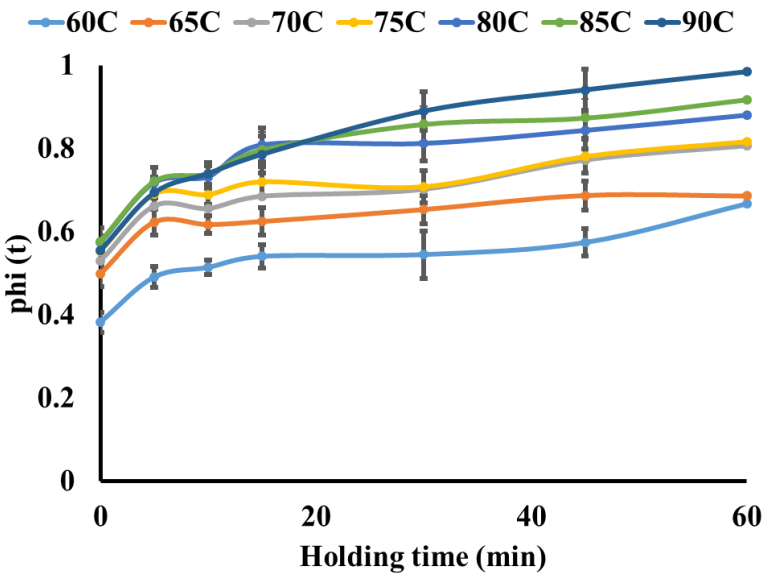

Figure 4.7: Volume fraction of 8 % w/w suspension of Waxy Rice Starch versus holding time at different temperatures.

4.5 Granule size distribution for normal rice starch

For normal rice starch, although the average size of granules heated for 60 min for all temperature is the highest (Figure 4.9), the size distribution of 60 min seem to shift to the left hand side of the 45 min. Polydispersity is lower than maize starches, indicating that rice starch swells at a relatively slow rate.

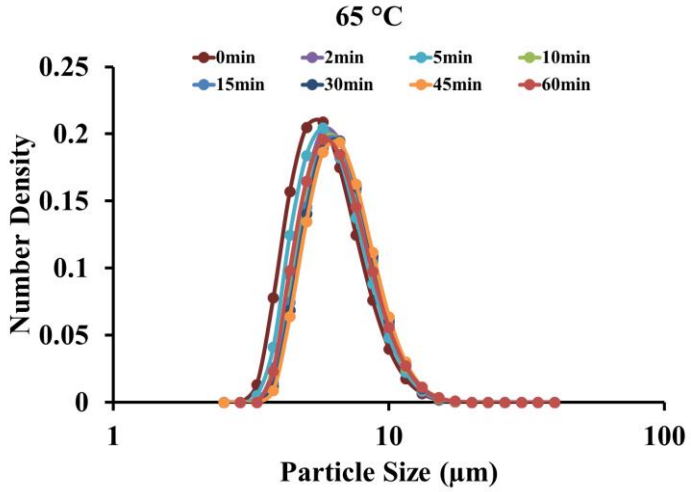

(a)

Figure 4.8: Size distribution of normal maize starch heated at (a) 65°C, (b) 70°C, (c) 75°C, (d) 80°C, and (e) 85°C for 1, 2, 5, 10, 15, 30, 45 and 60 min

Figure 4.8 continued

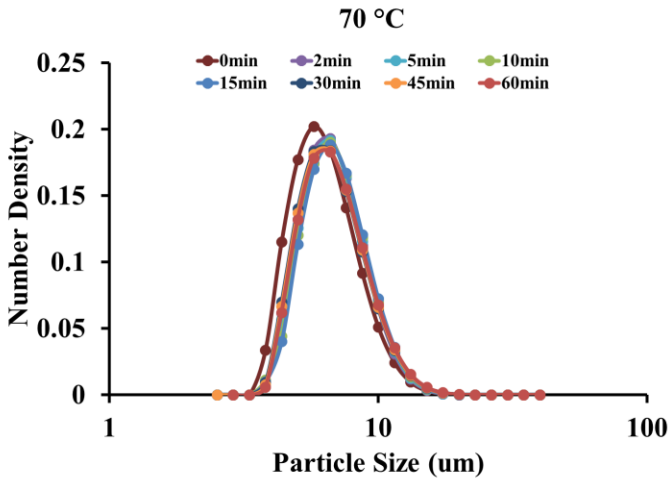

(b)

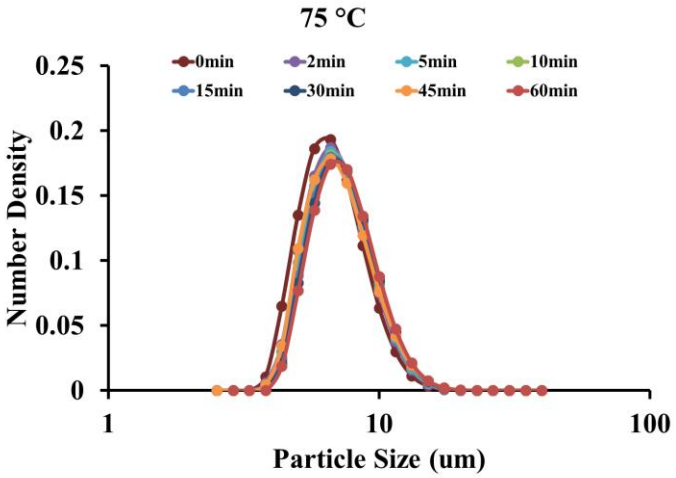

(c)

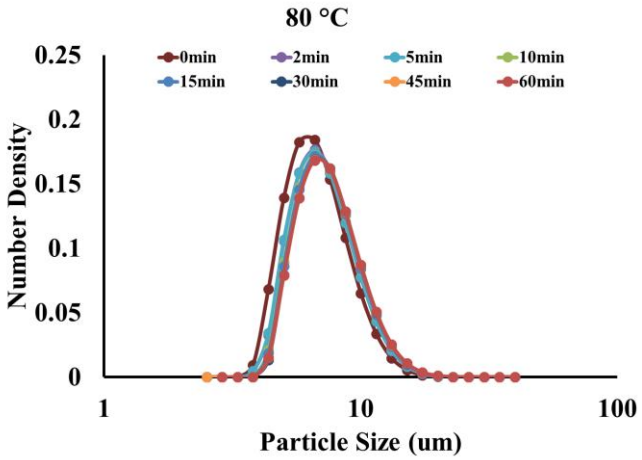

(d)

Figure 4.8 continued

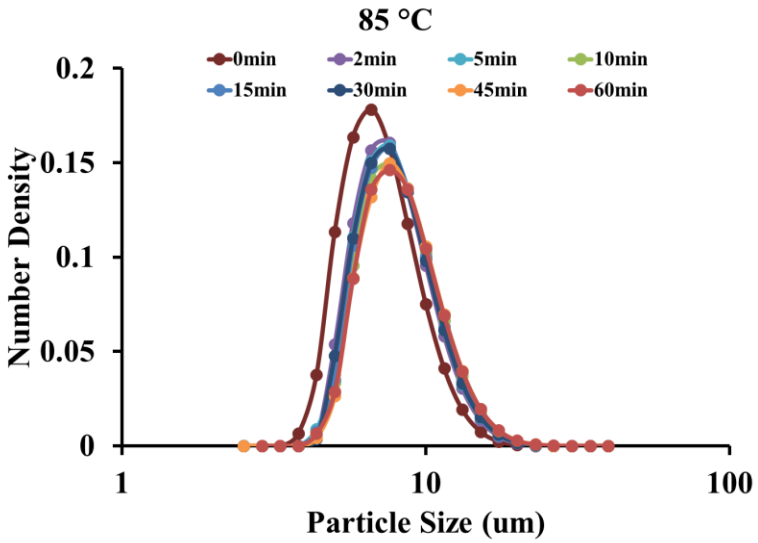

(e)

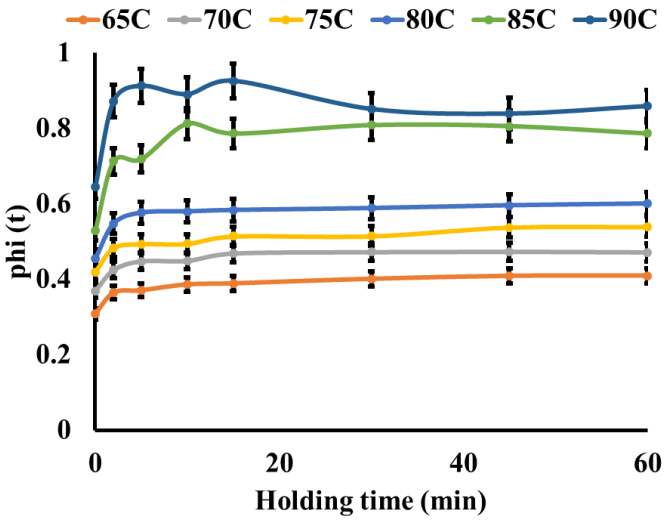

Figure 4.9: Volume fraction of 8 % w/w suspension of normal rice starch versus holding time at different temperatures.

4.6 Granule size distribution for STMP Cross-linked normal maize starch

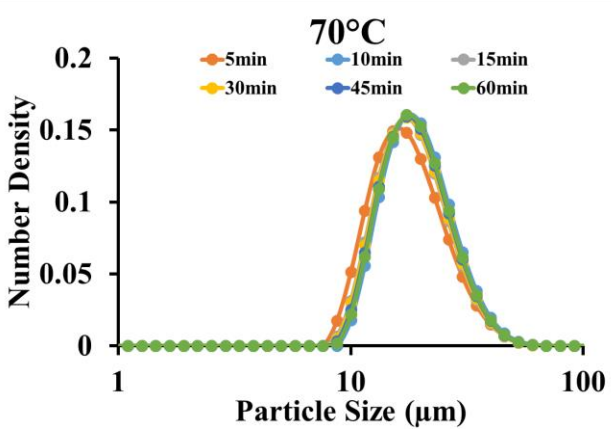

(a)

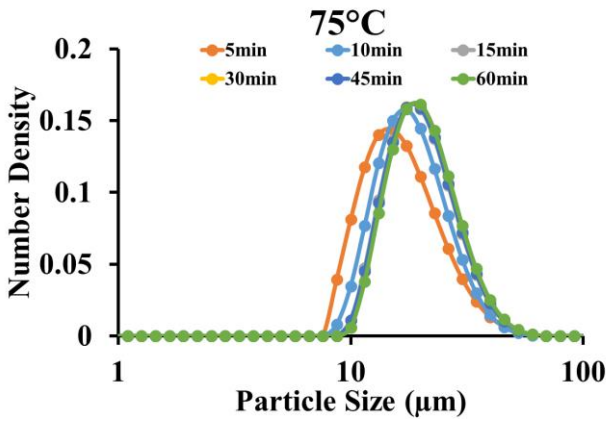

(b)

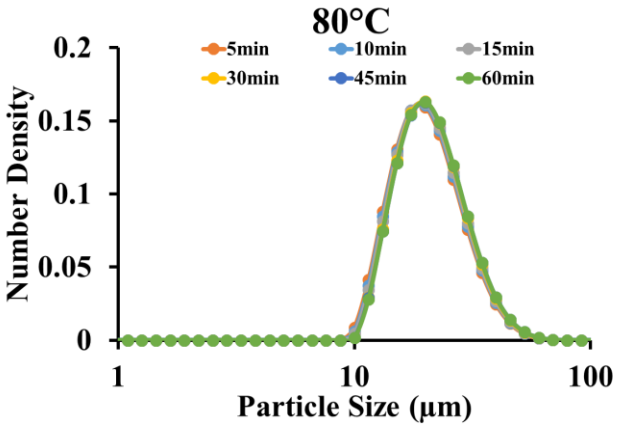

(c)

Figure 4.10: Size distribution of 0.1% STMP cross-linked normal maize starch heated at (a) 70°C, (b) 75°C, (c) 80°C, (d) 85°C, (e) 90°C and (f) 95°C for 5, 10, 15, 30, 45 and 60 min

Figure 4.10 continued

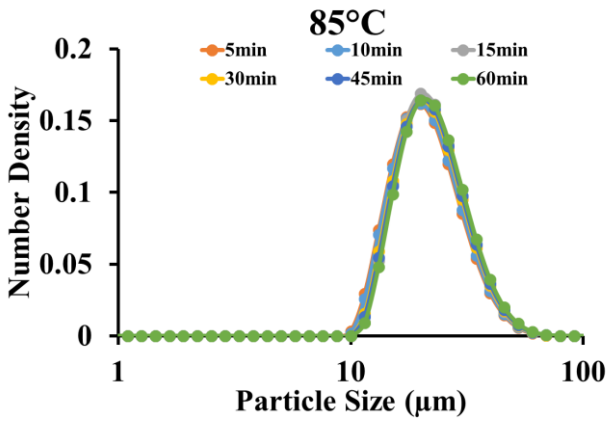

(d)

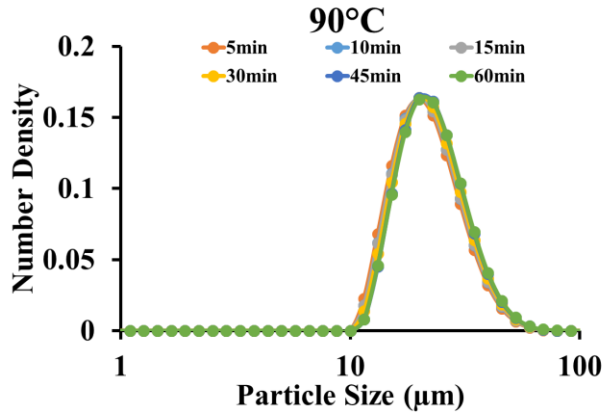

(e)

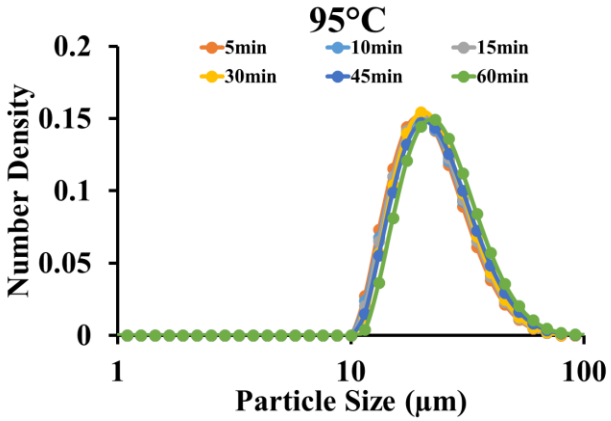

(f)

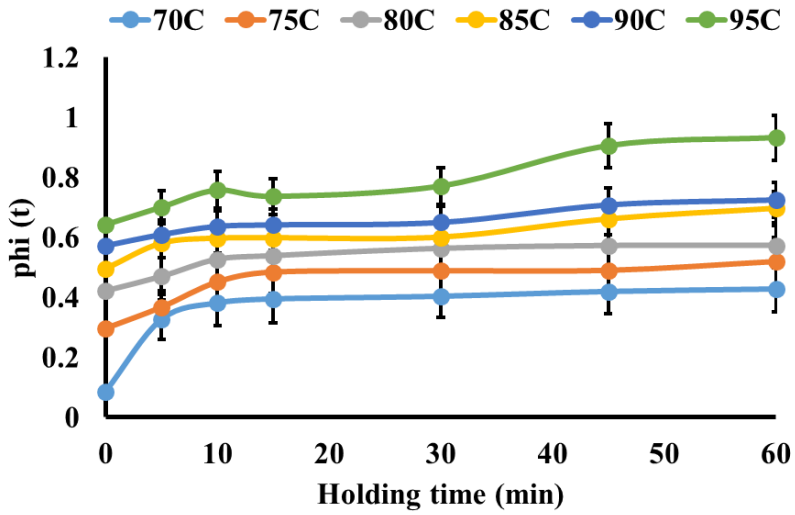

Figure 4.11: Volume fraction of 8 % w/w suspension of 0.1% STMP cross-linked normal maize starch versus holding time at different temperatures.

4.7 Light scattering of starch

Berry plot of static light scattering for waxy maize starch and normal maize starch in water at 25 C is shown in Figure 4.12 and Figure 4.13 . Starch sample for light scattering measurement was prepared as explained in methods section. The starch concentration range for these measurements is from 0.55 to 0.8383 g/dm^3. The inferred values from the Berry plot using the following equation:

$$\left(\frac{KC}{R_\theta}\right)^{1/2} = \left(\frac{1}{M_w}\right)^{1/2}\left(1+\frac{1}{6}q^2R_g^2\right) + A_2M_wC$$

q the scattering vector for vertically polarized light is denoted by $q = \frac{4\pi n_0 \sin(\theta/2)}{\lambda}$.

M_w= 1.477×10^7 (±7 %) g/mol; R_g= 1.562×10^2 (±3.2 ×10^{-13} %) nm, A_2= 2.762×10^{-8} (±12.6 %) mol dm^3/g^2. The Flory Huggins χ parameter is inferred from the second virial coefficient using

$$\left(\frac{1}{2}-\chi\right) = A_2\frac{\bar{v}_1}{\bar{v}_2^{\,2}} \qquad (1)$$

where $\bar{v}_1$ is the molar volume of solvent and $\bar{v}_2$ is the partial specific volume of waxy maize starch.

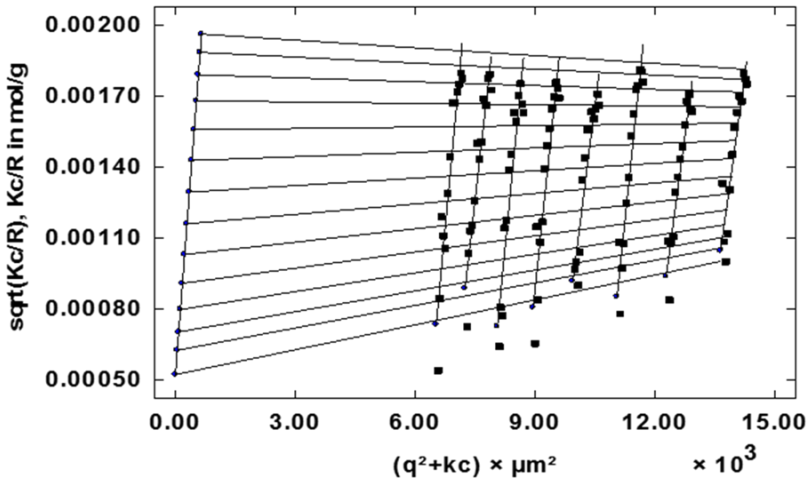

Figure 4.12: Berry plot obtained for the waxy maize starch dissolved in aqueous medium at 25°C.

Different vertical lines refer to different concentrations in the range of 1.15 to 0.55 g/dm^3 with 10% dilutions (the right most is the highest concentration) and different horizontal lines refer to different angles in the range of 30 to 150° with 10° increments (with top most referring to 150°C). The bottom most and left most refer to the extrapolated zero angle and zero concentrations respectively.

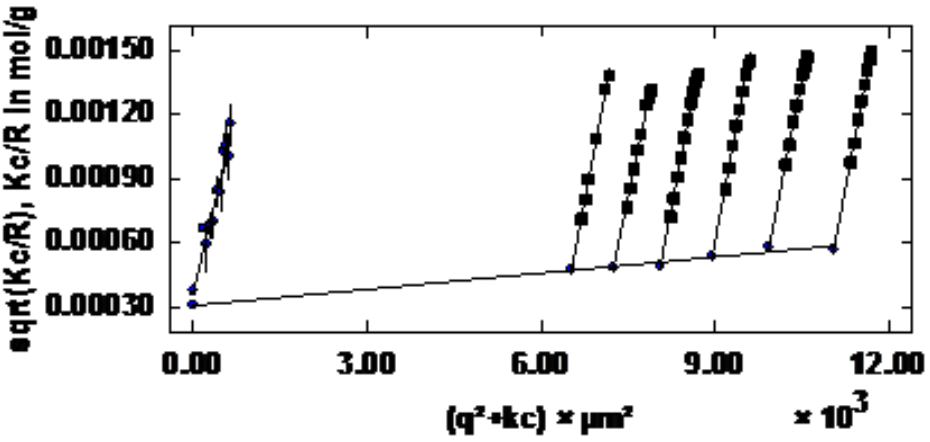

Figure 4.13: Berry plot obtained for the normal maize starch dissolved in aqueous medium at 25°C. Different vertical lines refer to different concentrations and different horizontal lines refer to different angles in the range of 30 to 150 ° with 10 ° increments (with top most referring to 150°)

4.8 Morphology of Starch Granules

Photomicrographs of starch granules at 25°C, 60°C, 75°C and 90°C at 2 min of exposure are shown in Figure 4.14 (a)-(d), respectively. The size of starch granules are much larger at 75°C compared to 60°C, while the difference between 75°C and 90°C are minor. One can also see that for this particular kind of waxy maize starch, the granules remain intact even heated to as high as 90°C. This evidence confirmed that temperature range from 60°C to 90°C is valid for the swelling kinetic model where breakage was not considered. Increase in granule size from 2 min to 10 min of heating can be clearly observed at both temperatures, but more prominent at 65°C (Figure 4.15).

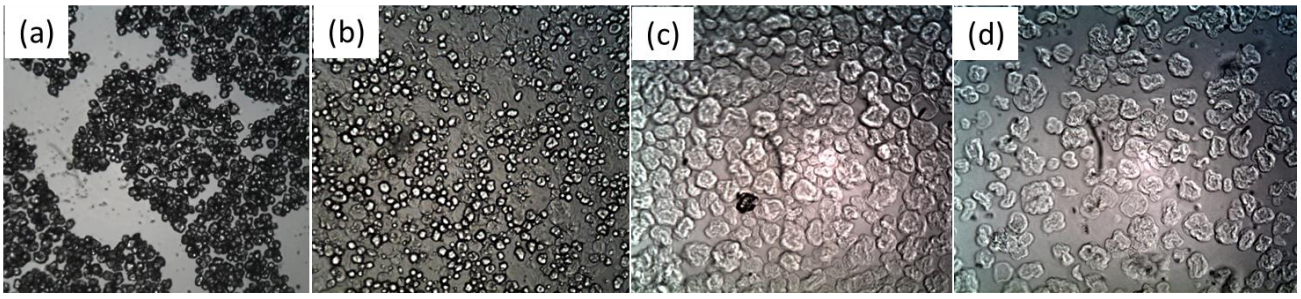

Figure 4.14: Photomicrographs for waxy maize starch granules at (a) 25°C, (b) 60°C. (c) 75°C and (d) 90°C indicate that majority of swelling occurs between 60°C and 75°C. Starch granules remain intact when heated as high as 90°C.

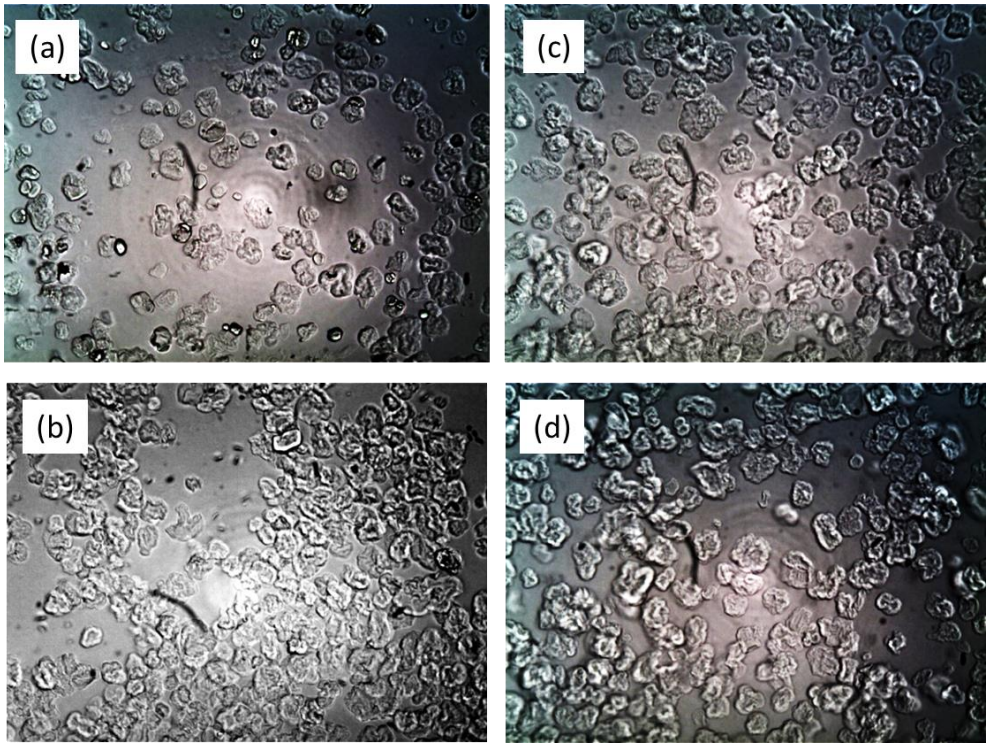

Figure 4.15: Photomicrographs for waxy maize starch granules at (a) 65°C for 2 min, (b) 65°C 10min, (c) 85°C for 2 min and (d) 85°C for 10min

Cryo images of starch granule at 65 and 85°C at 2 min and 10 min of heating are shown in Figs. 4a and 4b respectively. The unswollen starch particles have a smooth surface and appear in a spherical shape with some granules having faceted sides (Figure 4.16 a). The granules with open structure seem to stick together, whereas the closed ones with intact surface are freely suspended in the solution. At 65°C, starch granules undergo incomplete swelling at 2 min, whereas at 10 min, most of the surface seems to be porous (Figure 4.17). When the temperature was raised to 85°C, granules are completely swollen even at 2 min. Due to rapid and uneven heating at 85°C, some area of the granule might be exposed more to heat and therefore swell faster than the rest of the surface. This might be the cause to the wrinkles appear on the starch granule surface. This phenomenon was amplified at longer heating time at 85°C.

The cryo-SEM images of WRS at 85°C and 90°C show that granules remain intact at both temperature (Figure 4.18 and Figure 4.19). However, there are fewer intact NRS granules at 85 °C and almost none at 90 °C. The same phenomenon can be seen in cryo-SEM images of WMS

(Desam, Li, Chen, Campanella, & Narsimhan, 2018a) and NMS (Desam et. al., 2018b). This evidence can also support the hypothesis that granule became softer at higher temperature as they lose their structure.

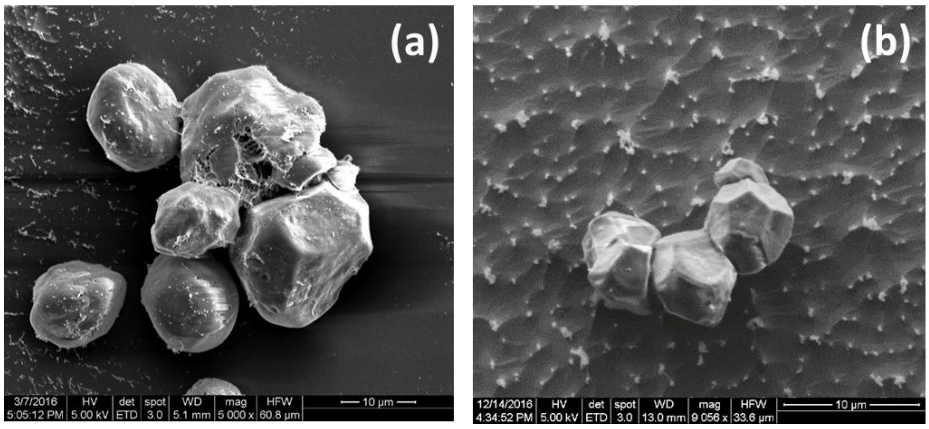

Figure 4.16: SEM images of a) waxy maize starch (× 5000) and b) waxy rice starch (× 9,056) at 25 °C

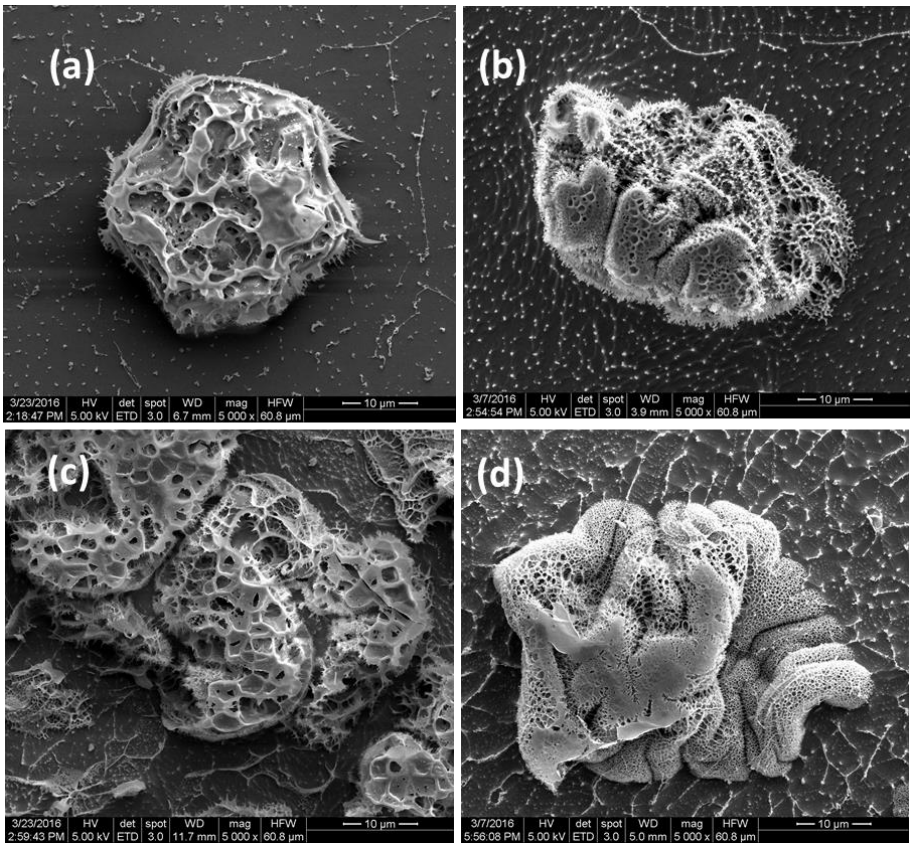

Figure 4.17: SEM image of waxy maize starch granules a) 65°C and 2 min, b) 85°C and 2 min, c) 65°C and 10 min, d) 85°C and 10 min

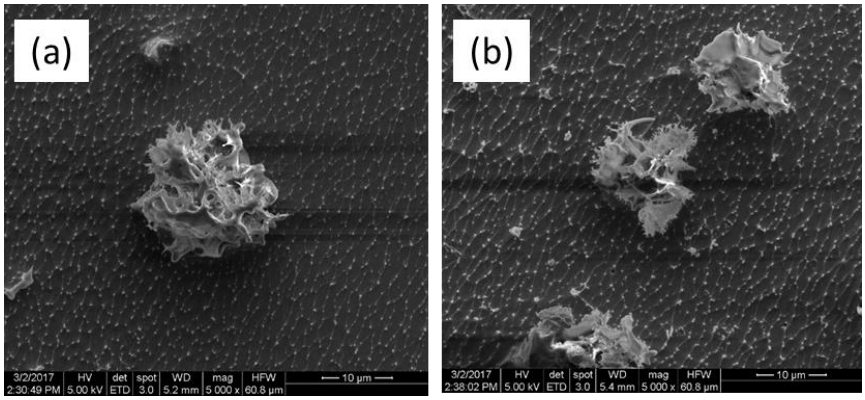

Figure 4.18: Cryo-SEM image of Waxy Rice Starch at room temperature As temperature increased to 85C and was held for 10 min, the facets became less defined and structure became more open (a). As it was held for 10 min, the starch granules still remian intact (b).

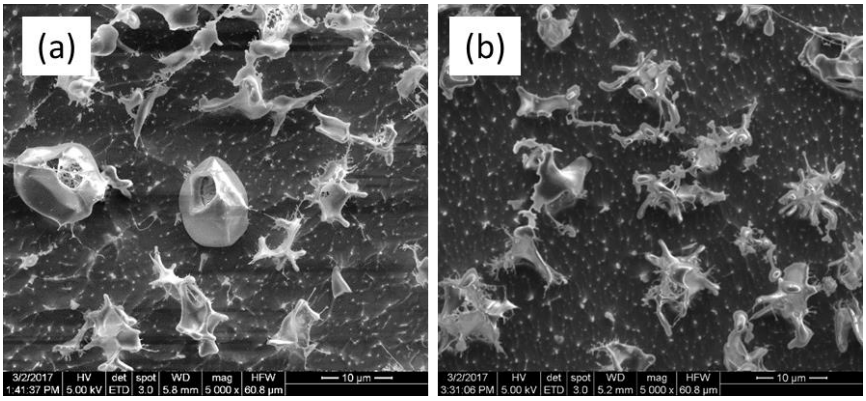

Figure 4.19: Cryo-SEM images of Normal Rice Starch at room temperature As temperature increased to 85ºC and was held for 10 min, the facets became less defined and structure became more open (a). At 90ºC and 10 min holding time, majority of the granules last their inregrity (b)

CHAPTER 5. CHARACTERIZATION OF PASTING BEHAVIORS OF CROSS-LINKED AND NATIVE MAIZE AND RICE STARCH

G’ and G” vs frequency (in the range of 0.01 to 10 Hz) for waxy maize starch at different temperatures and times are shown in Figure 5.1. G’ and G” increased with frequency. G’ is much greater than G” (Figure 5.2) indicating thereby that the elastic component of viscoelastic starch paste is more predominant than the viscous component. Therefore, only the evolution of G’ upon heating for maize and rice starch suspension is reported in this study.

5.1 G’ vs ω at different T and time for waxy maize (G” plots for a few cases)

G’ for waxy maize at 2 min and 5 min hold time increases as the temperature increases as can be seen from Figure 5.1. Also, by comparing the values at 2 min and 5 min, one can see that at 65°C, 70°C, 75°C and 80°C, G’ increases as hold time increases. For times greater than 10 min, the difference between G’ at different temperature becomes smaller because the extended hold time makes the starch granule more deformable at higher temperature and more swollen at lower temperature. Starting from 10 min, the G’ at 85°C and 90°C almost overlap. At 30 min, G’ is the highest at 80°C, with the values at 85°C and 90°C being lower. At holding time of 60 min, G’ decreased with temperature with the value at 65°C being the highest, Such a behavior is believed to be due to the opposite effects of swelling and softening of granules on G’. Swelling increases G’ as a result of an increase in the volume fraction of granules in the suspension. Softening of granules, on the other hand, results in a decrease in G’ because of the deformability of granule which enable them to pack more efficiently at higher volume fraction. At sufficiently large holding times, the latter effect is predominant thereby leading to a decrease in G’ with temperature. At smaller holding times, the former effect (swelling) is predominant thus leading to an increase in G’ with temperature as shown in Figure 5.1 (a)-(c). At intermediate holding times, however, the effect of temperature would depend on the relative magnitudes of the two effects as can be seen in Figure 5.1 (e)-(g).

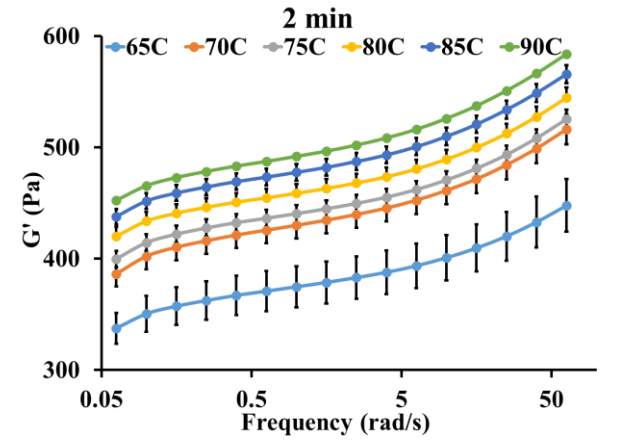

(a)

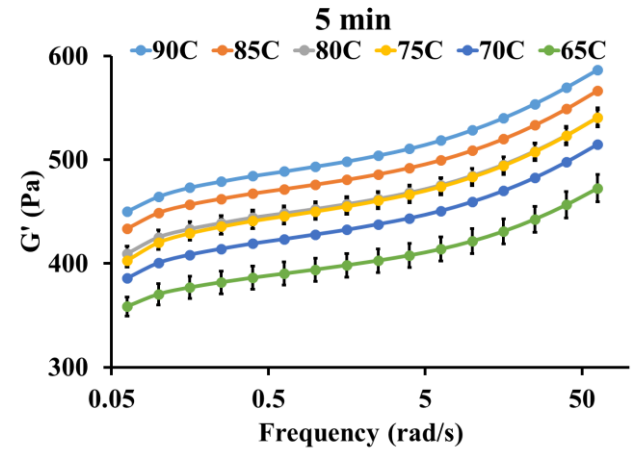

(b)

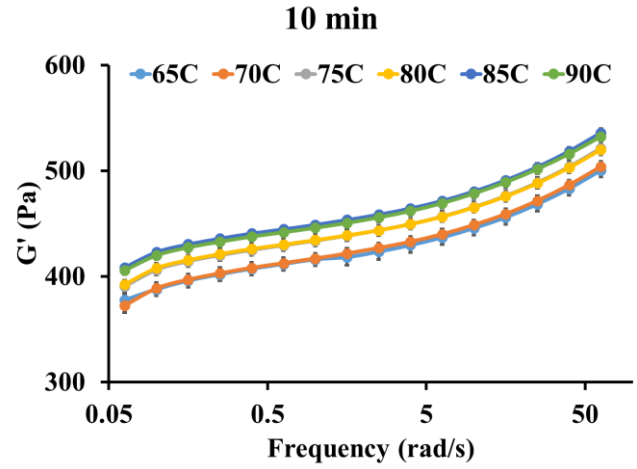

(c)

Figure 5.1: Storage modulus of waxy maize starch heated for (a) 2min, (b) 5 min, (c) 10 min, (d) 15 min, (e) 30 min, (f) 45 min and (g) 60 min at 65°C, 70°C, 75°C, 80°C, 85°C and 90°C.

Figure 5.1 continued

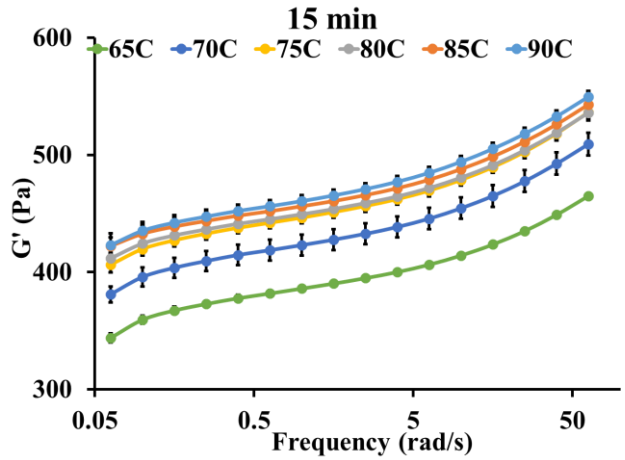

(d)

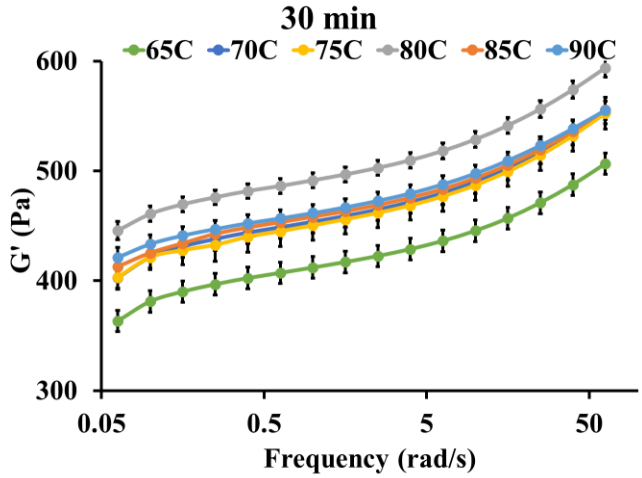

(e)

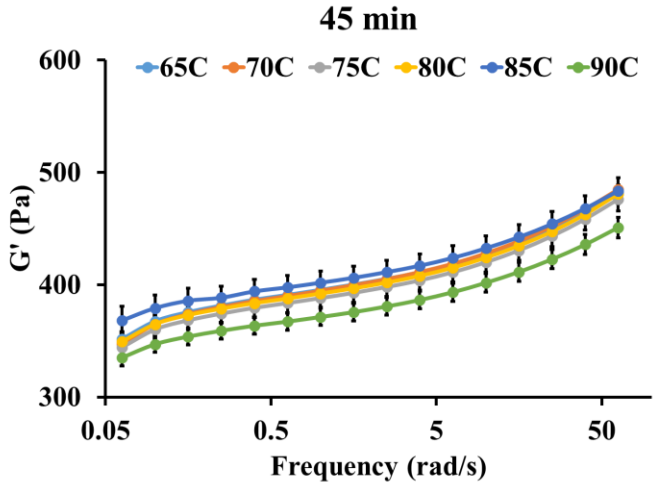

(f)

Figure 5.1 continued

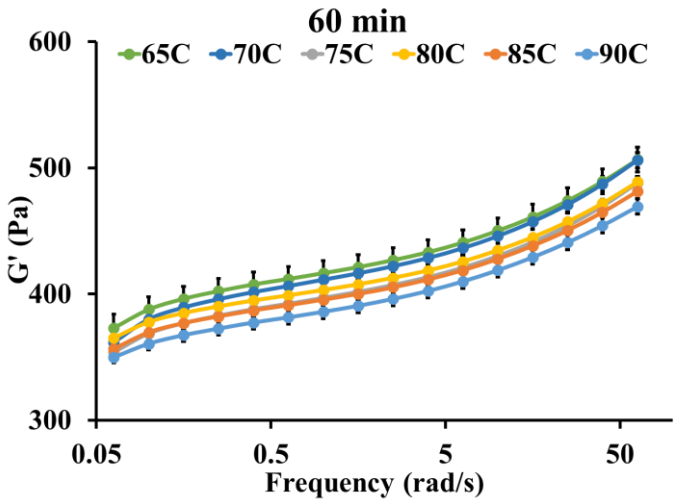

(g)

As can be seen from Figs. , G" increases with frequency exhibiting a shallow minimum at a frequency of around 0.2 rad/s. Since G" is much smaller than G', we focus our discussion only on G'.

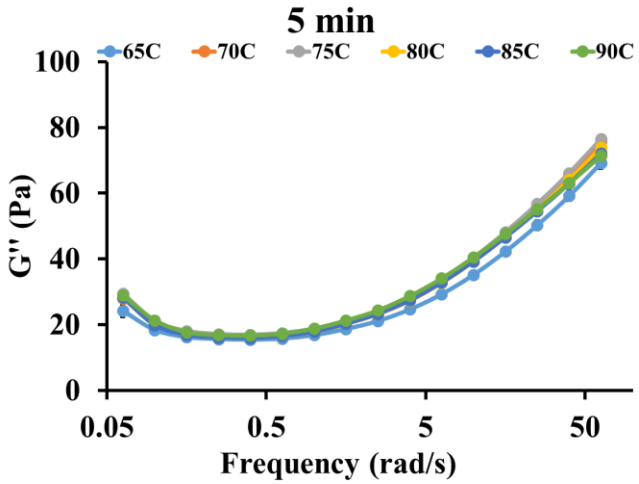

(a)

Figure 5.2: Loss modulus of waxy maize starch heated for (a) 5 min, (b) 15 min and (c) 60 min at 65°C, 70°C, 75°C, 80°C, 85°C and 90°C.

Figure 5.2 continued

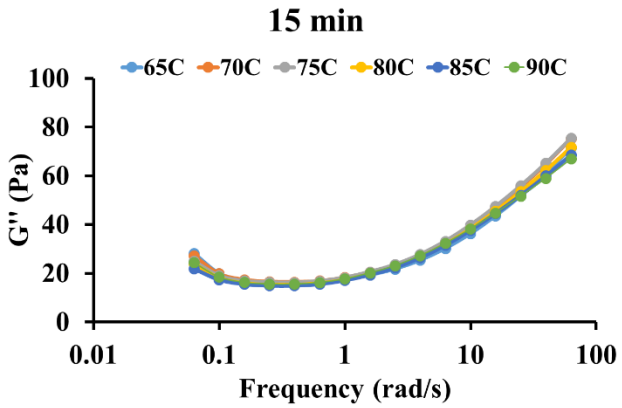

(b)

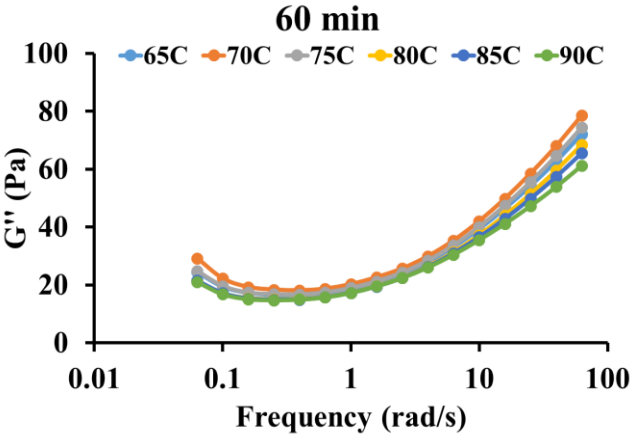

(c)

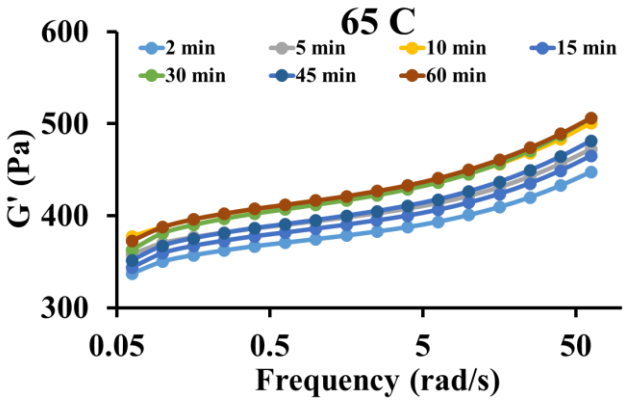

(a)

Figure 5.3: Storage modulus of waxy maize starch heated for (a) 65°C, (b) 70°C, (c) 75°C, (d) 80°C, (e) 85°C and (f) 90°C for 2, 5, 10, 15, 30, 45 and 60 min

Figure 5.3 continued

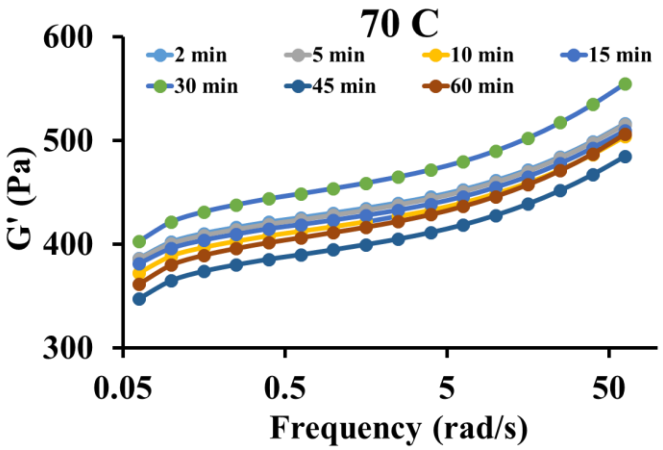

(b)

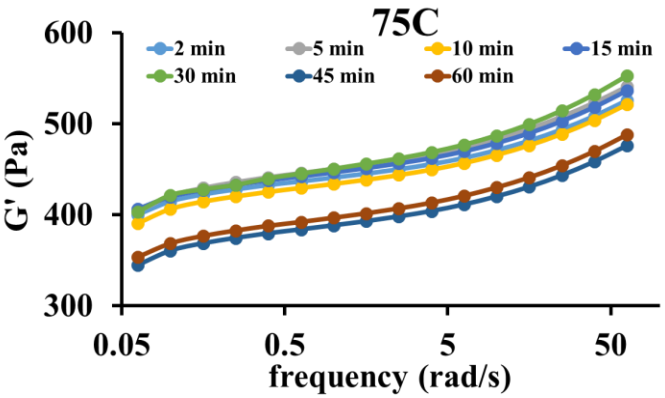

(c)

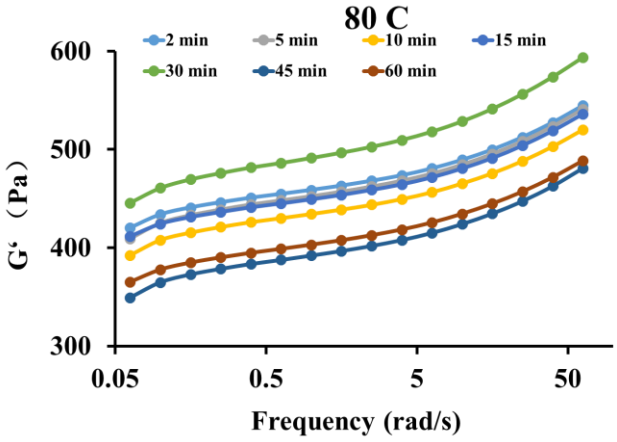

(d)

Figure 5.3 continued

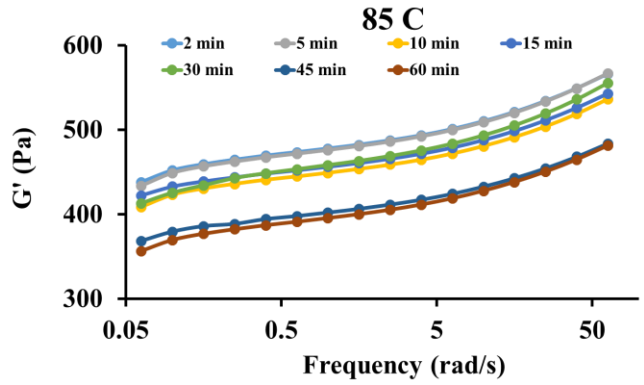

(e)

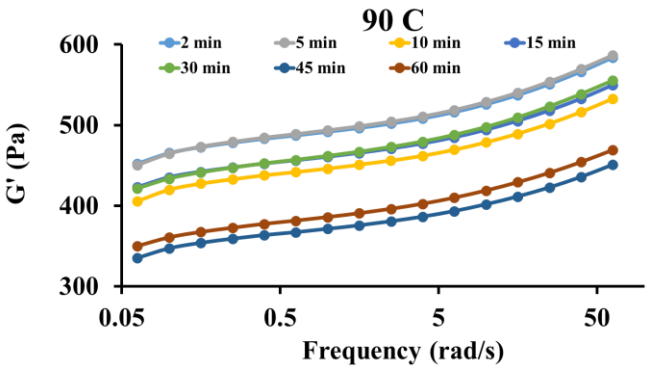

(f)

5.2 G’ vs ω at different T and time for normal maize

The normal maize starch has higher gelatinization temperature than waxy maize starch. Negligible swelling was observed at 65°C. This was reflected in the negligible G’ values. G’ was found to be significant only at 70°C. Figure 5.4 (a) and (b) show that hold time 5 and 10 min are not sufficient to heat the starch suspension into a gel at 70°C. Therefore, G’ values at these hold times were negligible. For longer hold times of 15-60 min of heating, however, G’ is measurable and increases in the order of 70°C, 75°C and 80°C. However, G’ is found to decrease at a higher temperature of 85°C. This is also true for 90°C. Similar to waxy maize starch, the decrease in the G’ is believed to be influenced by competing effects of swelling, amylose leaching and softening of granules.

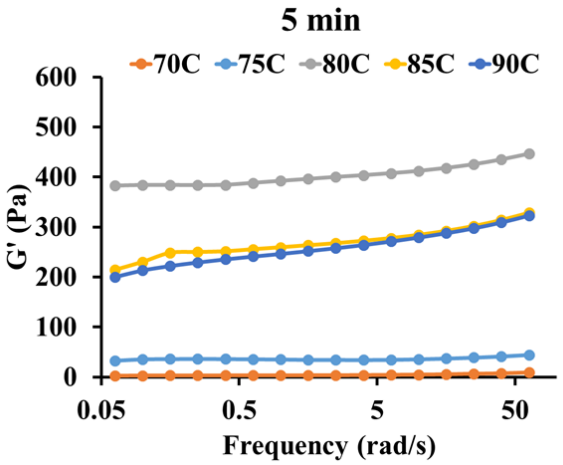

(a)

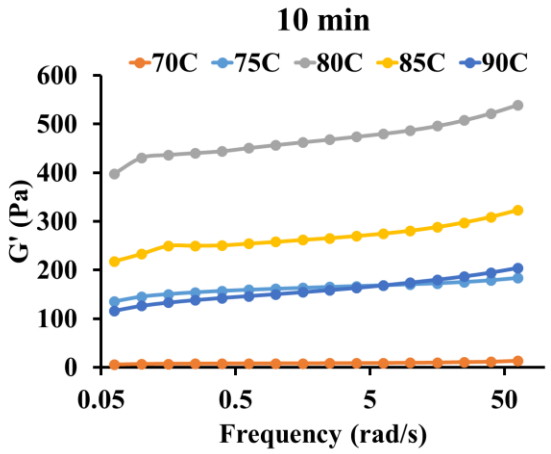

(b)

Figure 5.4: Storage modulus of normal maize starch heated for (a) 5 min, (b) 10 min, (c) 15 min, (d) 30 min, (e) 45 min and (f) 60 min at 70°C, 75°C, 80°C, 85°C and 90°C

Figure 5.4 continued

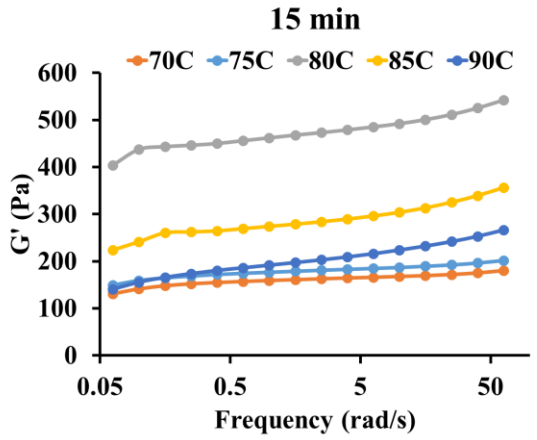

(c)

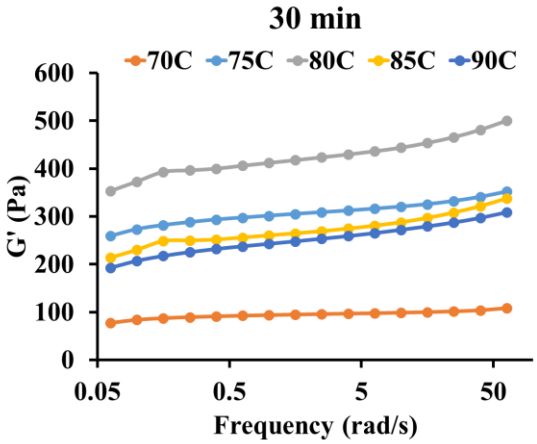

(d)

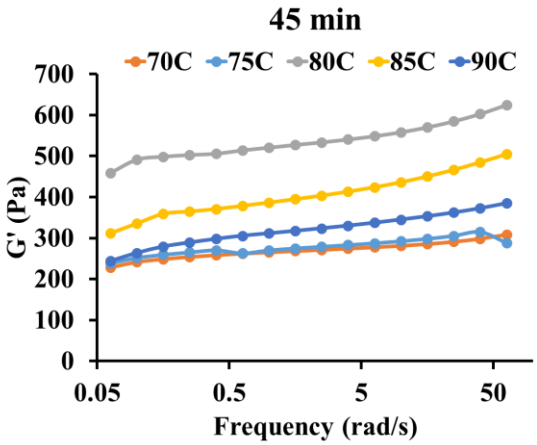

(e)

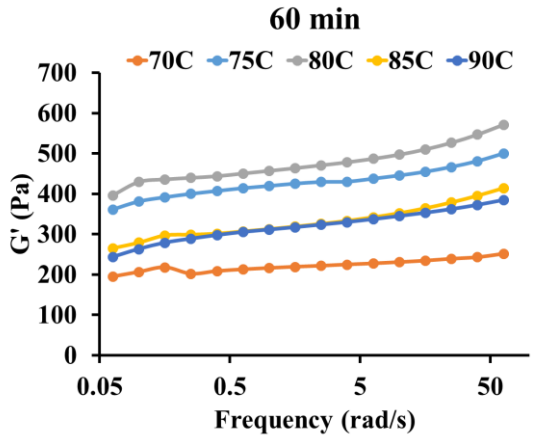

(f)

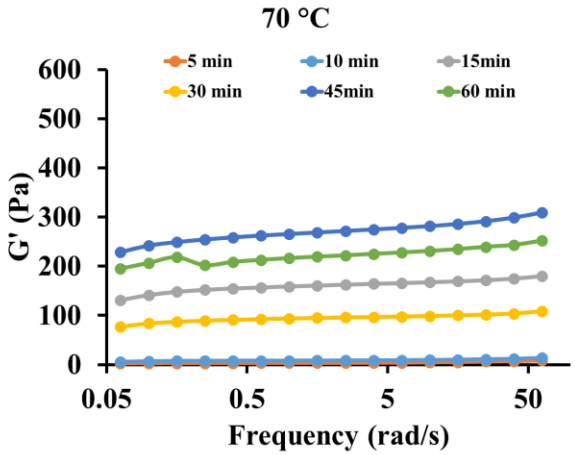

(a)

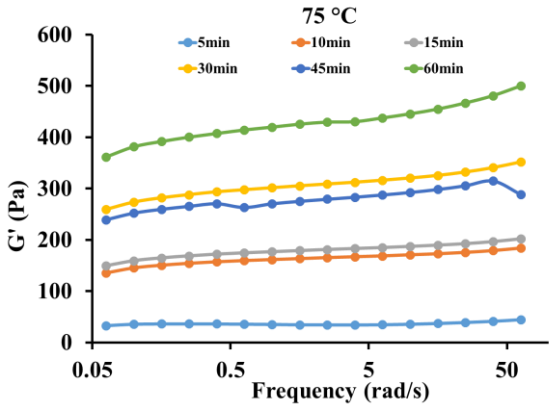

(b)

Figure 5.5: Size distribution of normal maize starch heated at (a) 70°C, (b) 75°C, (c) 80°C, (d) 85°C and (e) 90°C for 5, 10, 15, 30, 45 and 60 min

Figure 5.5 continued

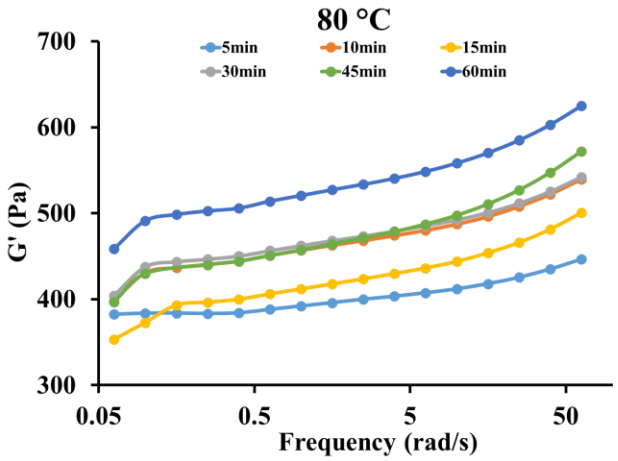

(c)

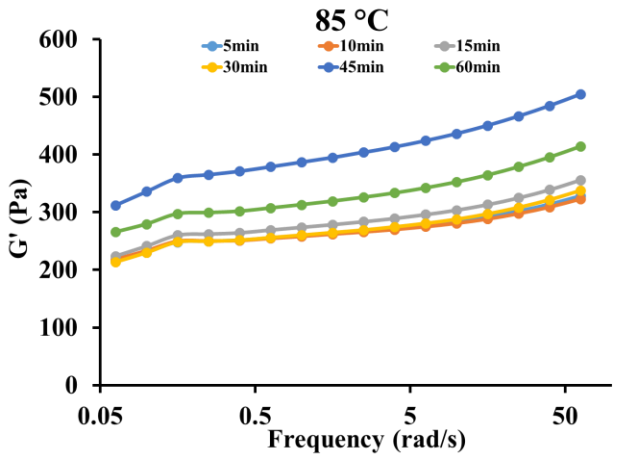

(d)

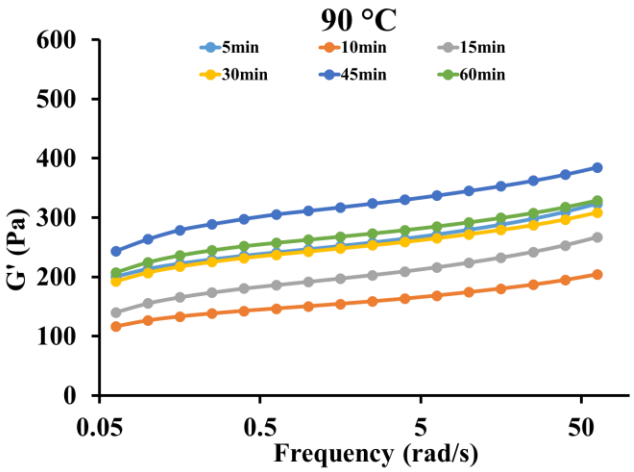

(e)

5.3 G’ vs ω at different T and time for waxy rice starch

Similar to waxy maize starch, the G’ of waxy rice starch at all hold times increase as the heating temperature increases (Figure 5.6). At holding time of 45 min, G’ at 85°C and 90°C overlap. At holding time of 60 min, G’ at 90°C dropped lower than that at 85°C. Unlike waxy and normal maize, the G’ for waxy rice starch does not vary much with the oscillatory frequency and therefore exhibit a more gel like behavior.

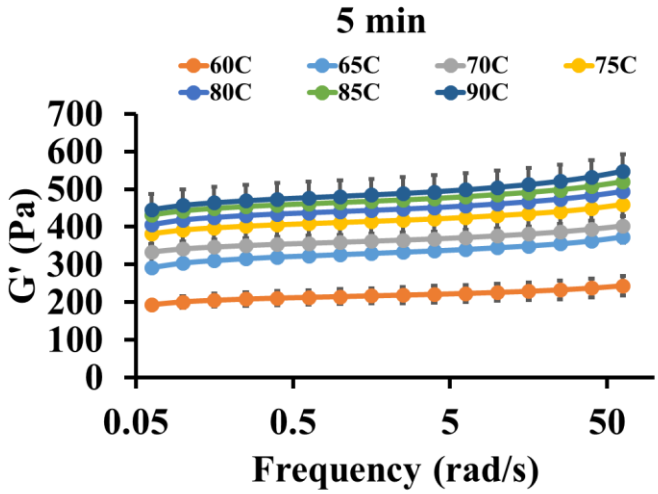

(a)

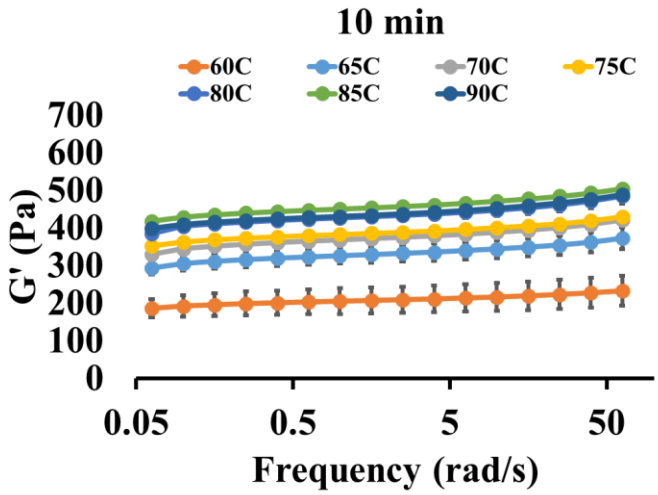

(b)

Figure 5.6: Storage modulus of normal maize starch heated for (a) 5 min, (b) 10 min, (c) 15 min, (d) 30 min, (e) 45 min and (f) 60 min at 60°C, 65°C, 70°C, 75°C, 80°C, 85°C and 90°C.

Figure 5.6 continued

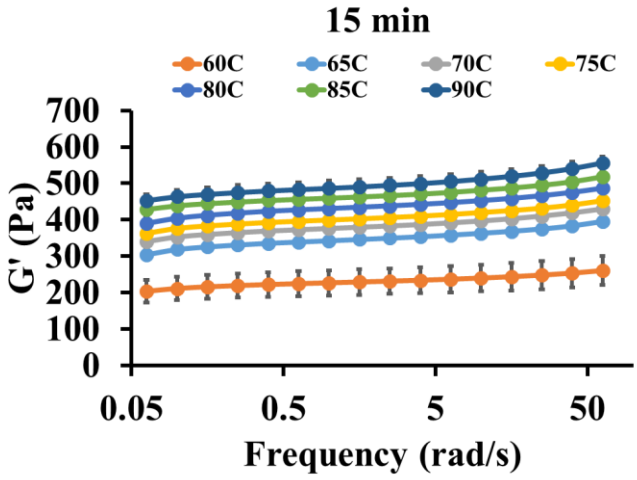

(c)

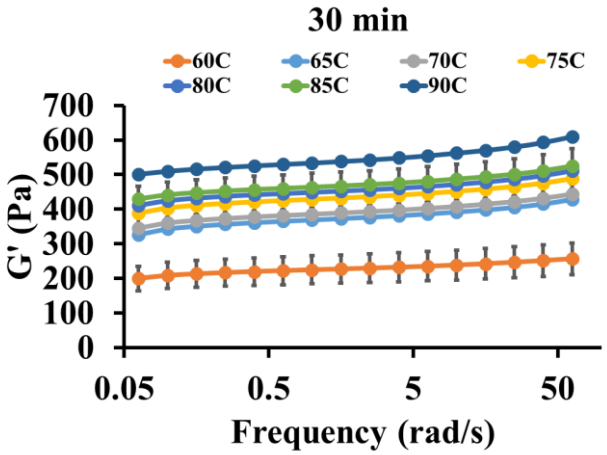

(d)

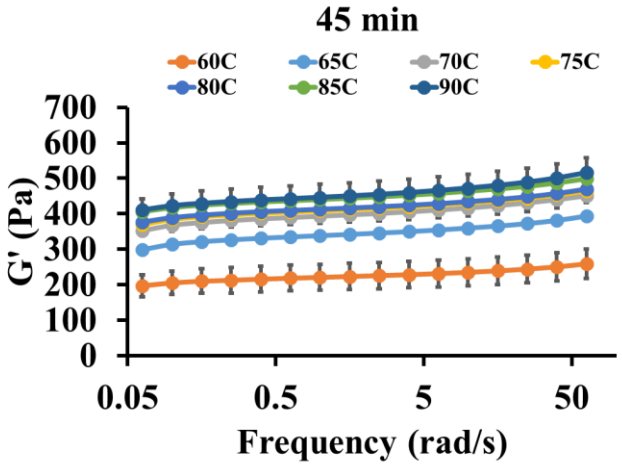

(e)

Figure 5.6 continued

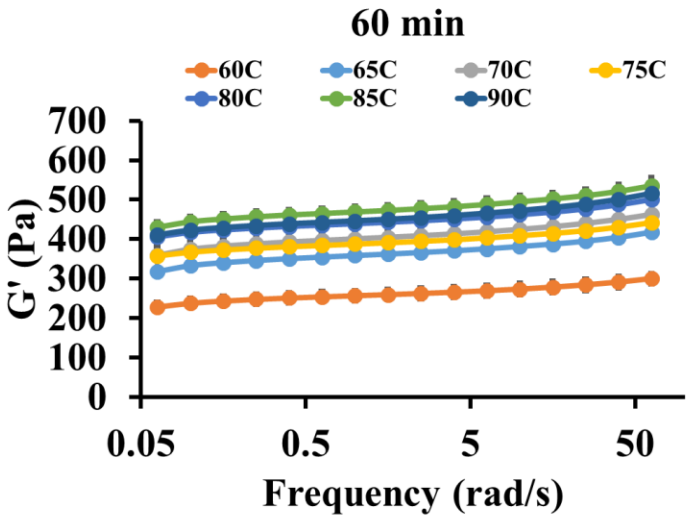

(f)

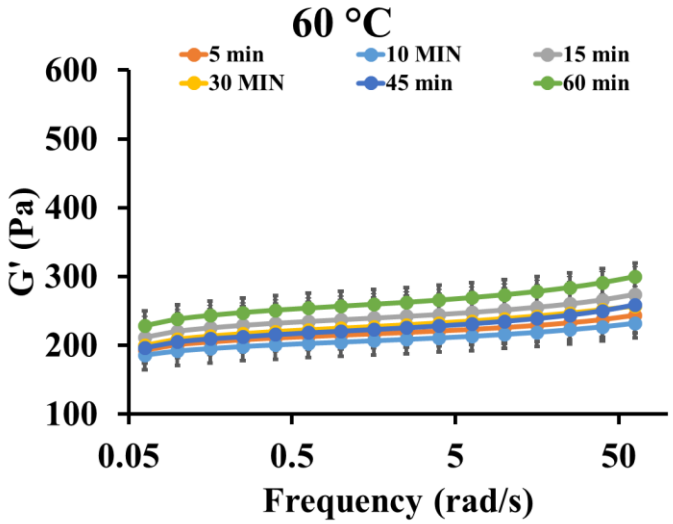

(a)

Figure 5.7: Size distribution of waxy rice starch heated at (a) 60°C, (b) 65°C, (c) 70°C**,** (d) 75°C, (e) 80°C, (f) 85°C and (g) 90°C for 5, 10, 15, 30, 45 and 60 min

Figure 5.7 continued

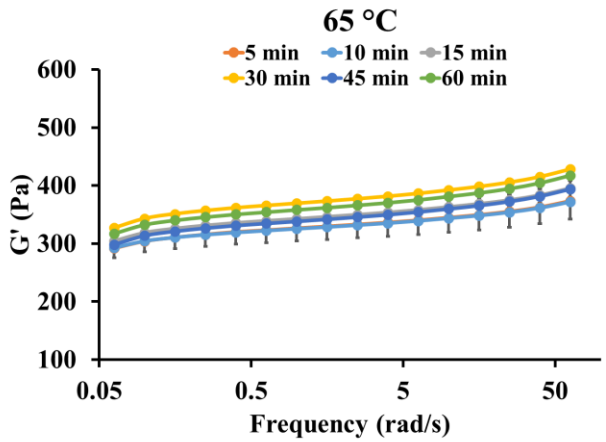

(b)

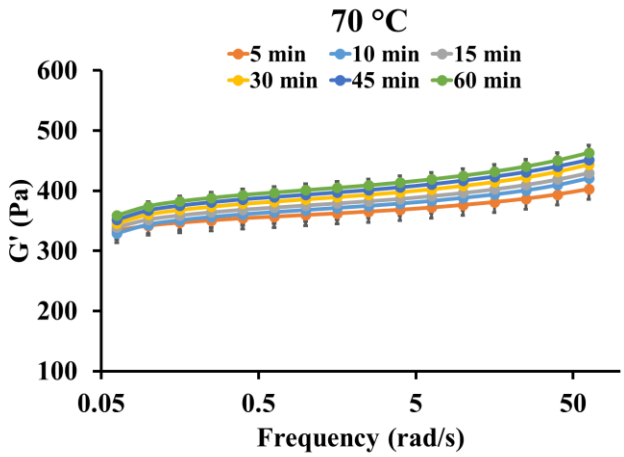

(c)

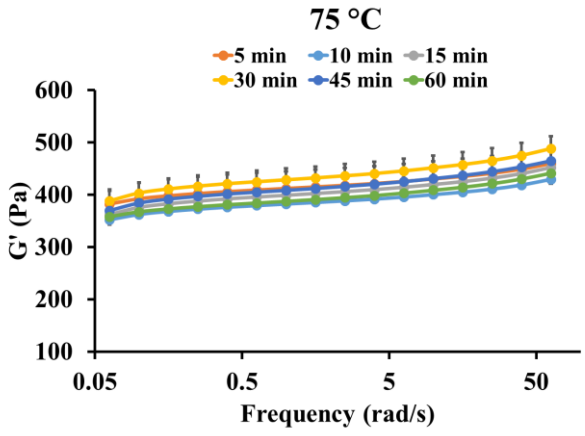

(d)

Figure 5.7 continued

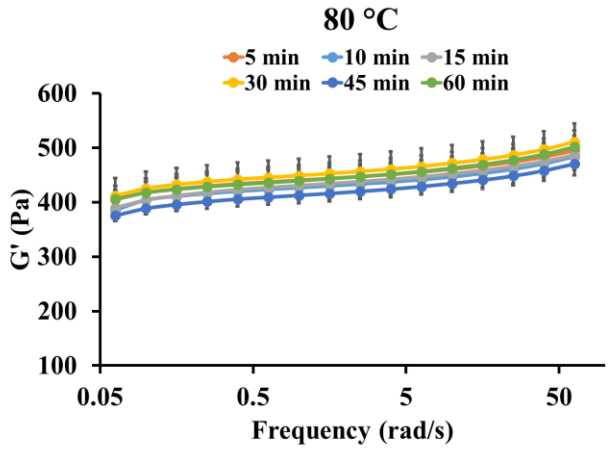

(e)

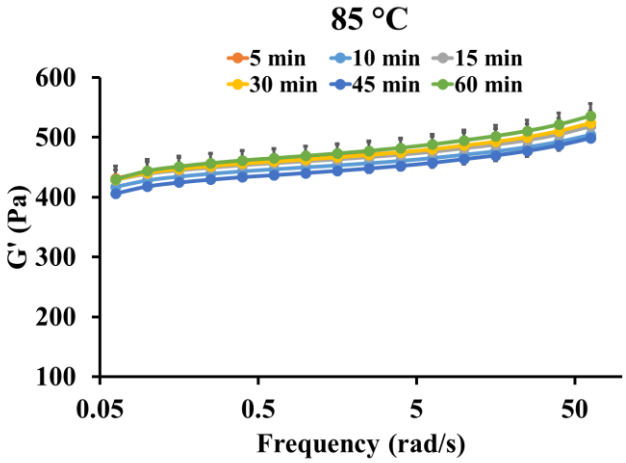

(f)

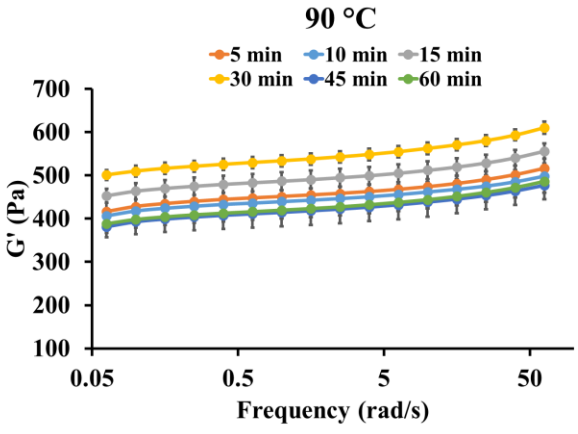

(g)

5.4 G’ vs ω at different T and time for normal rice starch

Similar trend for the change of G’ of normal maize starch has been observed for normal rice starch Figure 5.8. The difference is that at 70°C with 5 min of heating, the G’ of normal rice starch reaches close to 100 Pa, versus the G’ of normal maize starch at the same condition is almost zero. Same as normal maize starch, when heated at 90°C for however long, the G’ always decreases drastically. At 5 min of heating, G’ increases with temperature with 85°C being the highest G’ Figure 5.8 (a). Starting from 10 min, the G’ at 85°C becomes lower than the G’ at 80°C.

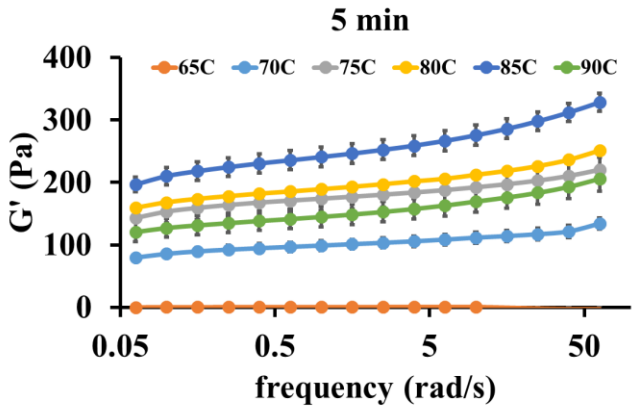

(a)

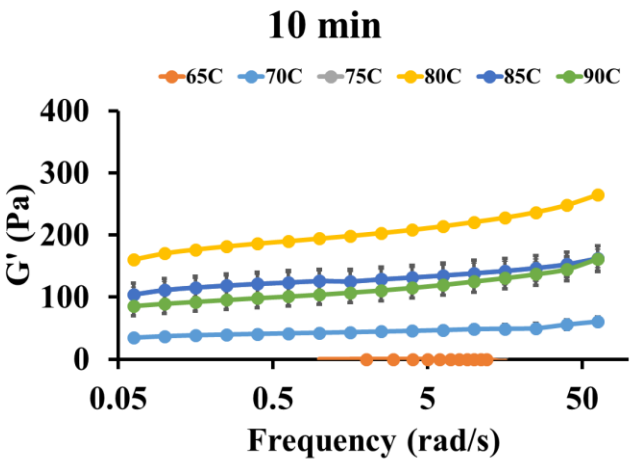

(b)

Figure 5.8: Storage modulus of normal rice starch heated for (a) 5 min, (b) 10 min, (c) 15 min, (d) 30 min, (e) 45 min and (f) 60 min at 65°C, 70°C, 75°C, 80°C, 85°C and 90°C.

Figure 5.8 continued

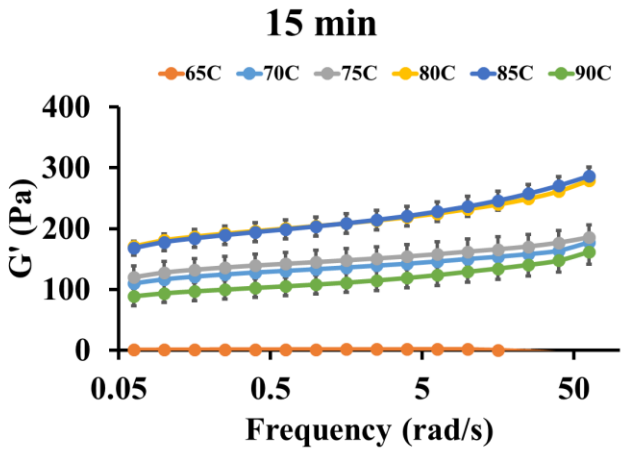

(c)

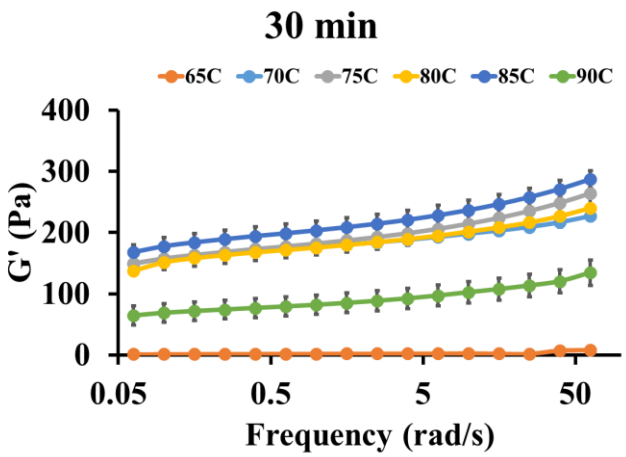

(d)

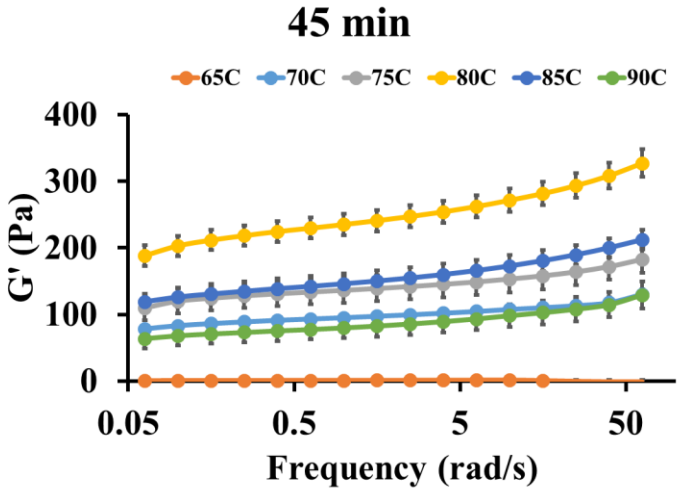

(e)

Figure 5.8 continued

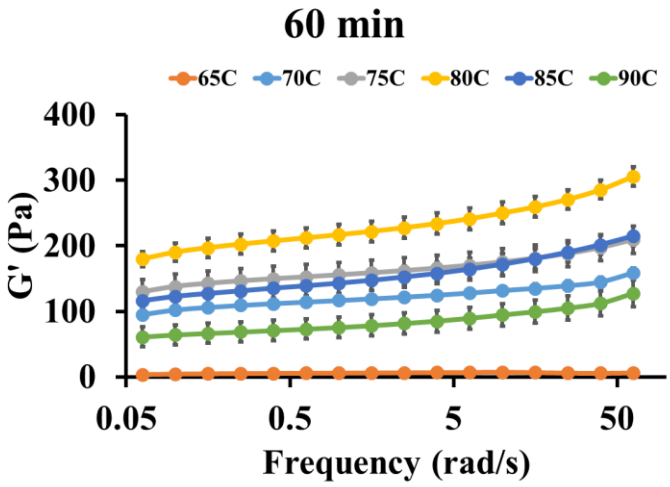

(f)

5.5 G’ vs ω at different T and time for STMP Cross-linked starch

With the STMP used to cross link starch granules, the swelling power becomes lower and integrity is higher against heat and shear. G’ is therefore lower for crosslinked starch and decreases with the extent of crosslink as a result of less swelling Figure 5.9 and Figure 5.10. Figure 5.9 shows that even after 30min of heating, the starch pasted at 80°C still has G’ below 100 Pa, indicating that crosslinking with STMP has effectively slower down the swelling, which in return, lowered the pasting.

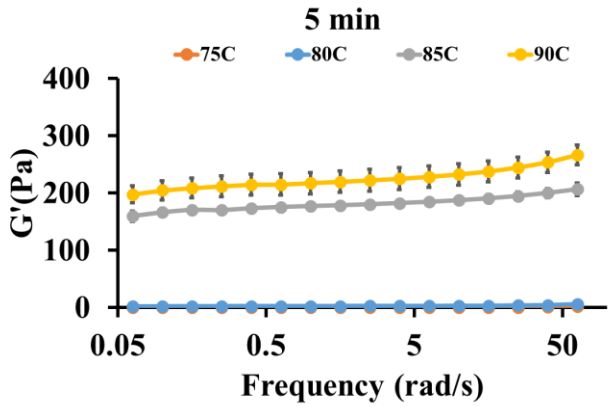

(a)

Figure 5.9: Storage modulus of 0.2% STMP cross-linked normal maize starch heated for (a) 5 min, (b) 10 min, (c) 15 min, (d) 30 min, (e) 45 min and (f) 60 min at 75°C, 80°C, 85°C and 90°C.

Figure 5.9 continued

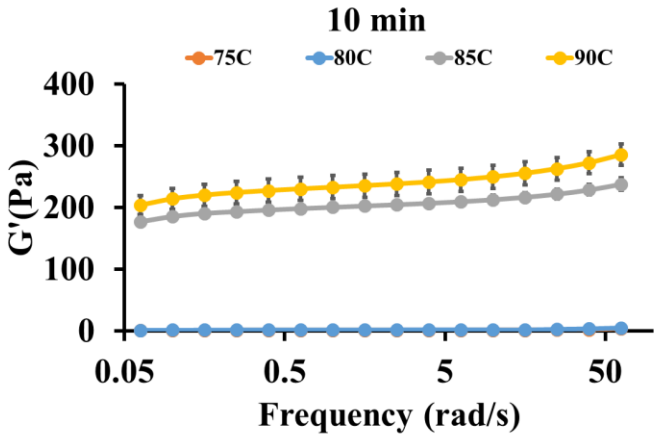

(b)

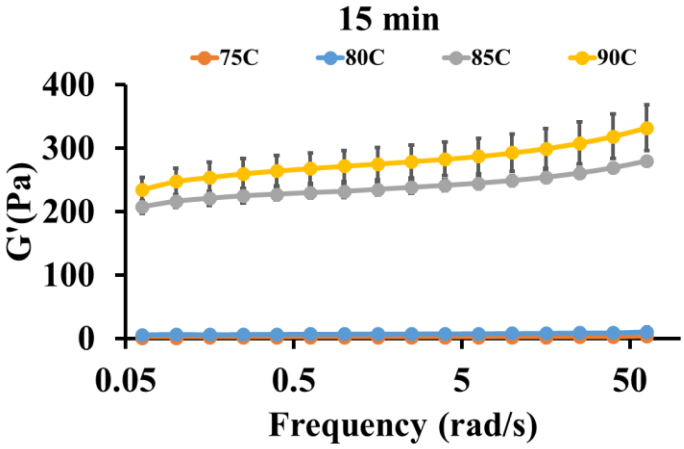

(c)

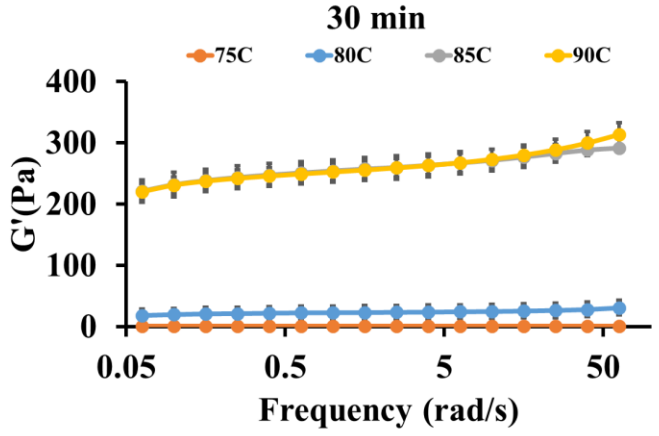

(d)

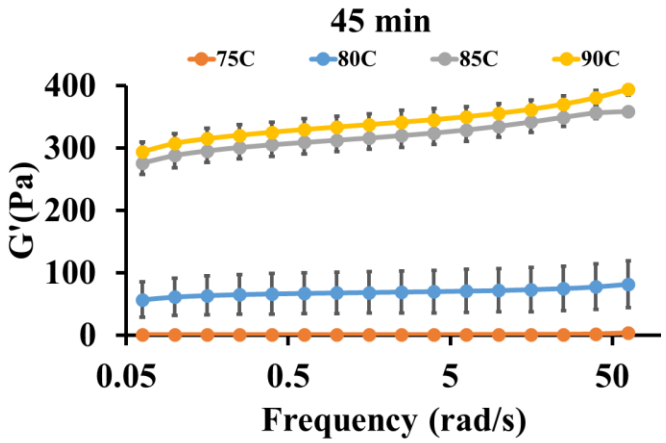

(e)

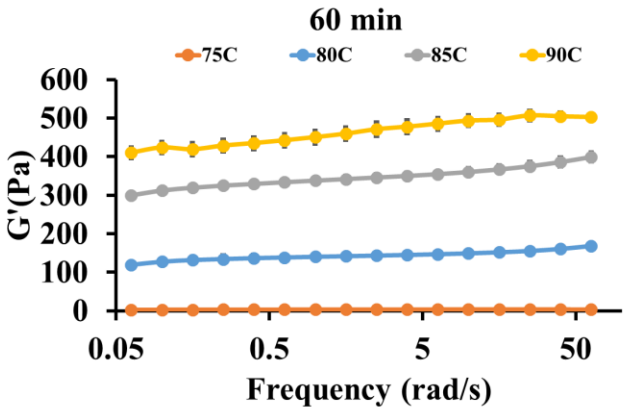

(f)

0.1% STMP Cross-linked

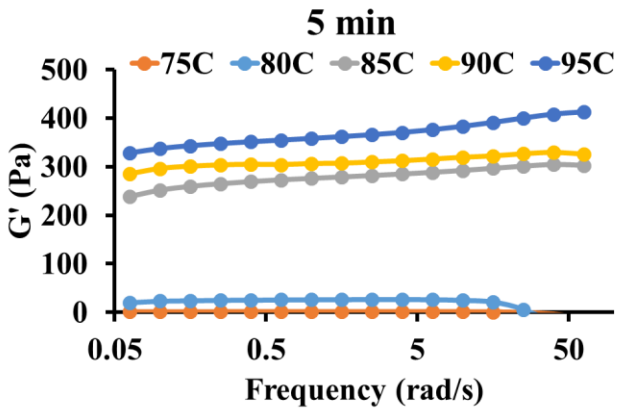

(a)

Figure 5.10: Storage modulus of 0.2% STMP cross-linked normal maize starch heated for (a) 5 min, (b) 10 min, (c) 15 min, (d) 30 min, (e) 45 min and (f) 60 min at 75°C, 80°C, 85°C, 90°C and 95°C

Figure 5.10 continued

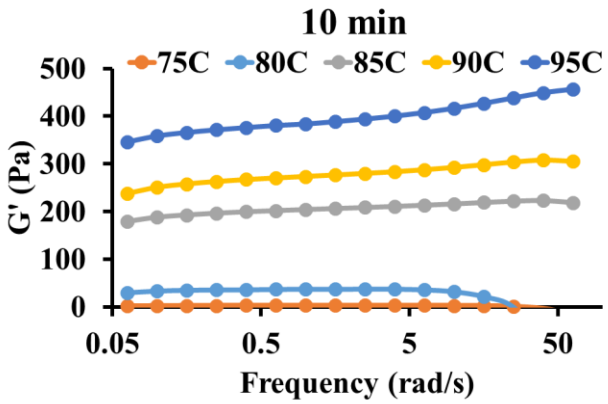

(b)

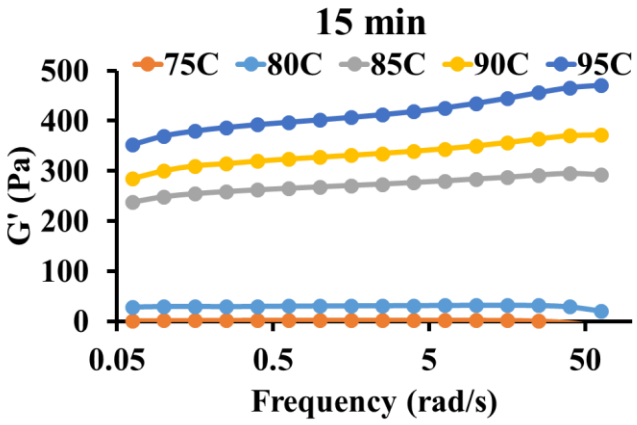

(c)

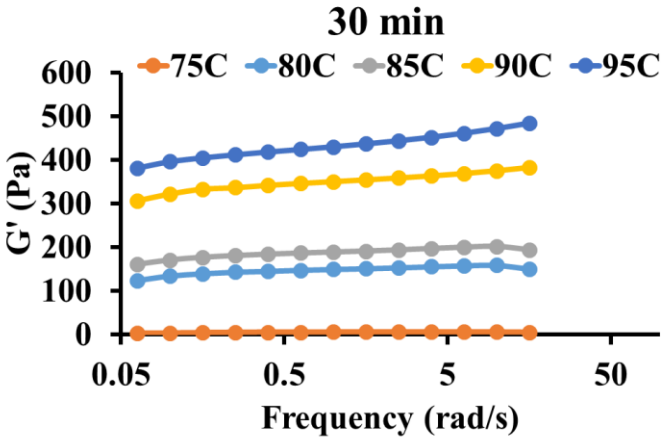

(d)

Figure 5.10 continued

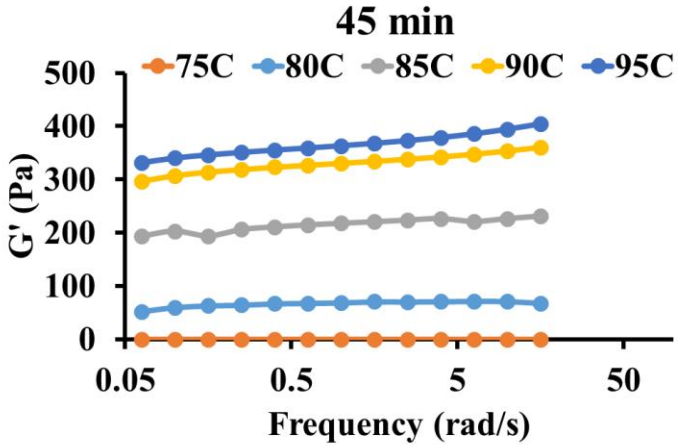

(e)

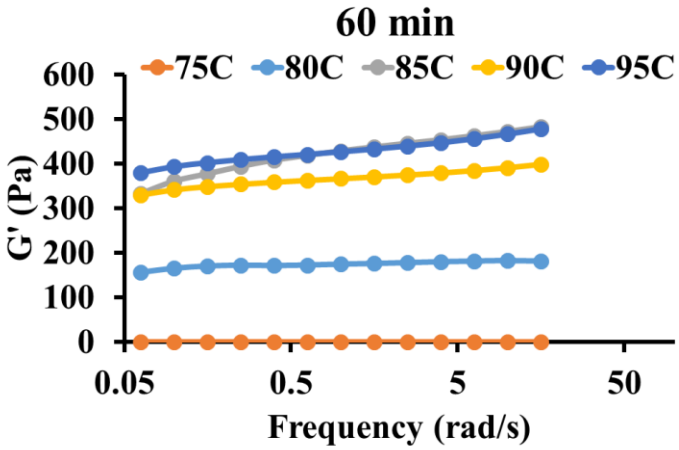

(f)

CHAPTER 6. VOLUME FRACTION DEPENDENT VISCOELASTICITY OF NATIVE MAIZE AND RICE STARCH

Results presented in the previous chapters indicate that starch swells rapidly after it attains the gelatinization temperature. As a result, the volume fraction quickly goes beyond 0.64 when the starch suspension is highly concentrated (above maximum packing of solids). The granules become deformable and the microstructure appears similar to that of a solid foam. Theories similar to foam rheology was invoked to predict the low-frequency shear modulus of the mixture. The analytical models developed here quantify how granule composition, rigidity, adhesion, and volume fraction alter starch rheology. This work paints a more detailed mechanical picture of the dense concentration regime, an underexplored area in the starch literature that is important in food applications where one would like to control food texture.

In general, granules can attain larger volume fractions than monodisperse hard spheres, because they are polydisperse and highly deformable. Although the rheology of granules behave similar to rigid particles at low concentration (Crassous et al., 2005), the high concentration leads to permanent contacts of particles when the granules start to deform, which strongly affect the rheological behavior of the suspension (van der Vaart, 2013). In this highly deformable limit, the microstructure of the dispersion appears similar to a packed, solid foam. In a foam structure, deformed granules will assume a dodecahedral structure in which they are separated by thin aqueous films (Ganesan Narsimhan & Eli Ruckenstein, 1986). At low applied deformation (or shear stress), they behave like an elastic solid (Weaire, 2008). There exists a yield stress above which the dispersion becomes plastic with shear thinning behavior. Two dimensional foam models have been developed to describe the elasticity, yield stress and shear thinning viscosity (Khan & Armstrong, 1986, 1987).

6.1 Model prediction for swelling kinetics

As starch granules are exposed to aqueous medium, because of the difference in the chemical potential, the solvent (aqueous medium) diffuses into the granule thus resulting in its swelling. There is elastic resistance to the swelling of the starch network. Here, we consider only the granules that are neutral (not charged). This is a reasonable assumption for native waxy maize starch

granules. The current model assumes that all starch granules are uniform and therefore does not account for the internal granule architecture, i.e. the presence of alternate rings of crystalline and semi-crystalline regions of different tortuosity. Eventually, the granule attains equilibrium at which the net osmotic pressure acting on the granule is zero, i.e. the total free energy is at a minimum. The total free energy can be written as the sum of (i) free energy of mixing of the starch network with the solvent and (ii) free energy of elastic deformation of the network Therefore, from Flory Huggins theory, the chemical potential of water inside the granule is given by (Flory, 1953),

$$\mu_1 - \mu_1^0 = RT\left[\ln(1-\phi) + \phi + \chi(T)\phi^2 + v_1\left(\frac{\nu_e}{V}\right)(\phi^{1/3} - \frac{\phi}{2})\right] \qquad (6\text{-}1)$$

where, ϕ is the volume fraction of starch within the granule, $\chi(T)$ is the Flory Huggins parameter at temperature T, R is the gas constant, T is the temperature, v_1 is the molar volume of the unswollen starch granule, V is the total volume of starch network within the granule and ν_e is the effective number of moles of chains in the network. The first two terms on the right hand side arise from entropy of mixing, the third term involving Flory Huggins parameter arises from the enthalpy of mixing and the last term arises from the elastic resistance to swelling. $v_1(\nu_e/V) = \nu^*$, ν^* being the fraction of chains that are crosslinked. Flory Huggins χ parameter gives the change in enthalpy of interaction when a starch segment is transferred from its own environment to solvent (water) and is therefore a measure of starch-solvent interaction. Now,

$$\frac{\partial \chi}{\partial T} = -\frac{\Delta H}{RT^2} \qquad (6\text{-}2)$$

where ΔH is the molar enthalpy of interaction of starch with water (solvent). It has been observed that starch swelling occurs mainly when the temperature is above gelatinization temperature. Consequently, it is reasonable to assume that the molar enthalpy of interaction with water does not change appreciably below the gelatinization temperature T_g. In case of amylopectin, gelatinization occurs due to interaction of water with part of the starch granule in the semi-crystalline region as well as its interaction with amylopectin in the crystalline region. Gelatinization is mainly due to formation of hydrogen bonds by water with starch molecule. Since the number of such hydrogen bonds per starch molecule as well as the actual moisture content of crystalline regions are not

known, it is difficult to predict ΔH . It is therefore taken as a parameter. Integrating the above equation, one obtains,

$$\chi(T) = \chi(T_0) \qquad \text{if } T \le T_g$$
$$\chi(T) = \chi(T_0) - \frac{\Delta H}{RT_g}\left(1 - \frac{T_g}{T}\right) \qquad \text{if } T > T_g \tag{6-3}$$

since χ parameter is assumed not to change below T_g. Experimental measurement of average granule size as a function of temperature during heating indicate that swelling starts at 45 °C with granule size not changing for lower temperatures. This is consistent with reported results in the literature (Tester & Morrison, 1990). Therefore, T_g is taken as 45 °C in the model calculations. In most of the experiments, the suspension of starch granules of weight fraction of 8 % was placed in the pasting cell and heated from room temperature to 45 °C at a heating rate of 15 °C/min, holding the sample at that temperature for 1 min followed by further heating of the sample at a heating rate of 15 °C/min to the desired temperature and holding the sample at that temperature . Because of the difference in the chemical potential, water (solvent) will diffuse into the granule thereby resulting in the swelling of the granule. The rate of diffusion of water is governed by the gradient of its chemical potential and can thus be described by,

$$\frac{\partial \mu_1}{\partial t} = \frac{1}{r^2}\frac{\partial}{\partial r}\left(Dr^2 \frac{\partial \mu_1}{\partial r}\right) \tag{6-4}$$

In the above equation, D is the diffusion coefficient of water (solvent) into the granule at temperature T , t is the time and r is the radial position within the spherical granule. The pore diffusion coefficient D , being proportional to pore radius, temperature and inversely proportional to tortuosity is given by (Swinkels, 1985),

$$D(T) = D_0\left(\frac{T}{T_0}\right)\frac{(1-\phi)^{1/3}}{tor(\phi)} \tag{6-5}$$

where D_0 is the self-diffusion coefficient of water (solvent) at reference temperature T_0. Starch granules exhibit radial channels in the outer region and an inner compact region with much higher tortuosity. The proposed model assumes the granules to be uniform and therefore the pore diffusion has to be expressed in terms of a volume averaged tortuosity which is unknown. Several empirical models exist that relate tortuosity to porosity. Here, we adopt one such model, namely, $tor(\phi) = (1-\phi)^{-c}$ where c is a parameter (Matyka, Khalili, & Koza, 2008). As can be seen from

this expression, tortuosity decreases with an increase in parameter c . In order to account for the decrease in tortuosity due to swelling as well as softening of the granules, the parameter c is taken as $b\frac{R}{R_0}\frac{T}{T_0}$, where b is a constant and R and T refer to the granule radius and medium temperature respectively with the subscript 0 being the initial conditions. Since the granule is heated, the temperature profile within the granule is changing with time and is given by the following unsteady state heat conduction equation,

$$\frac{\partial T}{\partial t}=\frac{1}{r^2}\frac{\partial}{\partial r}\left(\alpha\left(\phi,T\right)r^2\frac{\partial T}{\partial r}\right) \tag{6-6}$$

Where $\alpha\left(\phi,T\right)$ is the thermal diffusivity of the starch granule. The thermal diffusivity is given by (Morley & Miles, 1997),

$$\alpha\left(\phi,T\right)=\frac{k\left(\phi,T\right)}{\rho\left(\phi,T\right)c_p\left(\phi,T\right)} \tag{6-7}$$

where (Morley & Miles, 1997),

$$\rho\left(\phi,T\right)=\rho_s\left(T\right)\phi+\rho_w\left(T\right)\left(1-\phi\right) \tag{6-8}$$

$$k\left(\phi,T\right)=\phi k_s\left(T\right)+\left(1-\phi\right)k_w\left(T\right) \tag{6-9}$$

$$c_p\left(\phi,T\right)=c_{ps}\left(T\right)\phi+c_{pw}\left(T\right)\left(1-\phi\right) \tag{6-10}$$

Defining the following dimensionless variables, the above equation can therefore be written in terms of dimensionless variables as,

$$\tau=\frac{\alpha_0 t}{R_0^2};\ r^*=\frac{r}{R_0};\ T^*=\frac{T-T_0}{T_0};\mu_1^*=\frac{\mu_1-\mu_1^0}{RT_0};Pe=\frac{D_0}{\alpha_0};D^*=\frac{D}{D_0};\alpha^*=\frac{\alpha}{\alpha_0};H^*=\frac{HR_0^2}{T_0\alpha_0} \tag{6-11}$$

Where H is the heating rate and subscript 0 refers to the value at reference temperature T_0 , eqs. (6-5) and (6-6) can be recast as

$$\frac{\partial\mu^*}{\partial\tau}=\frac{Pe}{r^{*2}}\frac{\partial}{\partial r^*}\left(D^*r^{*2}\frac{\partial\mu^*}{\partial r^*}\right) \tag{6-12}$$

$$\frac{\partial T^*}{\partial\tau}=\frac{1}{r^{*2}}\frac{\partial}{\partial r^*}\left(\alpha^*r^{*2}\frac{\partial T^*}{\partial r^*}\right) \tag{6-13}$$

The initial and boundary conditions are,

$$\tau = 0 \quad \phi = \phi_0; \quad T^* = 0 \tag{6-14}$$

$$r^* = 0 \qquad \frac{\partial \mu^*}{\partial r*} = 0; \quad \frac{\partial T^*}{\partial r^*} = 0 \tag{6-15}$$

$$r* = R*(\tau) \qquad \mu^*(\phi^s) = 0;$$
$$T^* = H^*\tau \quad \text{if } T^* < T^*_{final} \tag{6-16}$$
$$= T^*_{final} \quad \text{otherwise}$$

where ϕ_0 is the initial volume fraction of starch within the granule that is equilibrated at room temperature and $R*(\tau) = R(\tau)/R_0$, $R(\tau)$ being the radius of the swollen granule at dimensionless time τ, the evaluation of which is discussed below. The boundary condition (6-16) is the result of the assumption that the surface of the granule is in equilibrium with the solvent since the external resistance to mass transfer is negligible. In eq. (6-15) $T^*_{final} = (T_{final} - T_0)/T_0$, T_{final} being the desired final temperature. Eq. (6-15) reflects the two stages of heating, i.e. in the first stage the medium is heated at a constant heating rate until the temperature reaches the desired value after which it is maintained constant. This assumption is justified since mass transfer of water inside the granule is due to diffusion through very small tortuous pores. The second boundary condition in eq. (6-15) assumes that the external resistance to heat transfer is negligible since the sample is stirred during the measurement. .Eqs. (6-11) and (6-12) are solved with initial and boundary conditions eq. (6-13)-(6-15) to obtain the dimensionless chemical potential and temperature profiles within the granule at different times. The volume fraction profile of starch within the granule $\phi(r^*, \tau)$ can then be obtained from the dimensionless chemical potential profile $\mu^*(r^*, \tau)$ using,

$$\mu^*(r^*, \tau) = \ln(1 - \phi(r^*, \tau)) + \phi(r^*, \tau) + \chi(T)\phi(r^*, \tau)^2 + v*(\phi(r^*, \tau)^{1/3} - \frac{\phi(r^*, \tau)}{2}) \tag{6-17}$$

At equilibrium, we have,

$$\frac{1}{r^{*2}} \frac{\partial}{\partial r^*} \left(D^* r^{*2} \frac{\partial \mu^*}{\partial r^*} \right) = 0 \tag{6-18}$$

$$\frac{1}{r^{*^2}}\frac{\partial}{\partial r^*}\left(\alpha^* r^{*^2}\frac{\partial T^*}{\partial r^*}\right)=0 \qquad (6\text{-}19)$$

which implies

$$\frac{d\mu^*}{dr^*}=0\ ; \qquad \frac{dT^*}{dr^*}=0 \qquad (6\text{-}20)$$

which satisfies the boundary condition eq. (6-14). Eqs. (6-19) and boundary condition (6-15) imply that

$$\mu^*=0\ \ ;\ \ T^*=\frac{T-T_0}{T_0} \qquad (6\text{-}21)$$

Therefore, the granules eventually reach equilibrium at which there is no further swelling and the chemical potential inside the granule is equal to that of the solvent. In addition, the temperature inside the granule is uniform and equal to that of the medium. The equilibrium starch volume fraction $\phi_s(T)$ inside the granule is therefore given by the solution of the equation

$$\ln(1-\phi_s(T))+\phi_s(T)+\chi(T)\phi_s(T)^2+\nu^*(\phi_s(T)^{1/3}-\frac{\phi_s(T)}{2})=0 \qquad (6\text{-}22)$$

Granule size distribution measurements were made after heating for 3 h and compared with the distribution after 60 min heating at all temperatures (65,70,75,80,85 and 90 C) as given in an earlier paper we published (Desam et al., 2018a). It is reasonable to assume that the system has attained equilibrium after 60 min of heating. Experimental values of $\phi_s(T)$ at long times (60 min) at different temperatures are fitted to predicted values using eq. (24) to get the best fit of ν^* and ΔH. The best fit values for ΔH and ν^* are 12.81 kJ/mole and 0.004 respectively. The fitted value of $\nu^*=0.0041$ which falls within the calculated range of 0.0003-0.006 for the degree of polymerization of waxy maize starch (GluckHirsch & Kokini, 1997) and agrees reasonably with the upper bound . The fitted value of ΔH compares favorably with the enthalpy of gelatinization of 11.96 kJ/mole (Liu, Yu, Xie, & Chen, 2006)Since the total volume of starch network is conserved in a swelling granule, we have,

$$\left[R(t)\right]^3\bar{\phi}(t)=R_0^3\phi_0 \qquad (6\text{-}23)$$

Where $\bar{\phi}(\tau)$ is the average starch volume fraction in the granule at τ . Therefore,

$$R^*(\tau) = \left(\frac{\phi_0}{\bar{\phi}(\tau)} \right)^{1/3} \quad (6\text{-}24)$$

Granule radius vs time for different values of parameter b at 75 °C are shown in the earlier paper (Desam et al., 2018a) as well. The evolution of granule size distribution was obtained from the solution of population balance equation for the growth of granules. The model predicts the evolution of average granule size and granule size distribution accurately.

6.2 G' vs Volume fraction

The effect of heating temperature on G' is more significant at 5 min, increasing with temperature. At larger holding times, however, this effect becomes less significant. As a result, one cannot observe a definite trend for variation of G' with temperature. The variation of G' with volume fraction (at different heating times and temperatures) is shown in Figure 6.1. G' increased monotonically with volume fraction for waxy and crosslinked maize whereas G' exhibited a maximum at an intermediate volume fraction for normal maize. Such a behavior is believed to be due to competing effects of swelling and softening of starch granules upon heating. Swelling results in crowding of granules in the suspension as a result of an increase in granule volume fraction as discussed above. This results in an increase in G' and is observed at short times. At longer times, however, the starch granule becomes softer thereby facilitating its deformation, this effect being more pronounced at higher temperature and depends on the nature of the starch granule. Higher deformability enables the granules to pack more efficiently when subjected to shear thereby reducing G'. Hence the decrease in G' at longer holding times, especially at higher heating temperature.

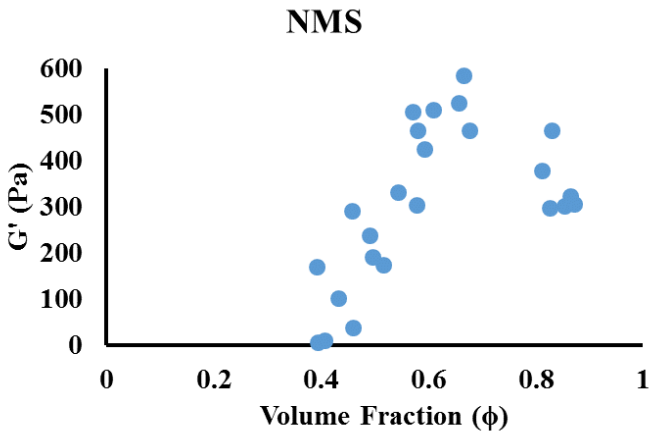

(a)

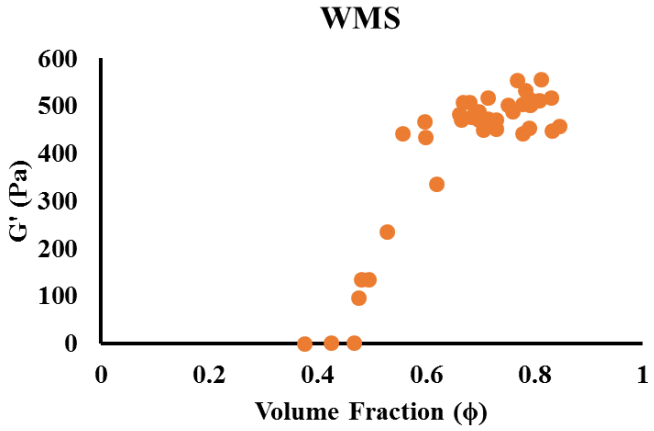

(b)

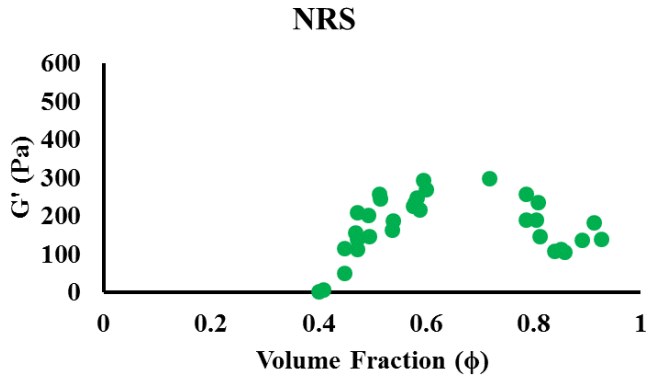

(c)

Figure 6.1: Storage modulus vs volume fraction for (a) normal maize starch, (b) waxy maize starch, (c) normal rice starch, (d) waxy rice starch, (e) 0.1% STMP cross-linked normal maize starch and (f) 0.2% cross-linked normal maize starch.

Figure 6.1 continued

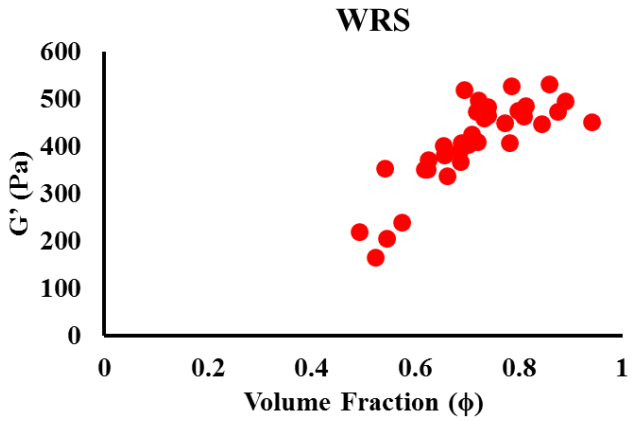

(d)

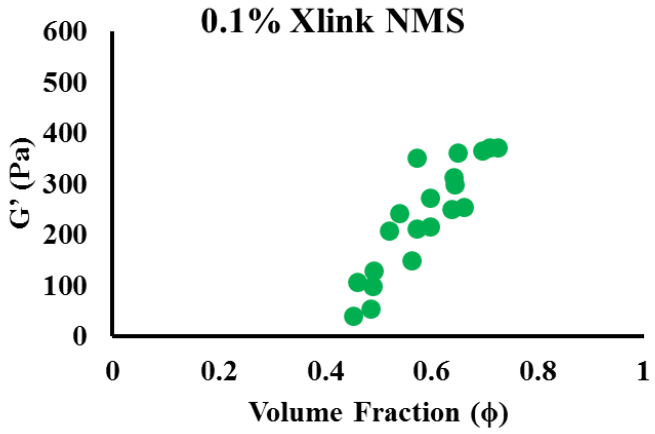

(e)

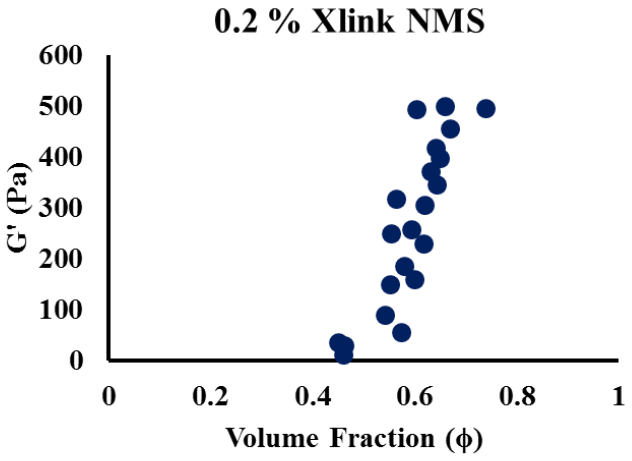

(f)

6.3 Master curve

It is well known that the viscosity of suspension increases with volume fraction (Ellis et al., 1989; I. D. Evans & Lips, 1992; Frith & Lips, 1995). Experimental observations of apparent viscosity and G' of starch suspensions were found to increase dramatically above a certain critical concentration (Wang and Lelieve, 1981). Interestingly, the increase in the relative viscosity (measure of relative increase in viscosity with respect to that of solvent) of wheat and maize starch suspensions at different heating rates correlated well with the ratio of actual volume fraction to that corresponding to maximum packing and collapsed into a single curve (Ellis et al., 1989). Evans and Lips (1990) also reported that the relative elasticity of sephadex dispersions, when plotted against notional volume fraction collapsed into a single curve. Since swelling of starch granules occur due to uptake of water from the suspending medium, it results in an increase in starch volume fraction and a concomitant increase in its apparent viscosity and G'. At higher temperatures, this swelling may result in some leaching of amylose (Ellis et al., 1989; I. D. Evans & Lips, 1992; Frith & Lips, 1995) into the suspending medium thereby increasing its viscosity. Our peak force measurements also seem to indicate that the granules become deformable under these conditions.

The normalized plots of $G'/G'_{0,\exp}$ vs ϕ for the three starch systems when subjected to different holding temperatures and times are shown in

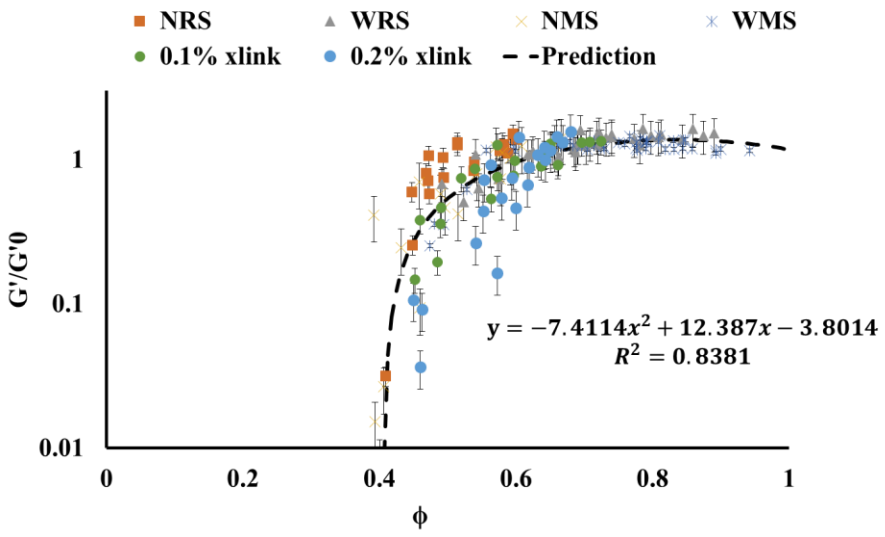

Figure 6.2. It is interesting to note that all the data points seem to fall into a single master curve.

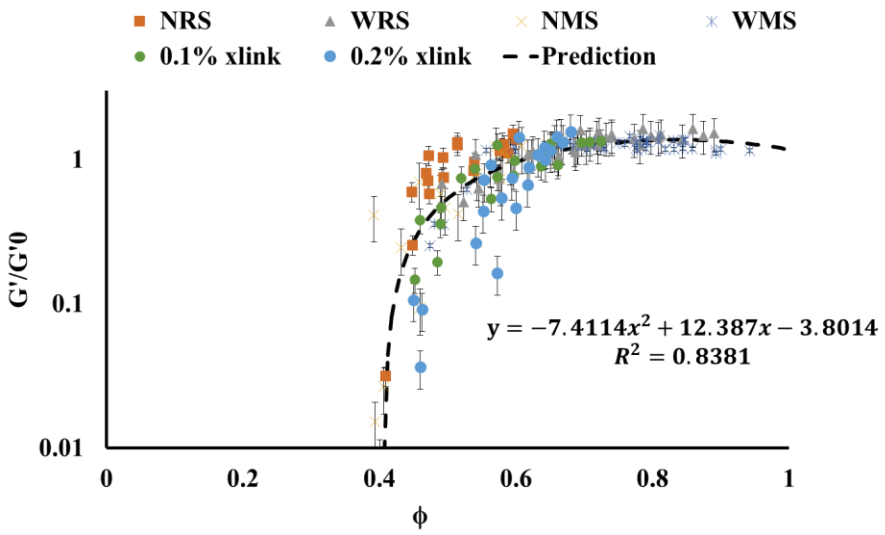

Figure 6.2: master curve of normalized G' of all starch at all heating condition vs volume Fraction

6.4 Deformation of Starch Granules

The peak force measurement gave a qualitative comparison of hardness of starch granules. It shows that as the temperature increases, the granule swells more and becomes less rigid. Softer the granules become, the less force it can withstand before deformation Therefore, higher temperature leads to a smaller peak force for all the starches (Figure 6.3). The decrease in peak force with temperature is more pronounced for NMS compared to WMS and cross-linked starch.

Table 6.1: Peak force of starch paste measure from compression test

	5min	10min
NMS	-0.0668 ± 0.0027	-0.0464 ± 0.0027
0.1% Xlink NMS	-0.0361 ± 0.0004	-0.0391 ± 0.0006
0.2% Xlink NMS	-0.0357 ± 0.0015	-0.0350 ± 0.0018
WMS	-0.0228 ± 0.0003	-0.0349 ± 0.0003

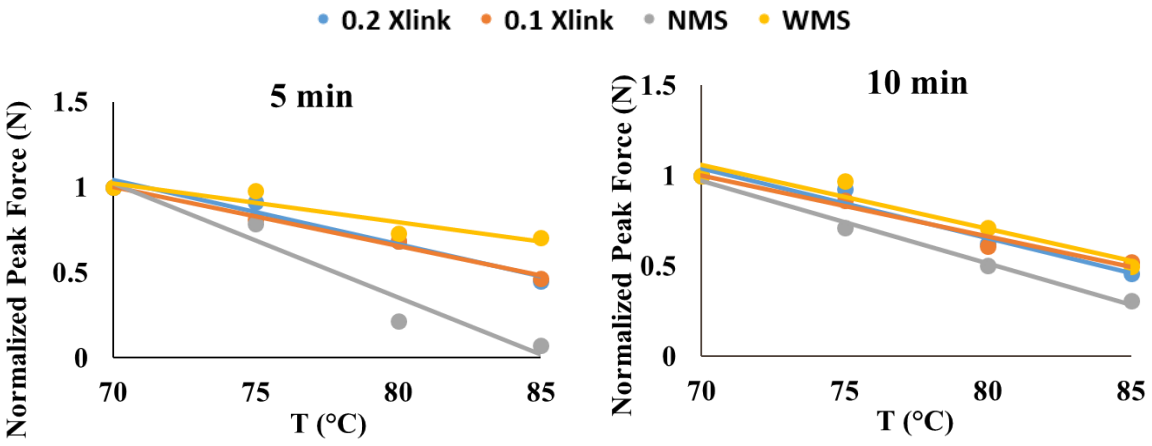

(a) (b)

Figure 6.3: Normalized peak force of cross-linked starch, normal maize starch and waxy maize starch

If the effects of leaching and deformability are not significant, one would expect G' of swollen starch paste to depend only on its volume fraction. We test this hypothesis by plotting G' vs φ for all starches subjected to different heating temperatures and holding times as shown in

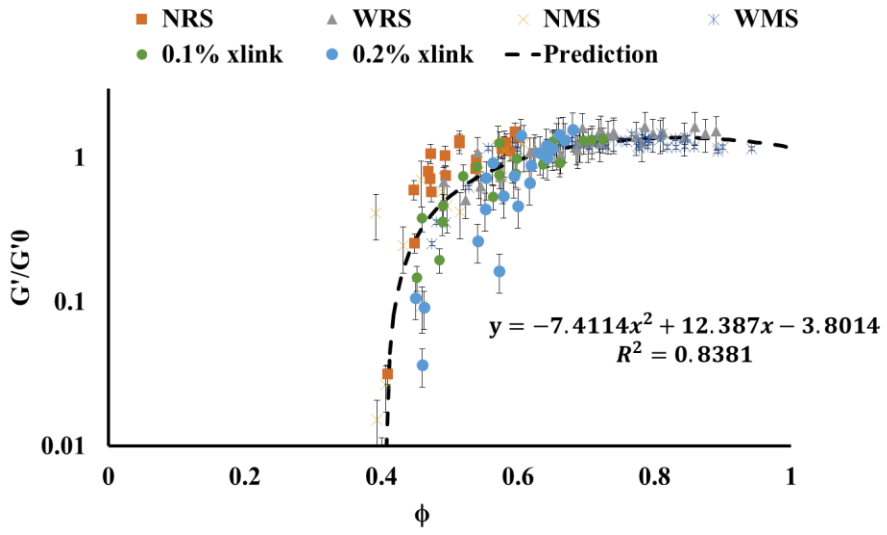

Figure 6.2. In this plot, the volume fraction of starch is calculated from the granule size distribution as discussed above in method section. The experimental data for waxy maize and waxy rice seem to fall into a single master curve. However, the data for NMS and NRS fall into the master curve only at lower temperatures and heating times, i.e. for 80 ºC for NMS and for 85 ºC for NRS.

For higher heating temperatures and times, G' for NMS and NRS fall below the master curve. This behavior is believed to be due to softening of the granules which is consistent with peak force measurement. If one discounts these data points, the remaining data points as shown in Figure 7b fall into a master curve confirming the hypothesis that G' of different starch suspensions depend only on its volume fraction. Interestingly, G' increases dramatically around the volume fraction of 0.4 and plateaus to a constant value as the volume fraction is that of close packed (0.64) or above. The equation of the fitted master curve is given in the inset of

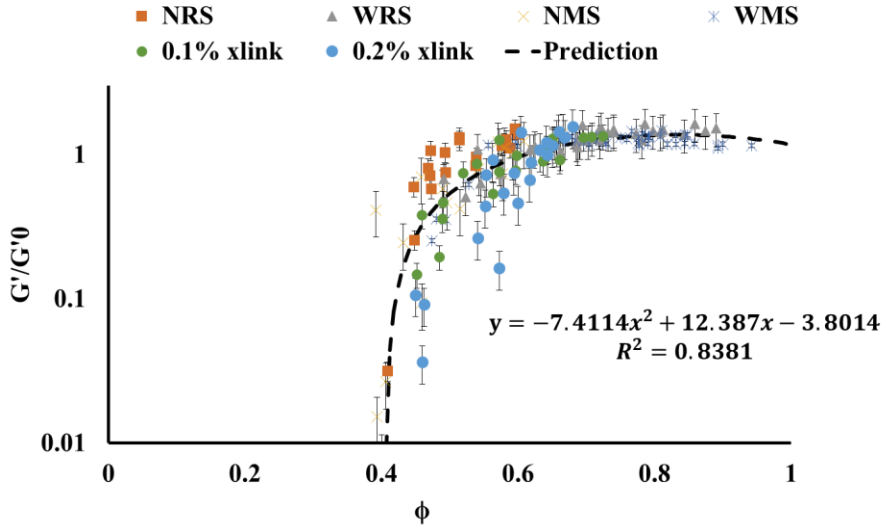

Figure 6.2. The correlation coefficient for the fit of master curve is 0.778.

6.5 Prediction of G' for Concentrated Starch Suspension

When the volume fraction of swollen granules becomes greater than 0.65, close packed volume fraction of spheres, granules deform and assume a dodecahedral structure, separated by thin films of aqueous phase. Three such films intersect at the dihedral angles of 120˚ in a channel called Plateau border. Four and only four these edges meet at a point at the angles of α (109˚28'16", the tetrahedral angles) to satisfy the laws of Plateau. The suspension therefore has a foam structure with thin films and interconnected Plateau borders.

At low strains, the starch paste (suspension of swollen granule) is elastic, i.e. applied stress is proportional to strain with an elastic modulus that is weakly dependent on the volume fraction. Above a yield stress, the paste would begin to flow and becomes plastic with a shear thinning behavior. In this project, we will be mainly concerned with the elastic behavior of the paste. The solid foam structure of high volume fraction suspension of swollen granules can be pictured as

interconnected randomly oriented elastic thin films. The surface area of a microstructural element is given by

$$S_0 = 6l_0^{\,2} \sin\alpha \qquad (6\text{-}25)$$

Where l_0 is the length of microstructural element. For dodecahedral structure, $l_0 = 0.816R$, R being the average particle radius. It is assumed that foam does not rotate upon the application of shear. Let us consider a uniaxial extension of foam. The surface area of microstructural element S is given by

$$S = 2l_0^{\,2}\left(2\lambda_1\lambda_2 + \lambda_2^{\,2}\right) \qquad (6\text{-}26)$$

Where λ_1 and λ_2 are principles stretches during uniaxial extension such that $\lambda_1 > \lambda_2$. For an incompressible deformation,

$$\lambda_1\lambda_2^{\,2} = 1 \qquad (6\text{-}27)$$

Therefore,

$$S = 2l_0^{\,2}\left(2\lambda_1^{1/2} + \frac{1}{\lambda_1}\right) \qquad (6\text{-}28)$$

The principal stretch λ_1 is related to strain ε via

$$\lambda_1 = \left(1 + 2\varepsilon\right)^{1/2} \qquad (6\text{-}29)$$

The shear modulus for foam G' is given by

$$G_0' = \frac{1}{2}\left(\frac{\partial^2\left(S/S_0\right)}{\partial\varepsilon^2}\right)_0 \Delta p \qquad (6\text{-}30)$$

Where the subscript 0 refers to the reference un-deformed state, Δp is the pressure difference across the thin film and γ is the surface free energy. From eq. (6-28), we get,

$$\left(\frac{\partial^2\left(S/S_0\right)}{\partial\varepsilon^2}\right)_0=\frac{1}{2} \qquad (6\text{-}31)$$

For monodispersed granules, $\Delta p=2\gamma/R$ Therefore,

$$G_0^{'}=\frac{\gamma}{2R} \qquad (6\text{-}32)$$

The experimental data of G' vs ϕ for waxy and cross linked maize increase with volume fraction and asymptotically reach a limiting value of $G'_{0,\exp}$ as can be seen from Figure 6.1. One can estimate the asymptototic value of elasticity of suspension at high volume fraction using eq. (6-8) from the knowledge of interfacial free energy of stach granule.

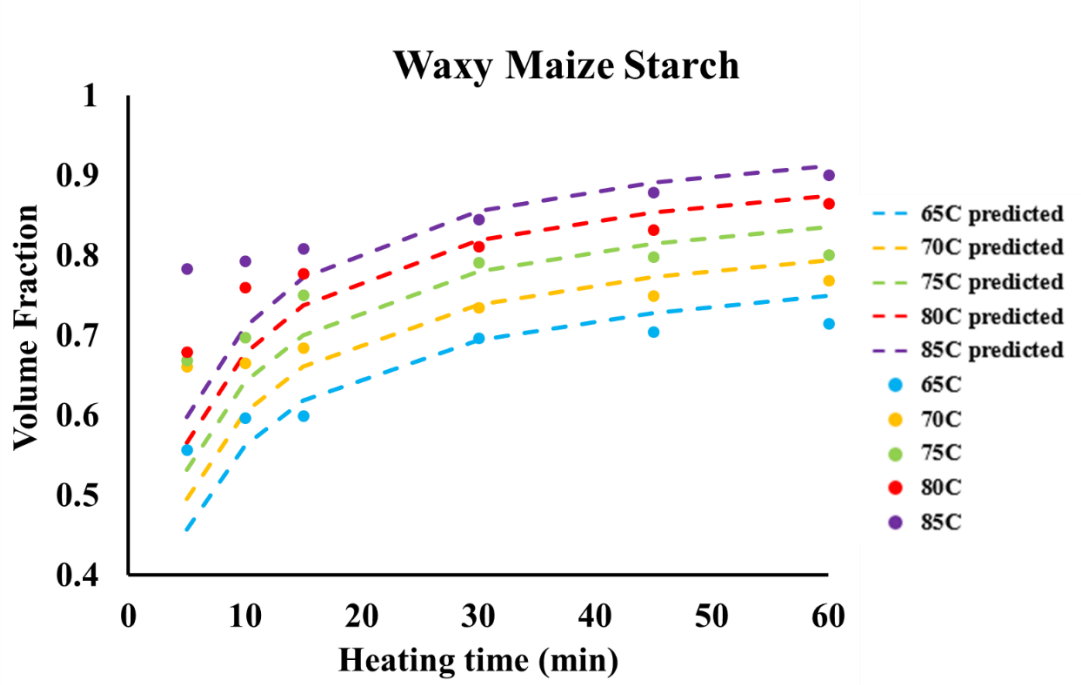

Figure 6.4: Predicted Volume fraction vs measured volume fraction for waxy maize starch

Table 6.2: Predicted and measured G’ at 4Hz oscillatory frequency of waxy maize starch heated at 65°C, 75°C and 85°C for 30 min

	Measured		Predicted	
	ϕ	G' (4 Hz)	ϕ	G' (4 Hz)
65C	0.70	470.92	0.68	428.88
75C	0.79	514.25	0.76	494.65
85C	0.84	519.32	0.84	531.86

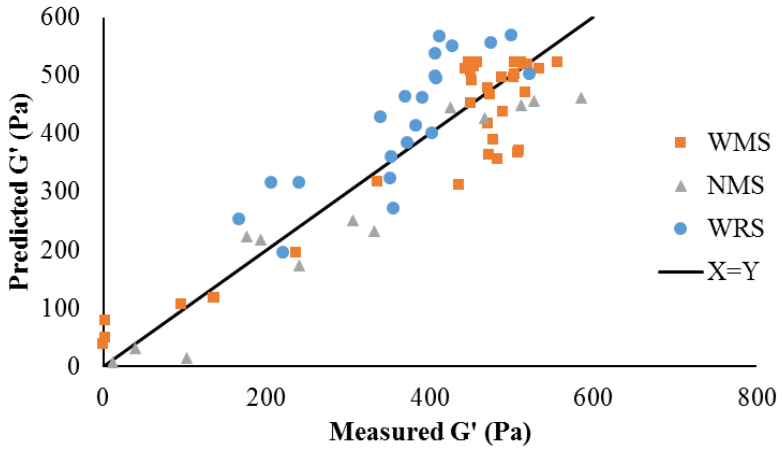

Figure 6.5: Plot of predicted and experimental G' of waxy maize starch, normal maize starch, and waxy rice starch.

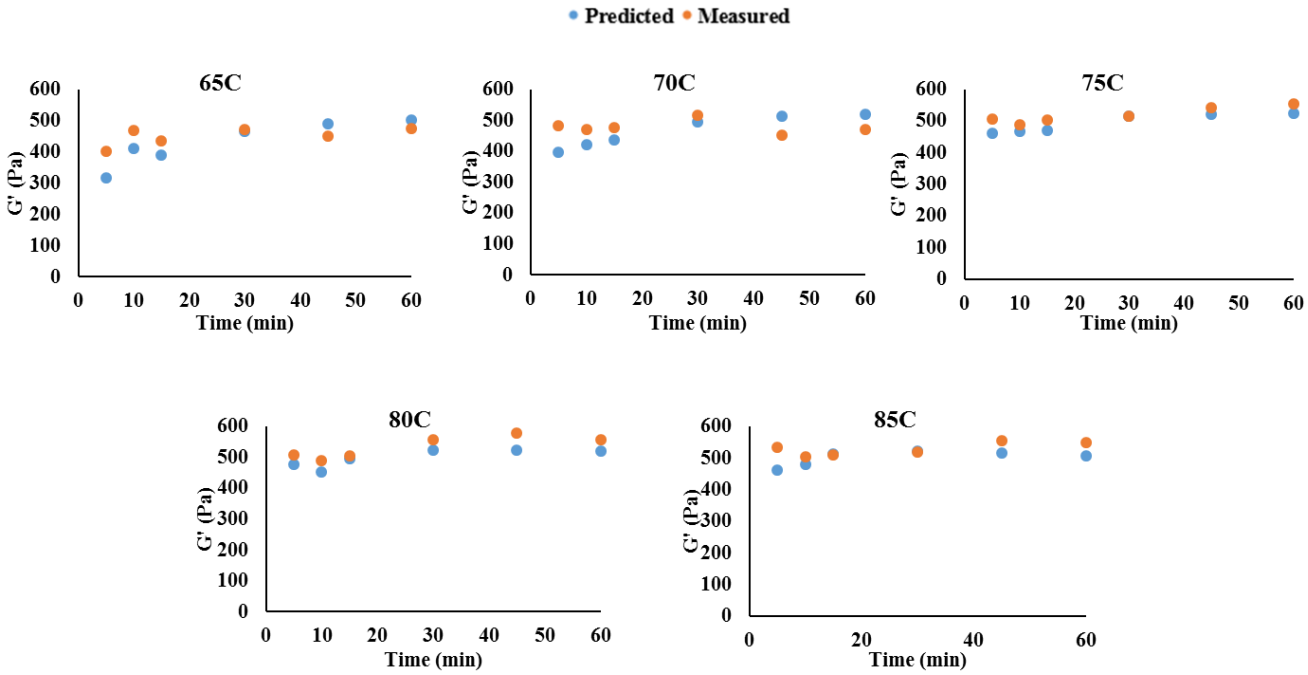

Figure 6.6: Predicted G' and measured G' versus hold time for waxy maize starch at 65, 70, 75, 80 and 85°C

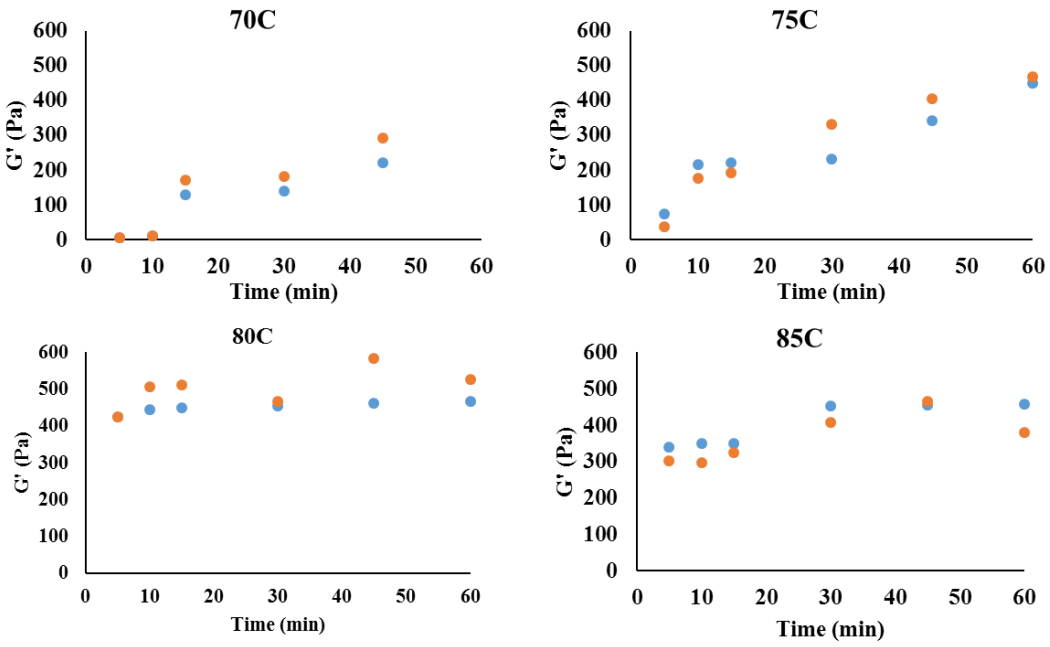

Figure 6.7: Predicted G’ and measured G’ versus hold time for normal maize starch at 70, 75, 80 and 85°C

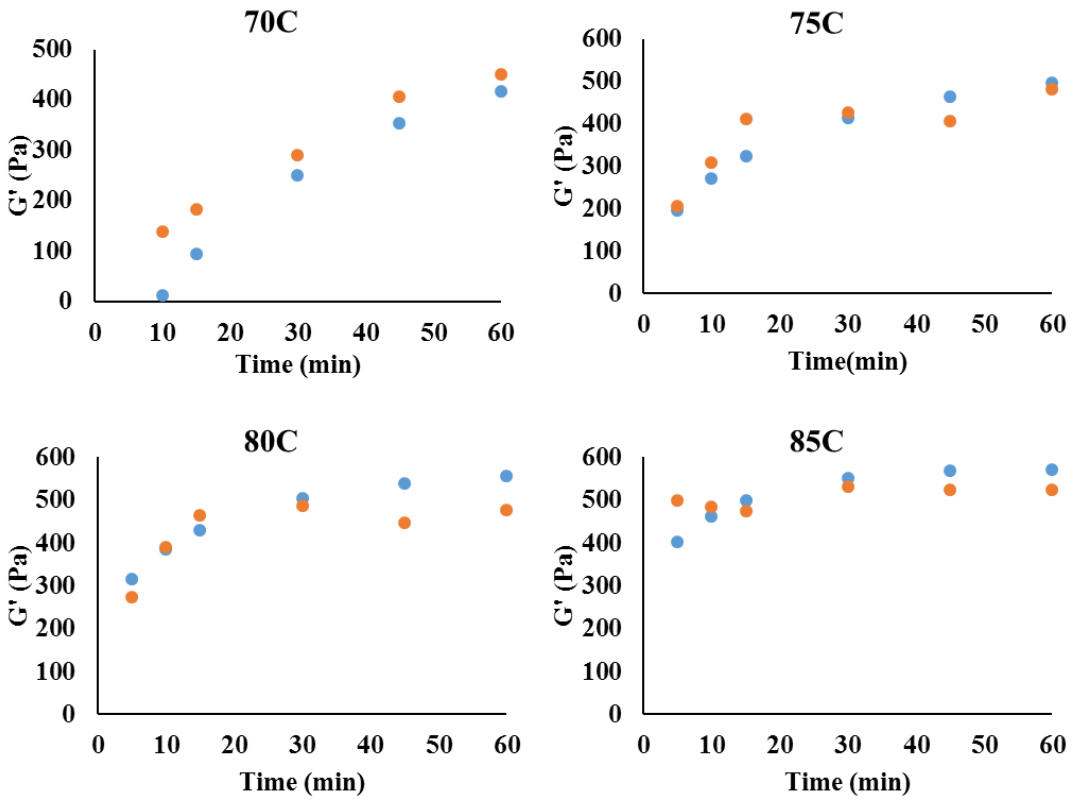

Figure 6.8: Predicted G' and measured G' versus hold time for waxy rice starch at 70, 75, 80 and 85°C

6.6 Apparent viscosity vs shear rate for all above cases

Figure 6.9- 6.11 plot the apparent viscosity of a starch suspension as function of shear rate and shear stress for different heating temperatures (60 min holding time). The suspension is shear thinning. The apparent viscosity increases dramatically with increasing temperature due to the more pronounced swelling of granules. At higher temperatures of 90 and 95 °C, the suspension appears to exhibit a yield stress – i.e., a diverging apparent viscosity below a critical shear stress (Fig. 6.9). This behavior is not observed at lower temperatures of 70 and 75 °C – in fact, at these temperatures, the suspension appears Newtonian at shear stresses below 10 Pa. These observations are consistent with previous studies (Bagley & Christianson, 1983; Christianson & Bagley, 1983).

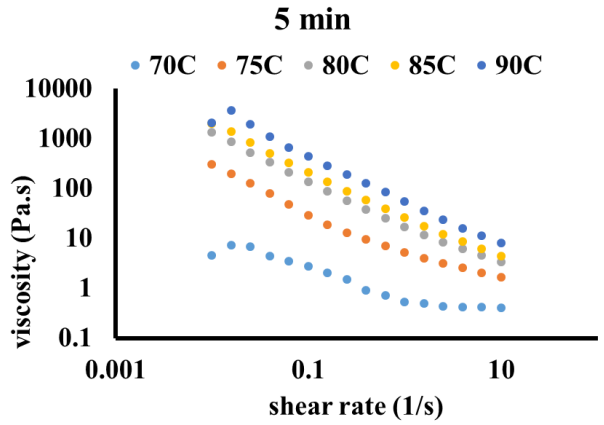

(a)

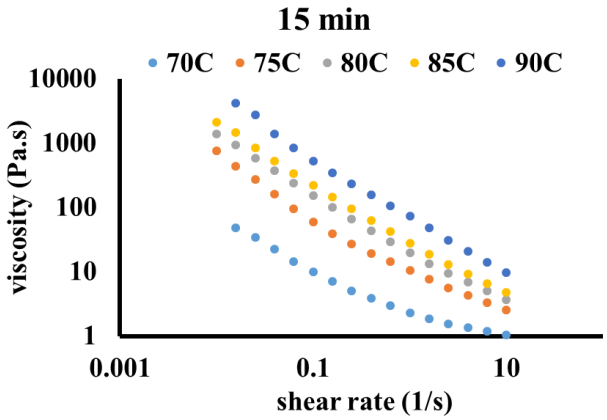

(b)

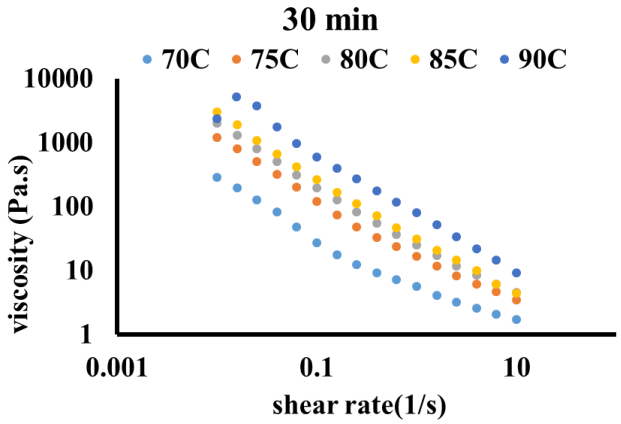

(c)

Figure 6.9: viscosity vs shear rate for normal maize starch heated for (a) 5 min, (b) 15 min and (c) 30 min at 70°C, 75°C, 80°C, 85°C and 90°C

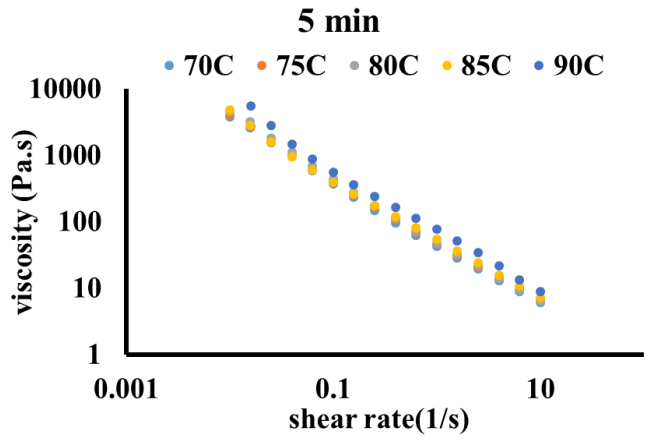

(a)

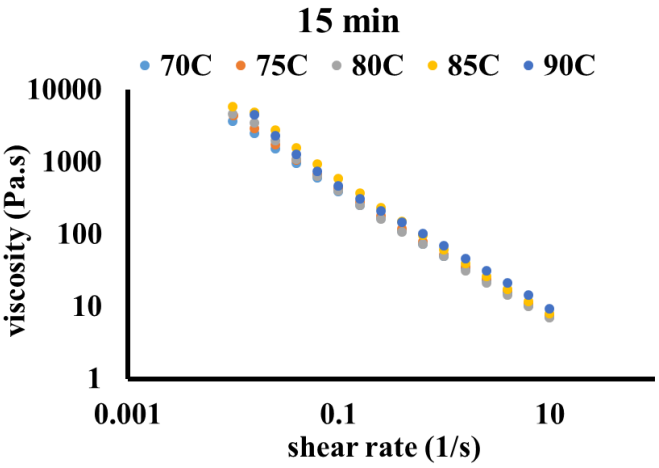

(b)

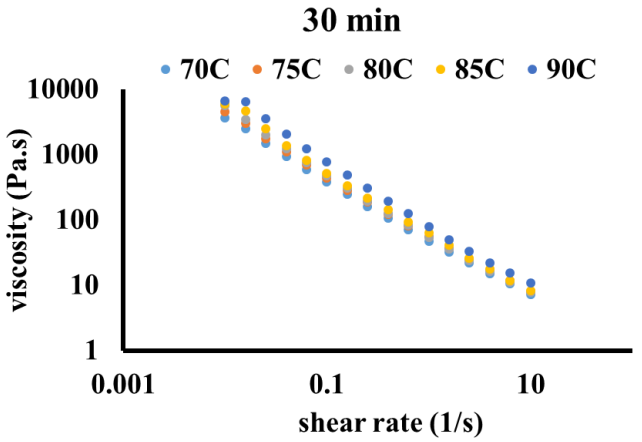

(c)

Figure 6.10: viscosity vs shear rate for waxy maize starch heated for (a) 5 min, (b) 15 min, (c) 30 min and (d) 45 min at 70°C, 75°C, 80°C, 85°C and 90°C

Figure 6.10 continued

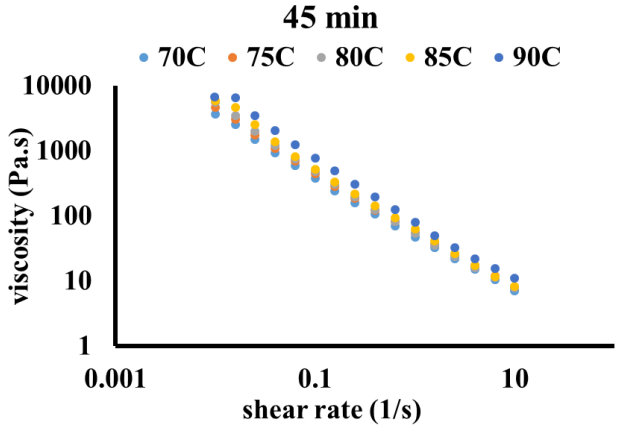

(d)

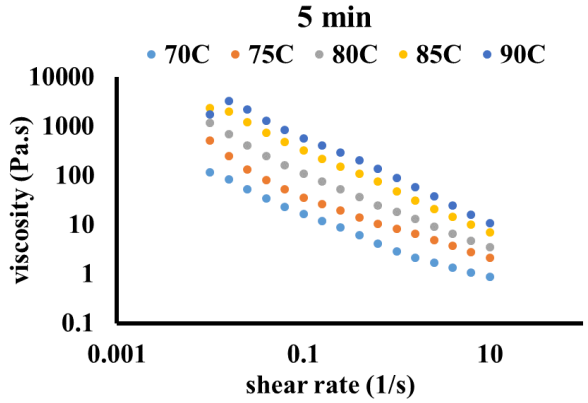

(a)

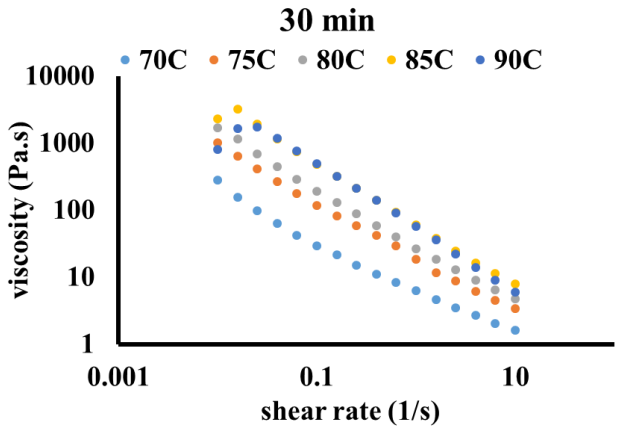

(b)

Figure 6.11: viscosity vs shear rate for normal rice starch heated for (a) 5 min, (b) 15 min, (c) 30 min and (d) 45 min at 70°C, 75°C, 80°C, 85°C and 90°C

Figure 6.11 continued

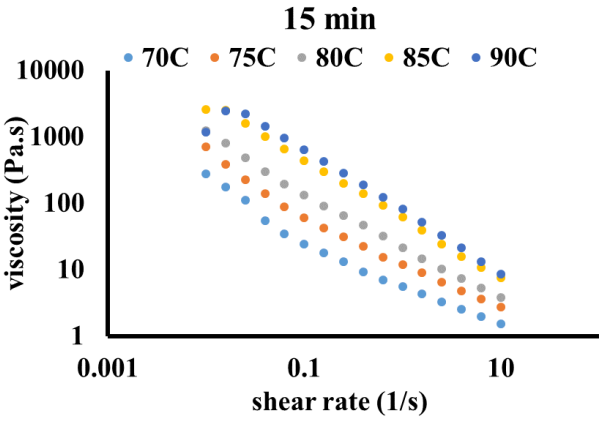

(c)

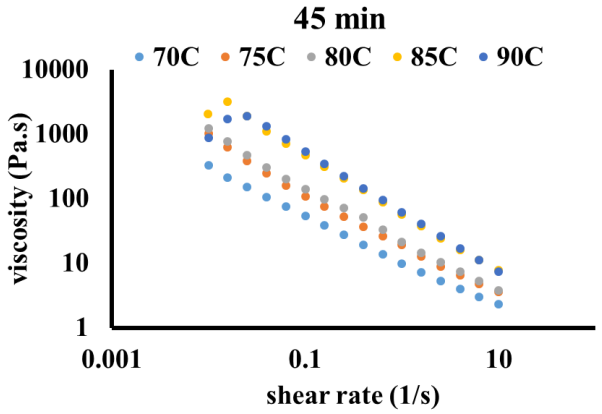

(d)

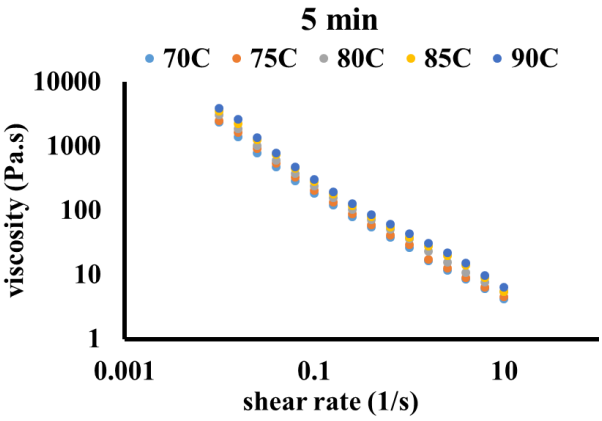

(a)

Figure 6.12: viscosity vs shear rate for waxy rice starch heated for (a) 5 min, (b) 15 min, (c) 30 min and (d) 45 min at 70°C, 75°C, 80°C, 85°C and 90°C

Figure 6.12 continued

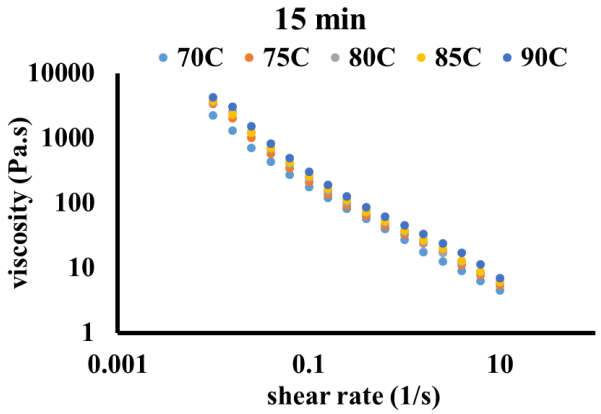

(b)

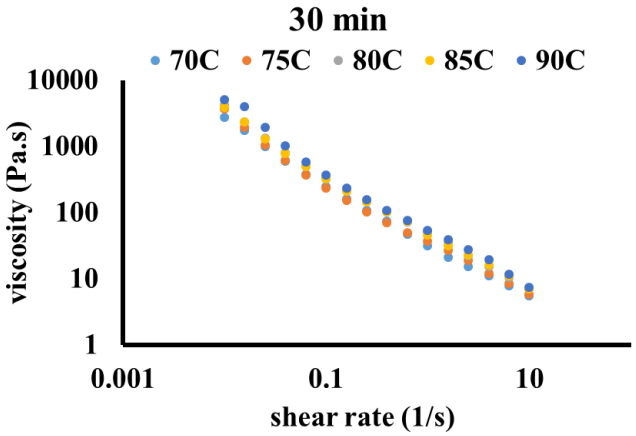

(c)

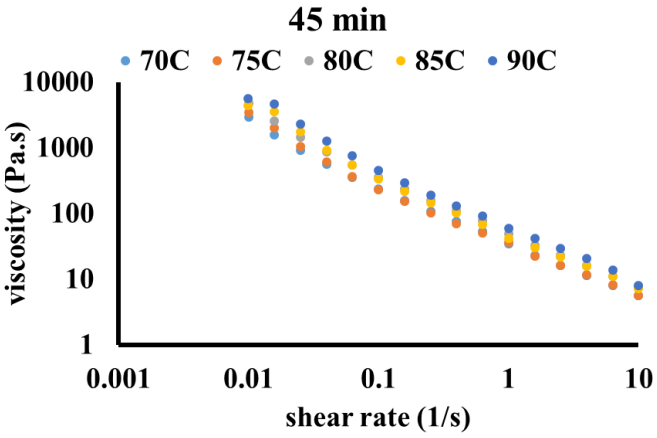

(d)

6.7 Yield stress values for different temperatures and holding times

The starch suspensions were found to exhibit a yield stress. The variation of yield stress for different heating temperatures and holding times for different starch samples are shown in Fig. . The yield stress is found to increase with holding temperature as well as time with this increase being more pronounced at lower temperatures. The yield stress is also plotted as a function of volume fraction of starch suspension for different heating times and temperatures in Figure 6.14. The actual number of the measurement is shown in Table 6.3. Interestingly, yield stress when expressed in terms of volume fraction falls into a single curve for different heating times and temperatures. The yield stress is the lowest for normal maize (varying from 0.367 to 55.876 Pa) and highest for waxy maize. In addition, the rate of increase of yield stress with volume fraction was highest for waxy and lowest for normal. Yield stress behavior of cross linked starches were found to be the same as that of waxy maize as can be seen from the superposition of yield stress data for the three systems.

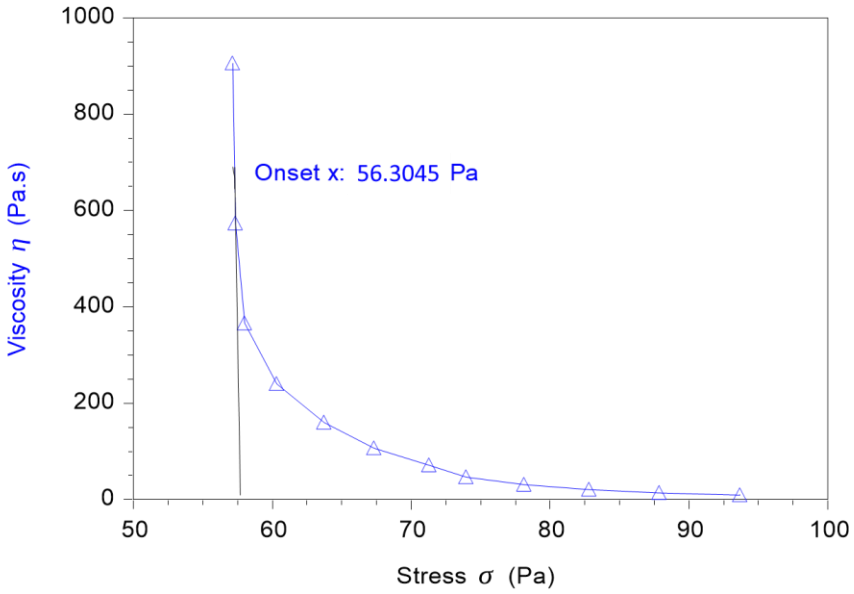

Figure 6.13: Plot of apparent viscosity vs stress for normal rice starch heated at 90°C for 5 min. The stress at which viscosity goes to infinity is the yield stress.

Table 6.3: Yield stress of starch paste at fixed time and temperature

WMS (Novation2300)					
	70°C	75°C	80°C	85°C	90°C
5	16.9073	38.7784	43.9202	47.9548	56.3045
15	20.6285	40.4258	43.7776	47.0241	59.2806
30	22.6263	43.0776	47.7057	51.4916	78.0865
45	24.1015	43.5813	49.7124	60.4	76.3126
NMS (Melojel)					
5	0.366183	3.19375	13.2948	20.4167	43.7039
15	0.906123	6.28951	14.7452	21.2528	53.739
30	3.27312	12.9058	19.999	27.0119	62.1232
45	4.613146	17.48032	25.024	34.2429	55.876
WRS (Novation 8300)					
5	16.9073	20.8315	23.8219	25.7577	30.6831
15	18.1319	21.379	24.8015	28.3986	31.9162
30	22.4537	23.3712	31.4129	32.3959	36.7055
45	23.9293	24.2485	34.5518	35.614	45.457
NRS (Penpure30)					
5	1.32422	3.38899	10.441	31.2104	52.3614
15	2.46841	5.5333	12.2661	40.6682	56.4874
30	2.99662	9.65774	16.9384	44.6744	47.152
45	3.37897	10.261	19.3575	46.6605	53.1395
0.1% Xlink NMS					
	70	75	80	85	90
5	N/A	0.109	0.1682	5.4874	13.0092
15	N/A	0.07716	0.1888	7.00227	16.5192
30	0.00437	0.0754	0.3101	10.6389	21.619
45	0.02069	0.08109	0.9367	14.7737	30.0162
0.2% Xlink NMS					
	70	75	80	85	90
5N/A		0.07716	0.1888	4.00227	11.5192
15	0.01124	0.0712	0.87949	6.4355	13.8961
30	0.01148	0.080189	0.25607	9.1464	12.0739
45	0.0361	0.0965	0.9855	14.0606	17.2898

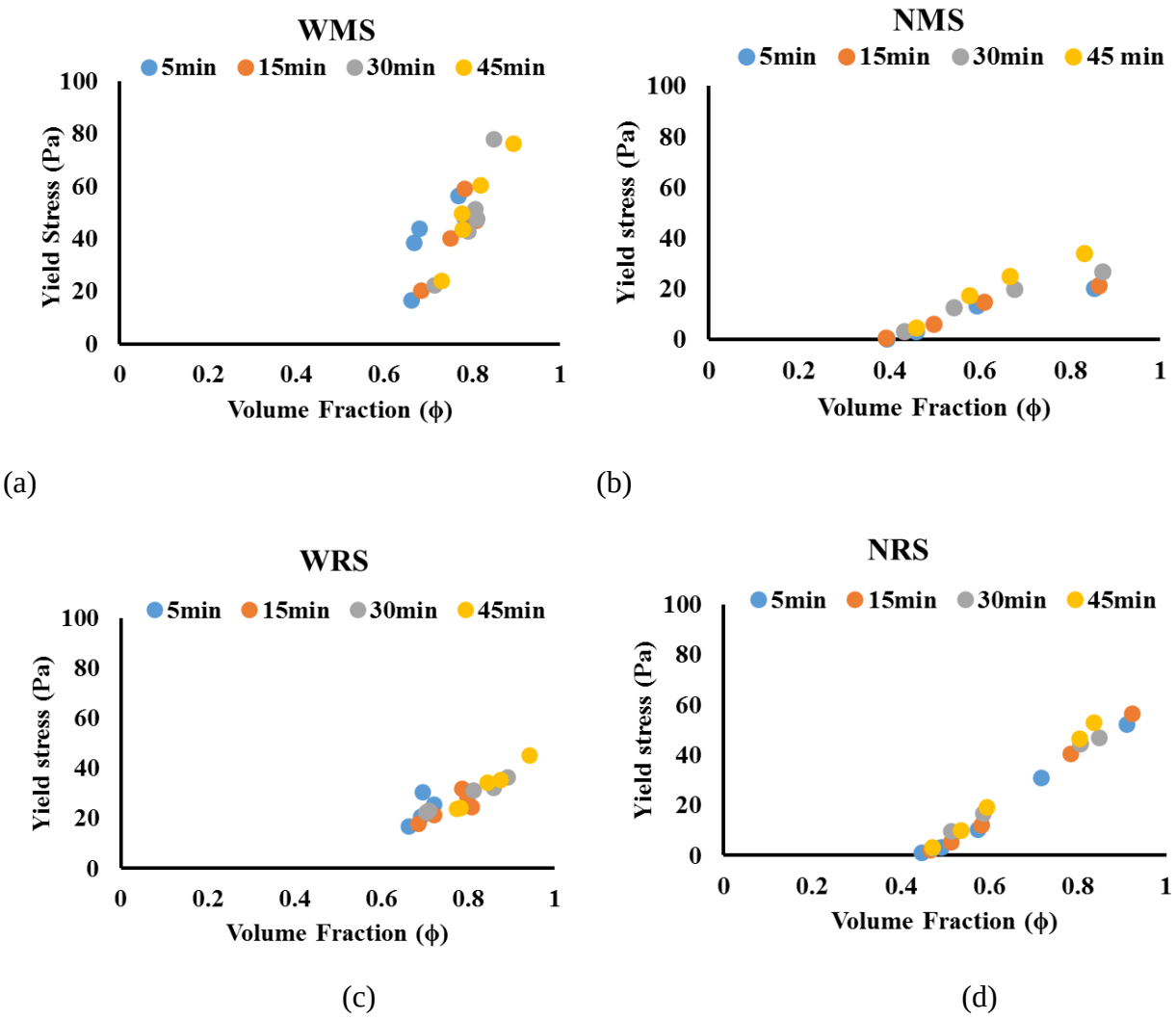

Figure 6.14: Yield stress vs volume fraction

6.8 Amylose leach-out during gelatinization

In order to investigate whether the increase in G' is due to amylose leached out over the time in normal maize starch, the amylose content in the continuous phase was measured. Result shows that there is not significant difference in amylose leached-out among different holding time at 75C and 80C (Figure 6.15).

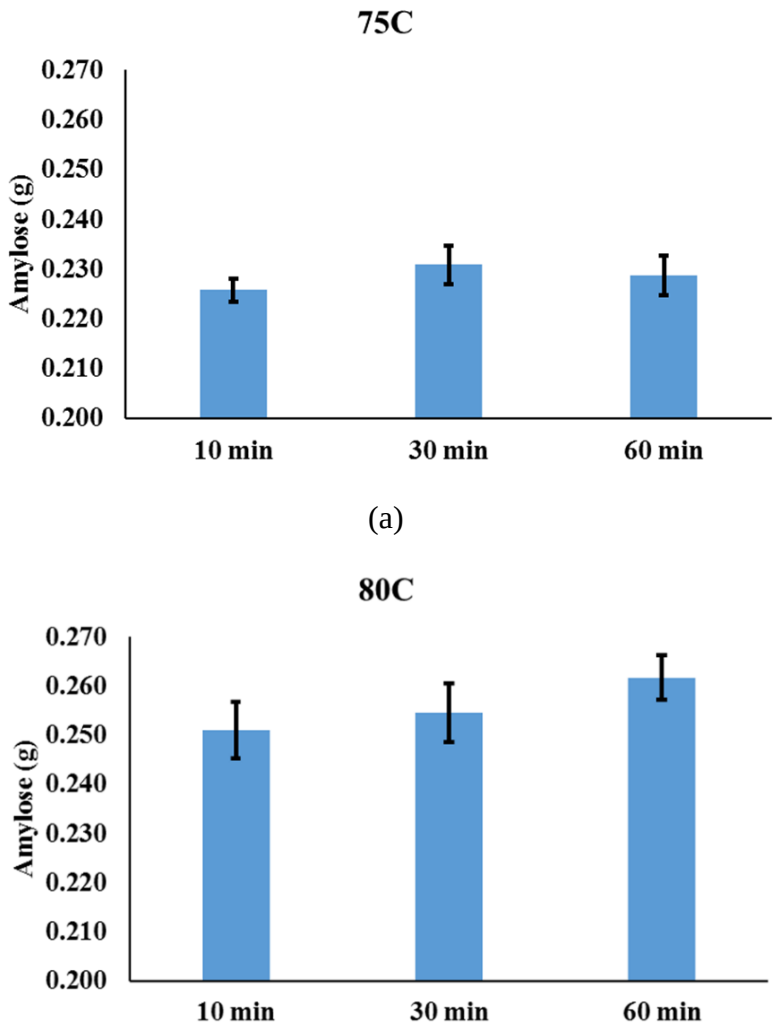

Figure 6.15: Amylose leached out from normal maize starch heated at (b) 75°C and (b) 80°C for 10, 30, and 60 min shows no significant difference

6.9 Interfacial free energy between starch paste and water

Precise characterization of solid material surfaces is studied by measuring contact angles of the substrate with a given liquid. Young equation (Eq. 6-33) describes the balance at surface contact of solid, liquid and gas. γ_{sv} is the surface energy of the solid, γ_{sl} is the interfacial tension between solid and liquid, γ_{lv} is the surface tension of liquid. The surface tension of liquid is a property of the chosen liquid. In order to calculate the surface free energy from contact angle, the other unknown variable γ_{sl} needs to be determined. Fowkes (Owens & Wendt, 1969) developed a way to calculate γ_{sl} based on the two surface tension γ_{sv} and γ_{lv} and the similar interactions between

the phases, which is approximated by taking geometric mean of a dispersive part and a non-dispersive part of the surface free energy or surface tension (Eq. 6-34). With Eq. 6-33 and Eq. 6-34 combined, the two unknown variables can be solved as written in OWRK equation (Eq. 6-35). γ_{lv}^{d} is dispersive component of liquid and γ_{lv}^{p} is polar component of liquid.

$$\gamma_{sv} = \gamma_{sl} + \gamma_{lv}\cos\theta_{\gamma} \tag{6-33}$$

$$\gamma_{sl} = \gamma_{sv} + \gamma_{lv} - 2\sqrt{\gamma_{sv}^{d}\gamma_{lv}^{d}} - 2\sqrt{\gamma_{sv}^{p}\gamma_{lv}^{p}} \tag{6-34}$$

$$\sqrt{\gamma_{sv}^{d}\gamma_{lv}^{d}} + \sqrt{\gamma_{sv}^{p}\gamma_{lv}^{p}} = 0.5\gamma_{lv}\,(1 + \cos\theta_{\gamma}) \tag{6-35}$$

These three variables are known properties of the liquid, which in this case is water. γ_{sv}^{d} is dispersive component of surface free energy, and γ_{sv}^{p} is the polar component of surface free energy. The OWRK method requires two liquids with known disperse and polar component to solve for the surface free energy of the solid. OWRK is one of the most common methods for surface free energy calculation.

In this study, Biolin Scintific's Theta tensiometer equipped with One Attention software was used to measure contact angle. The polar liquid is water and dispersive liquid is diiodomethane. Starch paste sample was evenly spread on a piece of glass slide to ensure there was no bubbles or lumps. The slide then was air-dried for 2 hours to ensure that no wet spot was left. During the contact angle measurement for water and diiodomethane, a droplet size of 2 µL was placed at a speed of 0.5 µL/s onto the glass slide.

It is to be noted that G' vs ϕ for normal maize exhibits a maximum at an intermediate volume fraction and therefore does not reach a limiting value (Figure 6.1). Such a behavior is believed to be due to breakage of granules as a result of swelling especially at high temperature (above 80°C) and longer holding time (above 45 min). Therefore, the surface free energy of normal maize could be calculated through the measurement in contact angles. The calculated values of surface free energy for the other three starch samples are given in Table 6-4. The surface free energy of NRS, WRS, NMS, WMS, 0.1% crosslinked NMS, and 0.2% crosslinked NMS are 6.98 mN/m, 4.36 mN/m, 14.6 mN/m, 11.31 mN/m, 7.25 mN/m, 8.32 mN/m respectively. These values are much smaller than corresponding interfacial tension values for organic solvent, such as Hexane and Octane against water (of the order of 50 mN/m) (Prince, 1967). The surface tension of water at

20°C is 72.62 mN/m (Vargaftik, Volkov, & Voljak, 1983). This seems to suggest that the granule surface is more compatible with water. The decrease in surface free energy for maize starch to that for rice starch implies that the higher G' is associate with higher hydrophilicity of granule surface. The decrease in surface free energy for crosslinked maize compared to that for normal maize implies that crosslinking makes the granule surface more hydrophilic. This is believed to be the result of higher charges as evidenced by our earlier reported results of zeta potential (Desam et. al.).

Table 6.4: Interfacial tension between starch paste and water

	condition	γ_{ls} (mN/m)	Std. dev
NRS	90°C, 15 min	6.98	0.45
WRS	90°C, 60 min	4.36	0.68
NMS	85°C, 30 min	14.6	1.50
WMS	90°C, 60 min	11.31	1.81
0.1% NMS	90°C, 60 min	7.25	0.77
0.2% NMS	90°C, 60 min	8.32	0.37

CHAPTER 7. CONCLUSION AND FUTURE RECOMMENDATIONS

7.1 Conclusion

In this study, we report the storage and loss moduli of different types of starch suspensions when heated to different temperatures. We develop a correlation between the storage modulus and volume fraction of starch granules which is able to collapse the experimental data apparently into a master curve. We also characterize the deformability of granules due to softening when heated to high temperatures and discuss its effect on the modulus of elasticity.

From the experiment data, it is concluded that G' increases rapidly at small times and tends to level off at longer times approaching equilibrium. Additionally, G" is much smaller than G' indicating that the swollen starch suspension is more elastic and less viscous. The peak force measurement shows that deformability of starch granules in normal maize and rice resulted in a decrease in G'. With the STMP used to cross link starch granules, the swelling power becomes lower and integrity is higher against heat and shear. G' is therefore lower for crosslinked starch and decreases with the extent of crosslink as a result of less swelling

Key comparison among starches derived from different species shows that normal starch granules tend to rupture at a higher heating temperature and heating time. Under the same heating condition, waxy maize starch has the highest G'. Yield stress is highest for waxy maize starch and increased with volume fraction of starch suspension for all starches. Crosslinking resulted in a smaller yield stress. Granules swelling power is higher for rice starch compared to maize.

Last but not the least, G' for different types of starch subjected to different heating temperatures can be collapsed into a master curve in terms of volume fraction of suspension. The master curve can be normalized in terms of interfacial free energy of different types of starches. The normalized master curve can be used along with a mechanistic model for starch swelling to predict the evolution of viscoelasticity of any starch suspension subjected to different heating temperatures

7.2 Future Recommendations

7.2.1 Stokesian dynamics simulation for prediction of G' as a function of volume fraction for intermediate volume fractions of starch suspension (moderately concentrated)

Particles suspended in a fluid medium are very common in nature and engineering field. There is a large body of literature on non-Newtonian rheological behavior of these multiphase materials. The general observations for dense suspensions can be summarized as following:

1. As shear rate increase, it is observed that at first the shear viscosity decreases; at higher shear rates, the shear viscosity goes to a minimum and they may increase to a much higher value if the suspension is shear thickening or dilatant.
2. As particle volume fraction increases, these rheological responses are intensified.
3. Discontinuing in shear viscosity, normal stress differences and yield stresses have also been reported.

There's still no clear physical understanding and explanation for these non-ideal rheological response of flowing suspensions because in many experiments the characterization for both chemistry and transport mechanisms operating in the suspensions is often difficult and incomplete. Predicting the rheological behavior of concentrated suspensions is a difficult and challenging theoretical problem. Theories must be able to address the physics of many body hydrodynamic interactions and the important near-field lubrication forces in dense suspensions.

Stokesian Dynamics simulation programs can be used for modeling a wide variety of particulate flows. Phung's thesis work focused the "rheological" behavior that includes the shear viscosity, normal stress difference, as well as the short- and long-time self-diffusion coefficients. Molecular-dynamics-like computer simulations are a promising tool for studying concentrated colloidal suspensions. Simulation, together with experiments can provide the physical understanding which is necessary for theoretical development. Among the simulation methods, Stokesian Dynamics is an excellent choice because it is capable of treating dense flowing suspensions and the computational algorithm is efficient. The methods allows simulation of flowing suspension with particle volume fractions from infinite dilution to dense packing and a continuous range of Péclet number.

- Péclet number <1 → strong Brownian motion

- Péclet number ~ 10, sus[ension no longer shear things and the shear viscosity is minimized. The balance of hydrodynamic and Brownina forces induce a strongly ordered flowing suspension with hexagonally packed strings of particles flowing with the bulk flow.
- Péclet number > 100, the suspension shear thickens due to formation of large elongated clusters of particles. Hydrodynamics contribute all particle stress as the direct Brownian contribution has essentially vanished.
- The complete relation of steady shear viscosity to particle volume fraction and Péclet number for concentrated hard-sphere suspensions is given.

The microstructural mechanics governing suspensions include hydrodynamic forces, stochastic forces which give rise to Brownian motion, internal and external forces acting on particles, as well as their temporal and spatial distribution which is commonly referred to as the suspension microstructure.

Phung's PhD dissertation also summarized study done on rheology of concentrated suspensions of hydrodynamically interacting colloidal particles in a simple shear flow by Stokesian Dynamics simulation. The simulation allows us to determine the microstructure and it's relation to the bulk properties according to the time evolution of particle configurations. In the 3D simulations developed by Phung, there was more details of microstructure provided and can be compared directly with experiment. For the shear viscosity, both 3D and monolayer simulations at comparable areal and volume fraction give similar results, indicating the correct physics in monolayer simulations. In the case of hard-sphere fluid, the interparticle potential is zero but becomes infinite when particles come in contact. We use hard-sphere model because it's fundamental and simple, yet it has a phase transition at high particle volume fraction. The only parameter in the equilibrium hard-sphere fluid is the particle volume fraction.

Bossis and Brady (1987 and 1989) developed and pioneered the application of Stokesian dynamics to study the rheology and self-diffusivities of hard sphere suspensions in simple shear flow. Puseu and van Megen Have reported a detailed study for colloidal hard spheres using PMMA/decalin/CS2 system, where they were able to determine the remarkable phase diagram for the hard-sphere model. This is a great motivation for engineers and scientist to predict the

rheological behavior of not just the equilibrium Brownian suspensions but also the more practical flowing hard spheres.

The rheology of suspension of particles can be predicted by evaluating the stress of a sample volume consisting of N particles when subjected to periodic shear strain. The particle motion can be described by N-body equation of motion

$$\mathbf{m}.\frac{d\mathbf{U}}{dt} = \mathbf{F}^H + \mathbf{F}^p$$

Where $\mathbf{m}$ is the generalized mass/moment of inertia tensor, $\mathbf{U}$ is the particle translational/rotational velocity vector of dimension 6N, and 6N force/torque vectors $\mathbf{F}$ represent (i) hydrodynamic forces $\mathbf{F}^H$ exterted on the particles as a result of relative motion of fluid and (ii) interparticle van der Waals and electrostatic forces $\mathbf{F}^p$. For small Reynolds number, the equation of motion is given by Stokes equation which is linear. As a result, the hydrodynamic interaction is given by,

$$\mathbf{F}^H = -\mathbf{R}_{FU}.\left(\mathbf{U} - \langle \mathbf{U} \rangle\right) + \mathbf{R}_{FE} : \langle \mathbf{D} \rangle$$

In the above equation, $\mathbf{R}_{FU}$ and $\mathbf{R}_{FE}$ are resistance tensors due to relative motion of liquid and external imposed flow respectively and $\langle \mathbf{D} \rangle$ is the rate of strain tensor. The interparticle van der Waals and electrostatic forces are already described in the earlier section. The evolution of separation of particles with time can be obtained by integrating the equation of motion of assemblage of particles twice to obtain,

$$\Delta \mathbf{x}^* = \left\{ \langle \mathbf{U} \rangle + \mathbf{R}_{FU}^{-1}.\left[\mathbf{R}_{FE} : \langle \mathbf{D} \rangle + \mathbf{F}^p \right] \right\} \Delta t^*$$

The above equation is non dimensionalized so that $\mathbf{x}^* = \mathbf{x}/a$ and $t^* = t\dot{\gamma}_{\max}$, $\dot{\gamma}_{\max}$ being the maximum shear rate. We would like to evaluate the stress due to imposition of a periodic strain in xy plane along x direction, i.e. $\gamma_{zx} = \gamma_0 \sin \omega t$ where γ_0 is the amplitude of imposed strain and ω is the frequency. The stress is given by

$$\langle \boldsymbol{\sigma} \rangle = -p\mathbf{I} + 2\eta \langle \mathbf{D} \rangle + \langle \boldsymbol{\sigma}_p \rangle$$

p is the pressure, η is the viscosity and $\langle \boldsymbol{\sigma}_p \rangle$ is the stress due to particles which is given by,

$$\left\langle \boldsymbol{\sigma}_p \right\rangle = n\left\{ \left\langle \mathbf{S}^H \right\rangle + \left\langle \mathbf{S}^p \right\rangle \right\}$$

The stress can then be evaluated on xy plane which can be expressed in terms of G' and G'' as

$$\left\langle \boldsymbol{\sigma} \right\rangle_{x,y} = \gamma_0 G'(\omega)\sin\omega t + \gamma_0 G''(\omega)\cos\omega t$$

The storage and loss moduli can be evaluated using

$$G'(\omega) = \frac{\omega}{\gamma_0 \pi}\int_0^{2\pi/\omega} \left\langle \boldsymbol{\sigma} \right\rangle_{x,y}(t)\sin\omega t dt$$

$$G''(\omega) = \frac{\omega}{\gamma_0 \pi}\int_0^{2\pi/\omega} \left\langle \boldsymbol{\sigma} \right\rangle_{x,y}(t)\cos\omega t dt$$

7.2.2 Characterization of the effect of starch-hydrocolloid and starch- oligosaccharide interactions on master curve for dependence of viscoelasticity in terms of volume fraction

The addition of hydrocolloids can modify and control the characteristics of starch granule swelling during processing, which determines the texture and stability of high-moisture starch-based foods. Starch is heated in excess water in an RVA or a Brabender Visco-Amylograph device. A lot of factors can affect the swelling of starch in excess water, including molecular weight distributions of amylopectin and amylose molecules, fine structures, the amount and type of the protein and lipid present, the amount of water available and the heating time, temperature, and shear(Bemiller, 2011). Gelatinization leads to pasting when starch granules are subjected to continuous heating in excess water. Granules undergo further swelling with more dissolved starch polymer molecules leaching out. This results in a viscoelastic paste, in which the dissolved starch polymer molecules form a network (continuous phase) while the swollen granules and other undissolved fragments form a discontinuous phase. The swelling of starch granule is the major factor to the viscosity rise in the paste. Factors that affect properties of paste include size distribution and nature of particles in the discontinuous phase(M. A. Rao, P. Okechukwu, P. M. S. Da Silva, & J. Oliveira, 1997), the composition and nature of continuous phase, and interactions between the two phases.

1. Granules became more swollen when heated in a hydrocolloid solution
2. Granule swelling was reduced in hydrocolloid solution. For example, the phosphate groups in potato starch granules and the negative charges on the hydrocolloid molecules.
3. There is little or no change in swelling power.

4. Xanthan can maintain the integrity of waxy maize starch granules. Maybe due to the association of xanthan with the surface of granules.
5. Xanthan reduces peak viscosity and inhibits swelling
6. Addition of hydrocolloid inhibits starch polymer (primarily amylose) leaching.

Take the xanthan and guar gum in waxy maize starch as an example, Abdulmola (1996) reported that the presence of xanthan did not change granule swelling of crosslinked waxy maize starch. In Biliaderis (1997)'s study, for example, guar gum retarded G' development and network formation, but enhanced the crystallization rate in concentrated waxy maize starch gels (40% w/w). Closs et al (1999). Concluded that the preparation method for hydrocolloid and starch granule mix influenced the rheological properties of composite pastes. Moreover, the addition of guar gum can also increase the peak temperature T_p of starch melting in the presence of a limited amount of water (Y. Kim, 1999), but it didn't affect the gelatinization temperature T_{gel} (Gonera & Cornillon, 2002).

The addition of xanthan gum could accelerate the formation of new structure of the WMS/xanthan gum mixed pastes under shear conditions. It could also decrease the in-shear recoveries of the mixture(B. Wang et al., 2009). Here is the proposed method for conducting this study in the future:

The pasting properties of starch-gum mixtures suspensions is going to be determined by RVA. The slurry concentration of 6% (w/v) starch was dispersed in 25 ml distilled water or 0.35% w/w (dry basis) gym solutions(Chaisawang & Suphantharika, 2005). When preparing starch-gum mixtures, gums are first dispersed in distilled water under magnetic stirring, heat to 80°C for 5 min and cooled to room temperature. Then starch is added in the gum solutions. The dispersions were stirred with for sufficient duration to avoid the formation of lumps, especially in the xanthan gum solution.

REFERENCES

Abdulmola, N. A., Hember, M. W. N., Richardson, R. K., & Morris, E. R. (1996). Effect of xanthan on the small- deformation rheology of crosslinked and uncrosslinked waxy maize starch. *Carbohydrate Polymers, 31*(1), 65-78. doi:10.1016/S0144-8617(96)00065-3

Alloncle, M., Lefebvre, J., Llamas, G., & Doublier, J. (1989). A RHEOLOGICAL CHARACTERIZATION OF CEREAL STARCH-GALACTOMANNAN MIXTURES. *Cereal Chem., 66*(2), 90-93.

Bagley, E. B., & Christianson, D. D. (1982). SWELLING CAPACITY OF STARCH AND ITS RELATIONSHIP TO SUSPENSION VISCOSITY-EFFECT OF COOKING TIME, TEMPERATURE AND CONCENTRATION. *Journal of Texture Studies, 13*(1), 115-126. doi:10.1111/j.1745-4603.1982.tb00881.x

Bagley, E. B., & Christianson, D. D. (1983). Yield Stresses in Cooked Wheat Starch Dispersions. *Starch - Stärke, 35*(3), 81-86. doi:10.1002/star.19830350304

Baker, J. P., Hong, I. H., Blanch, H. W., & Prausnitz, J. (1994a). Effect of initial total monomer concentration on the swelling behavior of cationic acrylomide based hydrogels. *Macromolecules, 27*, 1446-1454.

Baker, J. P., Hong, I. H., Blanch, H. W., & Prausnitz, J. (1994b). Effect of initial total monomer concentration on the swelling behavior of cationic acrylomide based hydrogels *Macromolecules, 27*, 1446-1454.

Ball, S. G., & Deschamps, P. (2009). Chapter 1 - Starch Metabolism A2 - Harris, Elizabeth H. In D. B. Stern & G. B. Witman (Eds.), *The Chlamydomonas Sourcebook (Second Edition)* (pp. 1-40). London: Academic Press.

Banks, W., Greenwood, C. T., & Muir, D. D. (1974). Studies on Starches of High Amylose Content. Part 17. A Review of Current Concepts. *Starch/Starke, 26*(9), 289.

Bello-Perez, L. A., Roger, P., Colonna, P., & Paredes-Lopez, O. (1998). Laser light scattering of high amylose and high amylopectin materials,stability in water after microwave dispersion. *Carbohydr. Polym., 37*, 383-394.

Bemiller, J. N. (2011). Pasting, paste, and gel properties of starch–hydrocolloid combinations. *Carbohydrate Polymers, 86*(2), 386-423. doi:10.1016/j.carbpol.2011.05.064

BeMiller, J. N., & Huber, K. C. (2015). Physical Modification of Food Starch Functionalities. *Annu. Rev. Food Sci. Technol., 6*(1), 19-69. doi:10.1146/annurev-food-022814-015552

Biliaderis, C. G., Arvanitoyannis, I., Izydorczyk, M. S., & Prokopowich, D. J. (1997). Effect of Hydrocolloids on Gelatinization and Structure Formation in Concentrated Waxy Maize and Wheat Starch Gels. *Starch - Stärke, 49*(7-8), 278-283. doi:10.1002/star.19970490706

Blennow, A., Bay-Smidt, A. M., & Bauer, R. (2001). Amylopectin aggregation as a function of starch phosphate content studied by size exclusion chromatography and on-line refractive index and light scattering *Int J Biol Macromol, 28*, 409.

Brotzman, R. W., & Eichinger, B. E. (1982). Volume dependence of elastic equation of state. 3. Bulk cured poly(dimethylsiloxane). *Macromolecules, 15*, 531-535.

Budiansky, B., & Kimmel, E. (1987). Elastic moduli of lungs. *Journal of Applied Mechanics, Transactions ASME, 54*(2), 351-358. doi:10.1115/1.3173019

Chaisawang, M., & Suphantharika, M. (2005). Effects of guar gum and xanthan gum additions on physical and rheological properties of cationic tapioca starch. *Carbohydrate Polymers, 61*(3), 288-295. doi:10.1016/j.carbpol.2005.04.002

Chen, P., Yu, L., Chen, L., & Li, X. (2006). Morphology and microstructure of maize starches with different amylose/amylopectin content. *Starch/Starke, 58*, 611-615.

Cheng, Y., Meng, B., Chen, M., Liu, X., Hua, Y., & Ni, Z. (2006). Laser light scattering study of structure and dynamics of waxy corn amylopectin in dilute aqueous solution. *Carbohydr. Polym., 64*, 190-196.

Choi, S. g., & Kerr, W. L. (2004). Swelling Characteristics of Native and Chemically Modified Wheat Starches as a Function of Heating Temperature and Time. *Starch - Stärke, 56*(5), 181-189. doi:10.1002/star.200300233

Choi, S. G., & Kerr, W. L. (2004). Swelling characteristics of native and chemically modified wheat starches as a function of heating temperature and time. *Starch-Stärke, 56*(5), 181-189.

Christianson, D. D., & Bagley, E. B. (1983). Apparent viscosities of dispersions of swollen cornstarch granules. *Apparent viscosities of dispersions of swollen cornstarch granules., 60*(2), 116-121.

Christianson, D. D., & Bagley, E. B. (1984). Yield stresses in dispersions of swollen, deformable cornstarch granules. *Yield stresses in dispersions of swollen, deformable cornstarch granules*(6), 500-503.

Closs, C. B., Conde-Petit, B., Roberts, I. D., Tolstoguzov, V. B., & Escher, F. (1999). Phase separation and rheology of aqueous starch/ galactomannan systems. *Carbohydrate Polymers, 39*(1), 67-77. doi:10.1016/S0144-8617(98)00048-4

Crassous, J. J., Ŕgisser, R., Ballauff, M., & Willenbacher, N. (2005). Characterization of the viscoelastic behavior of complex fluids using the piezoelastic axial vibrator. *Journal of Rheology, 49*(4), 851-863. doi:10.1122/1.1917843

Cross, M. M. (1965). Rheology of non-Newtonian fluids: A new flow equation for pseudoplastic systems. *Journal of Colloid Science, 20*(5), 417-437. doi:10.1016/0095-8522(65)90022-X

de Paepe, K. (2002). Effect of Rice Starch as a Bath Additive on the Barrier Function of Healthy but SLS-damaged Skin and Skin of Atopic Patients. *Acta Dermato-Venereologica, 82*(3), 184-187. doi:10.1080/00015550260132460

Desam, G. P., Li, J., Chen, G., Campanella, O., & Narsimhan, G. (2018a). A mechanistic model for swelling kinetics of waxy maize starch suspension. *Journal of Food Engineering, 222*, 237-249. doi:10.1016/j.jfoodeng.2017.11.017

Desam, G. P., Li, J., Chen, G., Campanella, O., & Narsimhan, G. (2018b). Prediction of swelling behavior of crosslinked maize starch suspensions. *Carbohydrate Polymers, 199*, 331-340. doi:10.1016/j.carbpol.2018.07.020

Dickinson, E. (1992). *An introduction to food colloids*. Oxford ; New York: Oxford ; New York : Oxford University Press.

Durrani, C. M., & Donald, A. M. (2000). Shape, molecular weight distribution and viscosity of amylopectin in dilute solution. *Carbohydr. Polym., 41*, 207-217.

Dzuy, N. Q., & Boger, D. V. (1983). Yield Stress Measurement for Concentrated Suspensions. *Journal of Rheology, 27*(4), 321-349. doi:10.1122/1.549709

Eliasson, A. C. (1986). VISCOELASTIC BEHAVIOUR DURING THE GELATINIZATION OF STARCH II. EFFECTS OF EMULSIFIERS. *Journal of Texture Studies, 17*(4), 357-375. doi:10.1111/j.1745-4603.1986.tb00559.x

Eliasson, A. C., & Bohlin, L. (1982). Rheological Properties of Concentrated Wheat Starch Gels. *Starch - Stärke, 34*(8), 267-271. doi:10.1002/star.19820340805

Ellis, H. S., Ring, S. G., & Whittam, M. A. (1989). A comparison of the viscous behaviour of wheat and maize starch pastes. *Journal of Cereal Science, 10*(1), 33-44. doi:10.1016/S0733-5210(89)80032-3

Escobedo, F. A. (1996). Chemical potential and dimensions of chain molecules in athermal environments. *Molecular Physics, 89*(6), 1733 - 1754. Retrieved from http://www.informaworld.com/10.1080/002689796173057

Escobedo, F. A., & Pablo, J. J. (1997). Simulation and theory of the swelling of athermal gels. *J. Chem. Phys., 106*(2), 793-810.

Evans, I. D., & Haisman, D. R. (1980). RHEOLOGY OF GELATINISED STARCH SUSPENSIONS. *Journal of Texture Studies, 10*(4), 347-370. doi:10.1111/j.1745-4603.1980.tb00865.x

Evans, I. D., & Lips, A. (1990). Concentration dependence of the linear elastic behaviour of model microgel dispersions. *Journal of the Chemical Society, Faraday Transactions, 86*(20), 3413-3417. doi:10.1039/FT9908603413

Evans, I. D., & Lips, A. (1992). VISCOELASTICITY OF GELATINIZED STARCH DISPERSIONS. *Journal of Texture Studies, 23*(1), 69-86. doi:10.1111/j.1745-4603.1992.tb00512.x

FANNON, J., & BEMILLER, J. (1992). STRUCTURE OF CORN STARCH PASTE AND GRANULE REMNANTS REVEALED BY LOW-TEMPERATURE SCANNING ELECTRON-MICROSCOPY AFTER CRYOPREPARATION. *Cereal Chemistry, 69*(4), 456-460.

Ferry, J. D. (1980). *Viscoelastic properties of polymers* (3d ed.. ed.). New York: New York : Wiley.

Flory, P. J. (1953). *Principles of Polymer Chemistry*: Cornell University Press: Ithaca, NY,.

Fredriksson, H., Silverio, J., Andersson, R., A.-C, E., & Åman, P. (1998). The influence of amylose and amylopectin characteristics on gelatinization and retrogradation properties of different starches *Carbohydr. Polym., 35*, 119.

French, D. (1984). Organization of starch granules. In R. L. Whistler, J. M. BeMiller, & E. F. Paschall (Eds.), *Starch: Chemistry and Technology* (pp. 183-247): Academic Press,Orlando.

Frith, W. J., & Lips, A. (1995). The rheology of concentrated suspensions of deformable particles. *Advances in Colloid and Interface Science, 61*, 161-189. doi:10.1016/0001-8686(95)00264-Q

Fuchs, M., & Ballauff, M. (2005). Flow curves of dense colloidal dispersions: Schematic model analysis of the shear-dependent viscosity near the colloidal glass transition. *J. Chem. Phys., 122*(9). doi:10.1063/1.1859285

Galinsky, G., & Burchard, W. (1995). Starch fractions as examples for nonrandomly branched macromolecules.1. Dimensional properties. *Macromolecules, 28*, 2363-2370.

Galliard, T., & Bowler, P. (1987). Morphology and composition of starch. In T. Galliard (Ed.), *Starch: Properties and Potential* (pp. 55-78): John Wiley and Sons, New York.

Genovese, D., & Rao, M. (2003). Role of starch granule characteristics (volume fraction, rigidity, and fractal dimension) on rheology of starch dispersions with and without amylose. *Cereal Chemistry, 80*(3), 350-355.

Glenn, G. M., Gray, G. M., Orts, W. J., & Wood, D. W. (1999). Starch-based lightweight concrete: effect of starch source, processing method, and aggregate geometry. *Industrial Crops & Products, 9*(2), 133-144. doi:10.1016/S0926-6690(98)00024-7

GluckHirsch, J. B., & Kokini, J. L. (1997). Determination of the molecular weight between crosslinks of waxy maize starches using the theory of rubber elasticity. *Journal of Rheology, 41*(1), 129-139. Retrieved from <Go to ISI>://WOS:A1997WC06400007. doi:Doi 10.1122/1.550804

Gonera, A., & Cornillon, P. (2002). Gelatinization of Starch/ Gum/ Sugar Systems Studied by using DSC, NMR, and CSLM. *Starch - Stärke, 54*(11), 508-516. doi:10.1002/1521-379X(200211)54:11<508::AID-STAR508>3.0.CO;2-K

Gunasekaran, S., & Ak, M. M. (2000). Dynamic oscillatory shear testing of foods — selected applications. *Trends in Food Science & Technology, 11*(3), 115-127. doi:10.1016/S0924-2244(00)00058-3

Hanselmann, R., Burchard, W., Ehrat, M., & Widmer, H. M. (1996). Structure properties of fractionated starch polymer and their dependence on the dissolution process. *Macromolecules, 29*, 3277-3282.

Hirotsu, S., Hirokawa, Y., & Tanaka, T. (1987). Volume-phase transitions of ionized N-isopropylacrylamide gels. *J. Chem. Phys., 87*(2), 1392-1395.

Hooper, H. H., Baker, J. P., Blanch, H. W., & Prausnitz, J. M. (1990). Swelling equilibria for positively charged polyacrylamide hydrogels. *Macromolecules, 23*(4), 1096-1104.

Jacobs, H., Mischenko, N., Koch, M. H. J., Earlingen, R. C., Decour, J. A., & Reynaers, H. (1998). Evaluation of the impact of annealing on gelatinization at intermediate water content of what and potato starches: a differential scanning calorimetry and small angle x-ray scattering study. *Carbohydrate Res., 306*(1-2), 1-10.

Joanny, J. F., & Leibler, L. (1990). Weakly charged polyelectrolytes in a poor solvent. *J. De Physique, 51*(6), 545-557.

Katchalsky, A., Lifson, S., & Eisenberg, H. J. (1951). Equation of swelling for polyelectrolyte gels. *Polym. Sci., 7*(5), 571-574.

Katchalsky, A., Lifson, S., & Mazur, J. (1953). The electrostatic free energy of polyelectrolyte solutions. 1. Randomly kinked macromolecules. *Polym. Sci., 11*(5), 409-423.

Katchalsky, A., & Michaeli, I. (1955). Polyelectrolyte gels in salt solutions. *Polym. Sci., 15*(79), 69-86.

Khan, S. A., & Armstrong, R. C. (1986). Rheology of Foams .1. Theory for Dry Foams. *Journal of Non-Newtonian Fluid Mechanics, 22*(1), 1-22. Retrieved from <Go to ISI>://WOS:A1986E547300001. doi:Doi 10.1016/0377-0257(86)80001-5

Khan, S. A., & Armstrong, R. C. (1987). Rheology of Foams .2. Effects of Polydispersity and Liquid Viscosity for Foams Having Gas Fraction Approaching Unity. *Journal of Non-Newtonian Fluid Mechanics, 25*(1), 61-92. Retrieved from <Go to ISI>://WOS:A1987J495300002. doi:Doi 10.1016/0377-0257(87)85013-9

Kim, H. R., Muhrbeck, P., & Eliasson, A. C. (1993). Changes in rheological properties of hydroxypropyl potato starch pastes during freeze— thaw treatments. III. Effect of cooking conditions and concentration of the starch paste. *Journal of the Science of Food and Agriculture, 61*(1), 109-116. doi:10.1002/jsfa.2740610117

Kim, W. T., Franceschi, V. R., & Okita, T. W. (1989). Immunocytochemical localization of ADPglucose pyrophosphorylase in developing potato tuber cells. *Plant Physiology, 91*(1). doi:10.1104/pp.91.1.217

Kim, Y. (1999). Starch cooking with limited water as affected by zein and guar gum. *Journal of Food Science, 64*(1), 133-136.

Kolli, V. G., Pollauf, E. J., & Gadala-Maria, F. (2002). Transient normal stress response in a concentrated suspension of spherical particles. *Journal of Rheology, 46*(1), 321-334. doi:10.1122/1.1428320

Kornbrust, B. A., Forman, T., & Matveeva, I. (2012). 19 - Applications of enzymes in breadmaking A2 - Cauvain, Stanley P. In *Breadmaking (Second edition)* (pp. 470-498): Woodhead Publishing.

Larson, R. G. (1999). *The structure and rheology of complex fluids*. New York: New York : Oxford University Press.

Lii, C. Y., Tsai, M. L., & Tseng, K. H. (1996). Effect of amylose content on the rheological property of rice starch. *Effect of amylose content on the rheological property of rice starch., 73*(4), 415-420.

Lil, C., Shao, Y., & Tseng, K. (1995). GELATION MECHANISM AND RHEOLOGICAL PROPERTIES OF RICE STARCH. *Cereal Chem., 72*(4), 393-400.

Liu, H. S., Yu, L., Xie, F. W., & Chen, L. (2006). Gelatinization of cornstarch with different amylose/amylopectin content. *Carbohydrate Polymers, 65*(3), 357-363. Retrieved from <Go to ISI>://WOS:000240154300015. doi:10.1016/j.carbpol.2006.01.026

Lu, C. I., & Chen, L. H. (1980). factors in the gel- forming properties of hsian- tsao (Mesona procumbens Hemsl). I. Extraction conditions and different starches. In *Factors in the gel-forming properties of hsian-tsao (Mesona procumbens Hemsl). I. Extraction conditions and different starches [Consumed as a jello-type dessert]* (Vol. 4, pp. 438-442).

Lu, Z. Y., & Hentschke, R. (2002). Swelling of model polymer networks with different cross-link densities: a computer simulation study. *Phys Rev E Stat Nonlin Soft Matter Phys, 66*(4 Pt 1), 041803. Retrieved from http://www.ncbi.nlm.nih.gov/entrez/query.fcgi?cmd=Retrieve&db=PubMed&dopt=Citation&list_uids=12443224

Matyka, M., Khalili, A., & Koza, Z. (2008). Tortuosity-porosity relation in porous media flow. *Physical Review E, 78*(2). Retrieved from <Go to ISI>://WOS:000259263700057.

Meshram, M. W., Patil, V. V., Mhaske, S. T., & Thorat, B. N. (2009). Graft copolymers of starch and its application in textiles. *Carbohydrate Polymers, 75*(1), 71-78. doi:10.1016/j.carbpol.2008.06.012

Millard, M. M., Wolf, W. J., Dintzis, F. R., & Willett, J. L. (1999). The hydrodynamic characterization of waxy maize amylopectin in 90% dimethy sulfoxide-water by analytical ultracentrifugation, dynamic and static light scattering. *Carbohydr. Polym., 39*, 315-320.

Morley, M. J., & Miles, C. A. (1997). Modelling the thermal conductivity of starch-water gels. *Journal of Food Engineering, 33*(1-2), 1-14. Retrieved from <Go to ISI>://WOS:000071070400001.

Nara, S., & Tsu, T. (1983). Studies on the relationship between water-saturated state and crystallinity by the diffraction method for moistened potato starch. *35*, 407-410.

Narsimhan, G., & Ruckenstein, E. (1986). Effect of Bubble-Size Distribution on the Enrichment and Collapse in Foams. *Langmuir, 2*(4), 494-508. Retrieved from <Go to ISI>://WOS:A1986D333700021. doi:Doi 10.1021/La00070a020

Narsimhan, G., & Ruckenstein, E. (1986). Hydrodynamics, enrichment, and collapse in foams. *Langmuir, 2*(2), 230-238. Retrieved from https://doi.org/10.1021/la00068a021. doi:10.1021/la00068a021

Nelson, O., & Pan, D. (1995). Starch synthesis in maize endosperms. *Annual Review of Plant Physiology and Plant Molecular Biology, 46*, 475-496.

Okechukwu, P. E., & Rao, M. A. (1995). Influence of granule size on viscosity of corn starch suspensions. *Journal of Texture Studies, 26*, 501-516.

Owens, D. K., & Wendt, R. C. (1969). Estimation of the surface free energy of polymers. *Journal of Applied Polymer Science, 13*(8), 1741-1747. doi:10.1002/app.1969.070130815

Pither, R. J. (2003). CANNING | Quality Changes During Canning A2 - Caballero, Benjamin. In *Encyclopedia of Food Sciences and Nutrition (Second Edition)* (pp. 845-851). Oxford: Academic Press.

Pozueta-Romero, J., Frehner, M., Viale, A. M., & Akazawa, T. (1991). Direct transport of ADPglucose by an adenylate translocator is linked to starch biosynthesis in amyloplasts. *Proceedings of the National Academy of Sciences of the United States of America, 88*(13), 5769. doi:10.1073/pnas.88.13.5769

Prange, M. M., Hooper, H. H., & Prausnitz, J. M. (1989). Thermodynamics of aqueous systems containing hydrophilic polymers or gels. *AIChE J., 35*, 803.

Preiss, J. (1982). Regulation of the biosynthesis and degradation of starch. *Regulation of the biosynthesis and degradation of starch [in plants], 33*, 431-454.

Preiss, J. (1998). Biochemistry, molecular biology and regulation of starch synthesis. *Genetic Engineering, 20*, 177.

Prince, L. M. (1967). A theory of aqueous emulsions I. Negative interfacial tension at the oil/water interface. *Journal of Colloid And Interface Science, 23*(2), 165-173. doi:10.1016/0021-9797(67)90099-9

Pusey, P. N. (2008). Colloidal glasses. *Colloidal glasses, 20*(49), 494202. doi:10.1088/0953-8984/20/49/494202

Pérez, C. J., Alvarez, V. A., & Vázquez, A. (2008). Creep behaviour of layered silicate/starch–polycaprolactone blends nanocomposites. *Materials Science & Engineering A, 480*(1), 259-265. doi:10.1016/j.msea.2007.07.031

Rao, M. A., Okechukwu, P., Da Silva, P. M. S., & Oliveira, J. (1997). Rheological behavior of heated starch dispersions in excess water: role of starch granule. *Carbohydrate Polymers, 33*(4), 273-283.

Rao, M. A., Okechukwu, P. E., Da Silva, P. M. S., & Oliveira, J. C. (1997). Rheological behavior of heated starch dispersions in excess water: role of starch granule. *Carbohydrate Polymers, 33*(4), 273-283. doi:10.1016/S0144-8617(97)00025-8

Ratnayake, W. S., & Jackson, D. S. (2006). Gelatinization and solubility of corn starch during heating in excess water: new insights. *Journal of agricultural and food chemistry, 54*(10), 3712. doi:10.1021/jf0529114

Ravenelle, F., Marchessault, R. H., Légaré, A., & Buschmann, M. D. (2002). Mechanical properties and structure of swollen crosslinked high amylose starch tablets. *Carbohydrate Polymers, 47*(3), 259-266. doi:10.1016/S0144-8617(01)00169-2

Ricka, J., & Tanaka, T. (1984). Swelling of ionic gels-Quantitative performance of Donnan theory. *Macromolecules, 17*(12), 2916-2921.

Ricka, J., & Tanaka, T. (1985). Phase transition in ionic gels induced by copper complexation. *Macromolecules, 18*(1), 83-85.

Sarko, A., & Wu, H. C. (1978). The crystal structure of A,B, and C plymorphs of amylose starch. *Starch/Starke, 30*, 73-78.

Singh, J., Kaur, L., & McCarthy, O. J. (2007). Factors influencing the physico-chemical, morphological, thermal and rheological properties of some chemically modified starches for food applications—A review. *Food Hydrocolloids, 21*(1), 1-22. doi:10.1016/j.foodhyd.2006.02.006

Singh, N., Singh, J., Kaur, L., Singh Sodhi, N., & Singh Gill, B. (2003). Morphological, thermal and rheological properties of starches from different botanical sources. *Food Chemistry, 81*(2), 219-231. doi:10.1016/S0308-8146(02)00416-8

Sjoo, M., Nilsson, L., & Sjöö, M. (2018). *Starch in food : structure, function and applications* (Second Edition.. ed.). Duxford: Duxford : Woodhead Publishing.

Stamenovic, D., & Wilson, T. A. (1984). The Shear Modulus of Liquid Foam. *Journal of Applied Mechanics, 51*(2), 229. doi:10.1115/1.3167604

Stapley, J. A., & BeMiller, J. N. (2003). Hydroxypropylated Starch: Granule Subpopulation Reactivity. *Cereal chemistry, 80*(5), 550-552.

Steeneken, P. A. M. (1989). Rheological properties of aqueous suspensions of swollen starch granules. *Carbohydrate Polymers, 11*(1), 23-42. doi:10.1016/0144-8617(89)90041-6

Stevenson, D. G., Jane, J., & Inglett, G. E. (2006). Physicochemical properties of pin oak (*Quercus palustris Muench.*) acorn starch. *Starch/Starke*, 553-560.

Sun, A., & Gunasekaran, S. (2009). Yield Stress in Foods: Measurements and Applications. *International Journal of Food Properties, 12*(1), 70-101. doi:10.1080/10942910802308502

Swinkels, J. J. M. (1985). Composition and Properties of Commercial Native Starches. *Starke, 37*(1), 1-5. Retrieved from <Go to ISI>://WOS:A1985AAY2000001. doi:DOI 10.1002/star.19850370102

Tan, I., Torley, P. J., & Halley, P. J. (2008). Combined rheological and optical investigation of maize, barley and wheat starch gelatinisation. *Carbohydrate Polymers, 72*(2), 272-286. doi:10.1016/j.carbpol.2007.08.018

Tanaka, T. (1978). Collapse of gels and critical endpoint. *Phys. Rev. Lett., 40*(12), 820-823.

Tanaka, T., Fillmore, D., Sun, S. T., Nishio, I., Swislow, G., & Shah, A. (1980). Phase transitions in ionic gels. *Phys. Rev. Lett., 45*(20), 1636-1639.

Tattiyakul, J., & Rao, M. A. (2000). Rheological behavior of cross linked waxy maize starch dispersion during and after heating. *Carbohydrate Polymers, 43*, 215-222.

Teli, M. D., Rohera, P., Sheikh, J., & Singhal, R. (2009). Application of germinated maize starch in textile printing. *Carbohydrate Polymers, 75*(4), 599-603. doi:10.1016/j.carbpol.2008.09.001

Tester, R. F., & Morrison, W. R. (1990). Swelling and Gelatinization of Cereal Starches .1. Effects of Amylopectin, Amylose, and Lipids. *Cereal Chemistry, 67*(6), 551-557. Retrieved from <Go to ISI>://WOS:A1990EK09100010.

Tsai, M. L., Li, C. F., & Lii, C. Y. (1997). Effects of Granular Structures on the Pasting Behaviors of Starches. *Cereal Chemistry, 74*(6), 750-757. doi:10.1094/CCHEM.1997.74.6.750

Urayama, K., & Kohjiya, S. (1996). Crossover of the concentration dependence of swelling and elastic properties for polysiloxane networks crosslinked in solution. *J Chem Phys, 104*(9), 3352-3358.

Vamadevan, V., & Bertoft, E. (2015). Structure-function relationships of starch components. *Starch-Starke, 67*(1-2), 55-68. Retrieved from <Go to ISI>://WOS:000347545400005. doi:10.1002/star.201400188

van der Vaart, K. (2013). Rheology of concentrated soft and hard- sphere suspensions. *Journal of Rheology, 57*(4), 1195-1210. doi:10.1122/1.4808054

Vargaftik, N. B., Volkov, B. N., & Voljak, L. D. (1983). International Tables of the Surface Tension of Water. *Journal of Physical and Chemical Reference Data, 12*(3), 817-820. doi:10.1063/1.555688

Visser, R. G. F., Suurs, L. C. J. M., Steeneken, P. A. M., & Jacobsen, E. (1997). Some physicochemical properties of amylose-free potato starch. *Starch/Starke, 49*(11), 443.

Wang, B., Wang, L.-J., Li, D., Özkan, N., Li, S.-J., & Mao, Z.-H. (2009). Rheological properties of waxy maize starch and xanthan gum mixtures in the presence of sucrose. *Carbohydrate Polymers, 77*(3), 472-481.

Wang, S., Wang, J., Yu, J., & Wang, S. (2014). A comparative study of annealing of waxy, normal and high-amylose maize starches: The role of amylose molecules. *Food Chemistry, 164*, 332-338. doi:10.1016/j.foodchem.2014.05.055

Wani, A. A., Singh, P., Shah, M. A., Schweiggert-Weisz, U., Gul, K., & Wani, I. A. (2012). Rice starch diversity: Effects on structural, morphological, thermal, and physicochemical properties—A review. *Comprehensive Reviews in Food Science and Food Safety, 11*(5), 417-436.

Weaire, D. (2008). The rheology of foam. *Current Opinion in Colloid & Interface Science, 13*(3), 171-176. Retrieved from <Go to ISI>://WOS:000256735800010. doi:10.1016/j.cocis.2007.11.004

Whistler, R. L., & BeMiller, J. M. (1997). *Carbohydrate Chemistry for Food Scientists*: Eagan Press, St. Paul MN.

White Jr, D. R. (1999). Applications of gel permeation chromatography with multi-angle light scattering to the characterization of polysaccharides. *ACS Symposium Series, 737*, 299-316.

Wong, R., & Lelievre, J. (1981). Viscoelastic behaviour of wheat starch pastes. *An International Journal of Rheology, 20*(3), 299-307. doi:10.1007/BF01678031

Woo, K., & Seib, P. (2002). Cross-linked resistant starch: Preparation and properties. *Cereal Chemistry, 79*(6), 819-825. doi:10.1094/CCHEM.2002.79.6.819

Yoo, S. H., & Jane, J. L. (2002). Molecular weights and gyration radii of amylopectins determined by high performance size exclusion chromatography equipped with multi-angle laser light scattering and refractive index detectors. *Carbohydr. Polym., 49*, 307-314.

Zhao, Y., & Eichinger, B. E. (1992). Study of solvent effects on dilation modulus of poly(dimethylsiloxane). *Macromolecules, 25*, 6988-6995.

Zhou, X., Yang, J., & Qu, G. (2007). Study on synthesis and properties of modified starch binder for foundry. *Journal of Materials Processing Tech., 183*(2), 407-411. doi:10.1016/j.jmatprotec.2006.11.001

Zobel, H. F. (1984). CHAPTER IX - GELATINIZATION OF STARCH AND MECHANICAL PROPERTIES OF STARCH PASTES A2 - WHISTLER, ROY L. In J. N. Bemiller & E. F. Paschall (Eds.), *Starch: Chemistry and Technology (Second Edition)* (pp. 285-309). San Diego: Academic Press.

VITA

Jinsha Li started her Ph.D study with Dr. Narsimhan in the Department of Agricultural and Biological Engineering and has been working on project "Prediction of swelling kinetics and pasting behavior of starch granules" since August 2015. She completed her M.S. thesis in the same year with Dr. Engelberth's, titled "Adding Value To Bio-Ethanol Production: Quantification and Recovery of Lutein And Zeaxanthin From DDGS". Li is the recipient of Frederick N. Andrews Fellowship and Whistler Center for Carbohydrate Research Scholarship. In 2013, she graduated from Michigan State University with B.S. in Biosystem Engineering.

Li and Desam have been successful in developing a mechanistic model for swelling kinetics of starch granules in terms of its structure. The model has been validated by her through experimental measurements of swelling kinetics of waxy maize starch which has resulted in a recent publication in Journal of Food Engineering. She investigated the relationship between swelling and viscoelasticity of starch suspensions for a variety of starches and developed a master curve relating viscoelasticity and volume fraction of starch suspensions. Such a curve will have critical implication on development of food formulations with desirable texture. Li is a member of several scientific societies and has five presentations of her research at Institute of Food Technology, American Institute of Chemical Engineers and Conference of Food Engineering conferences.

Li served as former President (2015-2016) and Professional Development Coordinator (2014-2015) of Agricultural and Biological Engineering Graduate Students Association. She was Leadership Team member for the Graduate Women in Engineering Network (GWEN) from 2015 to 2017. She has been an active member of Confucius Institute at Purdue Performing Arts Troupe performing traditional Chinese dances at Greater Lafayette Area.